



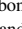














Carbon Mineralization in Fractured Mafic and Ultramafic Rocks: A Review

Key Points:

- Development of carbon mineralization operations in mafic and ultramafic rocks requires integrating field, laboratory, and modeling studies
- Fractures play an integral role in the mineralization of CO₂ in mafic and ultramafic rocks and must be considered in future studies
- Coupled geomechanical and geochemical processes in fractured mafic and ultramafic rocks require further experimental and modeling studies

H. Nisbet¹ , G. Buscarnera² , J. W. Carey¹ , M. A. Chen³ , E. Detournay⁴, H. Huang⁵, J. D. Hyman¹ , P. K. Kang³ , Q. Kang¹ , J. F. Labuz⁴ , W. Li¹ , J. Matter⁶ , C. W. Neil¹, G. Srinivasan⁷, M. R. Sweeney¹ , V. R. Voller⁴ , W. Yang³ , Y. Yang² , and H. S. Viswanathan¹ 

¹Earth and Environmental Sciences Division, Los Alamos National Laboratory, Los Alamos, NM, USA, ²Civil and Environmental Engineering, Northwestern University, Evanston, IL, USA, ³Department of Earth & Environmental Sciences, University of Minnesota, Minneapolis, MN, USA, ⁴Department of Civil, Environmental, and Geo-Engineering, University of Minnesota, Minneapolis, MN, USA, ⁵School of Civil and Environmental Engineering, Georgia Institute of Technology, Atlanta, GA, USA, ⁶School of Ocean and Earth Science, University of Southampton, Southampton, UK, ⁷X-Computational Physics Division, Los Alamos National Laboratory, Los Alamos, NM, USA

Correspondence to:

H. S. Viswanathan and H. Nisbet,
viswana@lanl.gov;
hayleanisbet@gmail.com

Citation:

Nisbet, H., Buscarnera, G., Carey, J. W., Chen, M. A., Detournay, E., Huang, H., et al. (2024). Carbon mineralization in fractured mafic and ultramafic rocks: A review. *Reviews of Geophysics*, 62, e2023RG000815. <https://doi.org/10.1029/2023RG000815>

Received 22 JAN 2024
Accepted 21 OCT 2024
Corrected 24 NOV 2024

This article was corrected on 24 NOV 2024. See the end of the full text for details.

Author Contributions:

Conceptualization: H. Nisbet, J. W. Carey, H. S. Viswanathan
Funding acquisition: E. Detournay, J. F. Labuz
Methodology: H. Nisbet, H. S. Viswanathan
Visualization: H. Nisbet, J. D. Hyman, H. S. Viswanathan
Writing – original draft: H. Nisbet, G. Buscarnera, J. W. Carey, M. A. Chen, E. Detournay, H. Huang, J. D. Hyman, P. K. Kang, Q. Kang, J. F. Labuz, W. Li, J. Matter, C. W. Neil, G. Srinivasan, M. R. Sweeney, V. R. Voller, W. Yang, Y. Yang, H. S. Viswanathan

Abstract Mineral carbon storage in mafic and ultramafic rock masses has the potential to be an effective and permanent mechanism to reduce anthropogenic CO₂. Several successful pilot-scale projects have been carried out in basaltic rock (e.g., CarbFix, Wallula), demonstrating the potential for rapid CO₂ sequestration. However, these tests have been limited to the injection of small quantities of CO₂. Thus, the longevity and feasibility of long-term, large-scale mineralization operations to store the levels of CO₂ needed to address the present climate crisis is unknown. Moreover, CO₂ mineralization in ultramafic rocks, which tend to be more reactive but less permeable, has not yet been quantified. In these systems, fractures are expected to play a crucial role in the flow and reaction of CO₂ within the rock mass and will influence the CO₂ storage potential of the system. Therefore, consideration of fractures is imperative to the prediction of CO₂ mineralization at a specific storage site. In this review, we highlight key takeaways, successes, and shortcomings of CO₂ mineralization pilot tests that have been completed and are currently underway. Laboratory experiments, directed toward understanding the complex geochemical and geomechanical reactions that occur during CO₂ mineralization in fractures, are also discussed. Experimental studies and their applicability to field sites are limited in time and scale. Many modeling techniques can be applied to bridge these limitations. We highlight current modeling advances and their potential applications for predicting CO₂ mineralization in mafic and ultramafic rocks.

Plain Language Summary Carbon mineralization is a developing environment-focused technology that aims to minimize the increasing levels of man-made CO₂ in the atmosphere to mitigate climate change. This approach works by injecting CO₂ into underground rock masses, where chemical reactions convert the CO₂ to mineral form, resulting in permanent storage. Initial field tests in basalt (mafic) and peridotite (ultramafic) rocks have demonstrated the promise of this technology, however, many processes are not well understood, which impedes further development of this technique. Moreover, while fractures are critical to the distribution and storage of CO₂ within the rock, their evolution and role during long-term and large-scale injection are not well understood. To fill these knowledge gaps, laboratory and modeling studies have been carried out to understand the fundamental science questions related to carbon mineralization. In this review, we highlight recent developments from field, laboratory, and modeling studies, and outline areas that should be studied to advance carbon mineralization to scales sufficient to minimize the effects of current and future emissions.

1. Introduction

A promising strategy to reduce anthropogenic CO₂ is to permanently mineralize carbon in mafic and ultramafic geologic reservoirs. These rock masses are advantageous due to their prevalence in the earth's subsurface and their ability to rapidly store CO₂ through carbon mineralization. Mafic and ultramafic rocks contain highly reactive silicate minerals abundant in metal cations (Mg²⁺, Ca²⁺, and Fe²⁺). When acidic CO₂-charged water reacts with these rock types, dissolution of the silicate minerals is promoted, releasing the cations into the pore fluid, where they can react with dissolved carbonate ions to precipitate carbonate minerals such as calcite (CaCO₃), magnesite (MgCO₃), siderite (FeCO₃), and ankerite [Ca(Fe, Mg, Mn) (CO₃)₂], “locking” the carbon in the subsurface

© 2024. The Author(s).

This is an open access article under the terms of the [Creative Commons Attribution License](https://creativecommons.org/licenses/by/4.0/), which permits use, distribution and reproduction in any medium, provided the original work is properly cited.

Writing – review & editing: H. Nisbet, J. W. Carey, E. Detournay, J. D. Hyman, P. K. Kang, J. F. Labuz, C. W. Neil, H. S. Viswanathan

(Figure 1) (Snæbjörnsdóttir et al., 2020; Xiong, Wells, & Giammar, 2017; Xiong, Wells, Menefee, et al., 2017). Successful pilot-scale mineral carbon storage projects in mafic rock, including CarbFix and CarbFix2 in Iceland (Clark et al., 2020; Pogge von Strandmann et al., 2019) and the Wallula basalt sequestration site in Washington, USA (S. K. White et al., 2020), have demonstrated rapid storage via mineralization on 2–3 year time scales. However, storing the levels of CO₂ needed to address the present climate crisis requires a significant up-scaling of these operations. An important consideration is how the CO₂ is injected into the reservoir. The injection of CO₂ that has been already dissolved in water, as done at the CarbFix sites, has the advantage of a more rapid conversion to mineral form, given that the CO₂ has already achieved “solubility trapping” prior to injection (Snæbjörnsdóttir et al., 2020). However, the requirement for immense quantities of water cannot be forgotten and may not be favorable in other locations. This issue can be avoided by injecting CO₂ as a supercritical fluid, as done at the Wallula basalt sequestration site. However, mineralization is expected to take longer, and requires favorable geologic formations that do not offer the possibility of leakage (Snæbjörnsdóttir et al., 2020). Therefore, determining the optimal injection conditions and having the ability to predict the impact of long-term, large-scale CO₂ mineralization on geologic reservoirs is pertinent to up-scaling CO₂ mineralization operations.

Promising targets for subsurface mineralization are basalt (mafic) and peridotite (ultramafic). Basalt, in particular, volcanic lava flows and flood basalts which have already been tested at the pilot scale, has the advantage of possessing inter-layer and fracture permeability that readily accommodates the injection of CO₂ (Raza et al., 2022). However, a significant fraction of the total mass of basalt contained in the flow centers is impermeable (Aubele et al., 1988). Peridotite has the advantage of containing a greater concentration of divalent cations, making the rock more reactive, but it is also not as widespread and generally has lower permeability (Raza et al., 2022). Thus, for both basalt and peridotite, efficient mineralization of the rock mass requires a penetrating fracture network or the development of fractures that accommodate the flow and reaction of CO₂-bearing fluids. This involves optimizing fully coupled thermal, hydrological, mechanical, and chemical processes that can sustain flow for long-term carbon mineralization. Complex feedbacks exist among fracture propagation, fluid flow, dissolution, precipitation, and fracture closure, including phenomena such as passivation of mineral surfaces that reduce reactive surface area (Béarat et al., 2006); carbonate precipitation that can clog pores and fractures (Jöns et al., 2017); subcritical fracture growth (Atkinson, 1984); and reaction-driven cracking (Kelemen & Hirth, 2012). These questions require a coupled understanding of fluid flow and transport in fractured media and the chemical and mechanical processes that occur during carbon mineralization.

Mineral carbon storage is a rapidly developing field of research, which has fostered the publication of review papers providing a broad overview of storage potential (Aminu et al., 2017; Oelkers & Gislason, 2023; Power et al., 2013; Snæbjörnsdóttir et al., 2020) and geochemical processes, primarily as they relate to porous materials (DePaolo & Cole, 2013; L. Zhang et al., 2019; Y. Zhang et al., 2019). There is also extensive research on flow and fracture processes that apply to impermeable materials, including reviews on (a) the physical characteristics of fractures and fracture patterns (NRC, 1996), (b) hydromechanical-thermomechanical processes in fractured rock (C. F. Tsang, 1991), and (c) flow and transport in fractured rock (Viswanathan et al., 2022; J. S. Y. Wang, 1991). To date, a review linking knowledge of fluid flow and transport, geochemistry, and the dynamic evolution of fractures during carbon mineralization in mafic and ultramafic rocks has not been published.

This review discusses recent developments in hydrological, geochemical, and geomechanics research domains highlighting new field, laboratory, and modeling studies that are relevant for carbon mineralization, combined with commentary on the implications for carbon mineralization in fractured mafic and ultramafic rocks. The current challenges that hinder our ability to accurately predict the outcome of long-term carbon mineralization in these rock masses will also be discussed. The review is organized as follows:

Section 2. Field Studies. Carbon mineralization in mafic and ultramafic rocks has been recently investigated at the pilot scale. At CarbFix in Iceland, over 95% of the injected CO₂ was mineralized in basalt after 2 years, while CarbFix2 mineralized >50% and 76% of the injected CO₂ and hydrogen sulfide, respectively, in 4 to 9 months, and is currently still in operation (Clark et al., 2020; Matter et al., 2016). The Wallula Basalt Project in Washington State, USA mineralized 60% of CO₂ in basalt after 2 years (S. K. White et al., 2020), while the injection of CO₂ into peridotite-rich Oman ophiolite is currently underway. Field observations and data derived from these tests provide invaluable information about the physicochemical processes occurring in the subsurface during and after CO₂ injection, which can guide experimental designs and inform model parameters. In this review, we delve into the key findings from these field tests and highlight the variances in site characteristics including rock types,

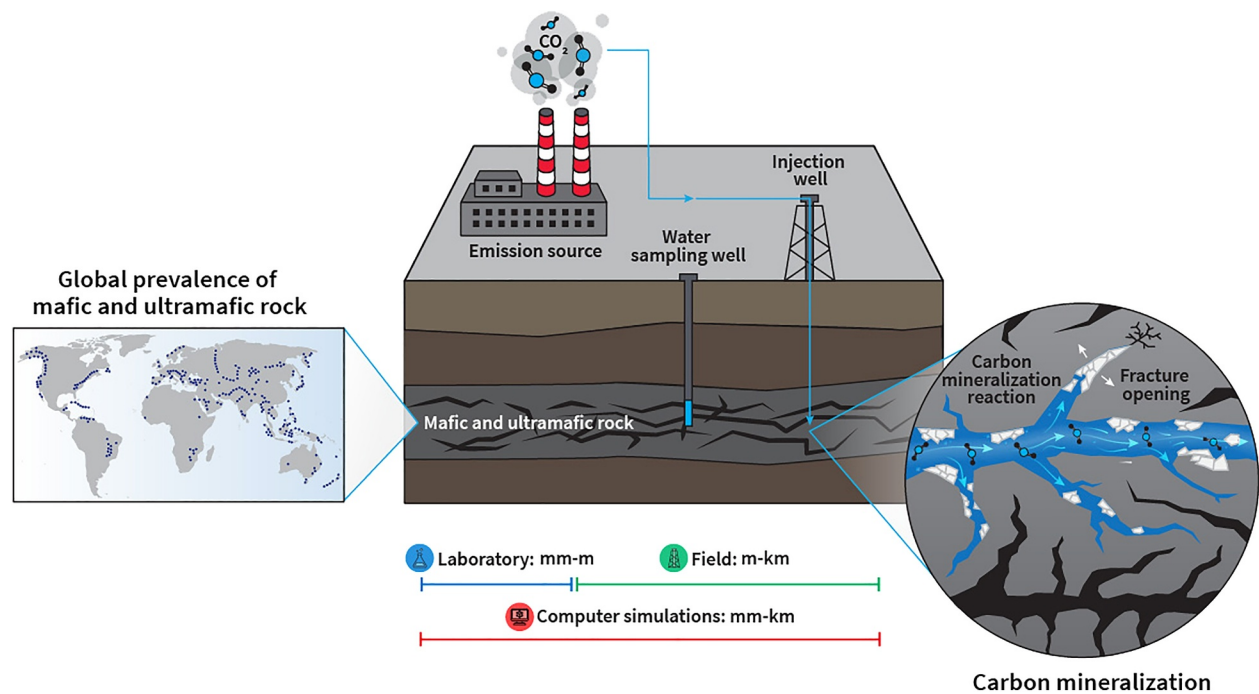


Figure 1. Carbon mineralization in mafic and ultramafic rocks is a promising strategy to permanently remove and store emitted CO₂ into the subsurface due to the prevalence of mafic and ultramafic rocks worldwide, and the ability for these rocks to rapidly convert CO₂ into minerals. This review highlights recent developments toward understanding the geochemical and geomechanical processes at the laboratory, field, and simulation scale.

fracture networks, carbon mineralization products, fluid composition, and rates of mineralization. In addition, we outline the current knowledge gaps and challenges that inhibit the scale-up of carbon mineralization to store the gigaton-per-year levels required to meet the needs of the climate crisis.

Section 3. Experimental Studies. Laboratory testing provides an opportunity to decipher the coupled flow, chemical and mechanical processes that occur during CO₂ injection and subsequent carbon mineralization in a controlled environment. An abundance of laboratory studies, including flow-through and batch-reactor experiments, have been carried out to understand the geochemical reactions that facilitate the carbonation of mafic and ultramafic rocks, producing data such as mineral dissolution and precipitation kinetics, mineralogy of reaction products, hydrodynamic parameters (e.g., Damköhler and Peclet numbers), and surface characteristics. Fundamental research on the mechanical behavior of mafic and ultramafic rocks exists, which can be combined with studies on other materials (e.g., analog systems) that examine clogging and passivation of mineral surfaces, stress-corrosion cracking, and reaction-driven cracking, to understand fluid flow and reactive transport in fractured rock. We describe the advances in experimental studies on the geochemistry of carbon mineralization in analog and real geomaterials under relevant reservoir conditions, and fluid flow and reactions in fractures, as well as address the challenges of accurately representing field-scale carbon mineralization processes in laboratory-scale experiments.

Section 4. Modeling and Simulation Studies. Field observations and controlled laboratory experiments constrain the multi-scale numerical models operating at the pore, single fracture, and fracture network scale that are used to predict the long-term carbon mineralization of a reservoir. The coupled geochemical-geomechanical processes that affect fracture creation and damage, fluid flow, and mineralization in current models do not include all the relevant processes. Numerous models exist that predict the evolution of fractures due to stress effects. Different models also exist to simulate flow through fractures. These models range in complexity from simple analytical models to mechanistic numerical models run on supercomputers. Few models couple flow and chemical reactions, while fully coupled studies of fracture, flow, and reaction are rare. For mafic and ultramafic rocks, answering key questions, such as whether stress-corrosion cracking or reaction-driven cracking will occur, requires a fully coupled approach. Models that are capable of describing fracture propagation rigorously with simplified assumptions for flow, transport, and reaction processes have been used for applications such as hydraulic fracturing. Other models that simulate flow, transport, and reactions once the fractures are created also

exist and have been used for enhanced geothermal systems and nuclear waste disposal. We describe a combination of reduced complexity models, the latest generation of high-performance computing physics-based models, and statistically based uncertainty quantification (UQ) techniques that together can be used to better understand first-order mechanisms to forecast carbon mineralization in reservoirs.

2. Field Studies of Carbon Mineralization in Mafic and Ultramafic Rock

2.1. Introduction

Over the past two decades, carbon mineralization in mafic and ultramafic rocks has developed from a conceptual idea to successful pilot-scale operations globally (Clark et al., 2020; Kelemen, Matter, et al., 2020; Kelemen, McQueen, et al., 2020; Matter et al., 2016; McGrail et al., 2011). Motivated by the naturally reactive nature of mafic and ultramafic rocks, these exploratory field sites offer a critical first-hand look at the feasibility and effectiveness of storing CO₂ in these rock masses. Among mafic/ultramafic rocks, subsurface basalt (mafic) and peridotite (ultramafic) have been tested at various pilot injection sites, which we review in this section. CarbFix (Section 2.2), the inaugural CO₂ mineralization project located in western Iceland's basalt, injected 230 tons of CO₂ and a CO₂-H₂S gas mixture dissolved in water (Matter et al., 2016), where an estimated ~95% of the CO₂ was mineralized after 2 years. The success of this operation resulted in the development of the CarbFix2 site, an up-scaled commercial injection site that is showing promise. In Eastern Washington, USA, the Wallula Basalt Sequestration Project (Section 2.3) was carried out and was the first site to inject supercritical CO₂ directly into flood basalts without first dissolving it in water. Here, after 2 years of injection, ~60% of the CO₂ was mineralized (S. K. White et al., 2020). More recently, the injection of CO₂ dissolved in water into peridotites in Oman (Section 2.4) is being tested and monitored.

The success of carbon mineralization field studies demonstrates the viability of storing CO₂ in mafic and ultramafic rocks. However, reaching the levels of stored CO₂ needed to reduce atmospheric CO₂ requires a significant up-scaling of the operations and the introduction of new field sites. Key parameters that are currently poorly understood govern the feasibility of injection sites, including the existing and induced fracture network that provides a conduit for fluid and solute transport, the geochemical properties of the reservoir including the mineral reaction rates and reactive surface area, and water availability and use. Basalt inter-layer zones tend to be highly porous and fractured, resulting in a “double-edged sword” effect where, while these sites have high CO₂ injectivity, they also have a greater potential for CO₂ leakage. In the case of CarbFix, this issue was avoided by injecting CO₂ already dissolved in water, reducing the risk of leakage through solubility-trapping (Snæbjörnsdóttir et al., 2020). However, the high quantity of water used for injection may limit the scalability of the site to inject larger amounts of CO₂. At Wallula, the injection of supercritical CO₂ eliminates the need for large quantities of water, however, careful reservoir characterization and highly impermeable (unfractured) basalt flow centers capping the injection zone are needed to prevent CO₂ migration (McGrail, Sullivan, et al., 2009). Furthermore, it is still not known how supercritical CO₂, often considered inert to chemical reactions in the absence of water, will govern the distribution and capacity of CO₂ mineralization within these rock masses during longer-term injection (McGrail, Schaef, et al., 2009). Peridotites are more reactive rocks than basalt, and thus, have a higher potential to store CO₂. However, these rocks tend to be relatively impermeable, and, thus, their effectiveness at mineralizing CO₂ will likely be contingent on a connected network consisting of pre-existing fractures, enhanced by hydraulic stimulation and aided by reaction-driven fracturing and sub-critical fracturing (discussed in Section 3.4). The total mass of CO₂ that can be stored in mafic and ultramafic reservoirs is also governed by the physicochemical properties of the rock.

For both basalt and peridotite, the relative reactivity of minerals and the available reactive surface area are important factors that will influence the amount of CO₂ mineralized at a given site. Furthermore, the precipitation of carbonates could lead to the passivation of reactive surfaces or the clogging of fluid pathways (Béarat et al., 2006; Jöns et al., 2017). Thus, analysis of coupled geochemical reactions, fluid flow, and the development of fracture networks in these systems is imperative. While it is impossible to visualize precisely what is occurring in the subsurface, we highlight key takeaways from the field sites discussed in the following sections and outline challenges (Section 2.5) that must be overcome to expand to large-scale carbon mineralization operations.

2.2. The CarbFix Project

2.2.1. Site Description

The CarbFix project was founded in 2007 by Reykjavik Energy, the University of Iceland, Columbia University, and CNRS Toulouse France. The aim of the CarbFix project was to demonstrate rapid CO₂ mineralization in basaltic rocks, which was achieved on different scales by the CarbFix1 and CarbFix2 pilots from 2013 to 2020 (e.g., Aradóttir et al., 2012; Clark et al., 2020; Gislason et al., 2010; Matter et al., 2016; Pogge von Strandmann et al., 2019; Sigfusson et al., 2015; Snæbjörnsdóttir et al., 2017). The CarbFix1 pilot injection site, located approximately 2 km west of the Hellisheiði geothermal power plant, consists of a series of lava flows and glassy hyaloclastite formations (Alfredsson et al., 2013). The site is equipped with a 2,000 m deep injection well (HN02) and eight monitoring wells with depths ranging from 150 to 1,300 m. The injection operation focused on utilizing HN02 as the injection well and HN04, an inclined borehole, as the closest monitoring well. The distance between the two wells is ~60 m at 400 m, 150 m at 650 m, and 360 m at 800 m depth, respectively (Alfredsson et al., 2013). The target CO₂ storage formation was between 400 and 800 m depth, consisting of olivine tholeiitic basaltic lavas and hyaloclastites. The lateral and vertical intrinsic permeabilities were 300 and 1,700 × 10⁻¹⁵ m², respectively (Aradóttir et al., 2012). A tracer test in combination with borehole logs revealed three distinct major flow paths or channels between wells HN02 and HN04, with the first flow path being located at 400 m, the second at 650 m, and the third at 850 m depth, respectively (Rezvani Khalilabad et al., 2008). The water level in the HN02 injection well was at ~100 m depth, and the groundwater temperature and pH in the target storage formation ranged from 20 to 33°C and from 8.4 to 9.4, respectively (Rezvani Khalilabad et al., 2008).

The CarbFix2 injection site is located 1.5 km north of the Hellisheiði geothermal power plant and is utilizing pre-existing multiple directionally drilled wells from the Hellisheiði geothermal field as injection and monitoring wells with total depths ranging from 2,204 to 2,606 m (Gunnarsson et al., 2018). The reservoir rocks consist of olivine tholeiitic basalt, with the top 1,000 m being dominantly hyaloclastites. The target storage reservoir is at depths greater than 1,300 m with an in-situ temperature of >250°C (Gunnarsson et al., 2018). Fluid flow within the reservoir is controlled by multiple high-permeability fractures and faults that intersect the injection and monitoring wells, as a result of the emplacement of intrusive rocks cross cutting the lava flows and hyaloclastites (Gunnarsson et al., 2018). In addition, fluid migration within the reservoir is influenced by the hydraulic gradient imposed by the far-field injection and production wells (Ratouis et al., 2022). Tracer tests confirmed fast-flowing pathways from the injection to the monitoring wells along NE-SW trending faults and fractures (e.g., Gunnarsson et al., 2018).

2.2.2. CO₂ Injection and Post-Injection Monitoring

CarbFix1 consisted of two injections, which were conducted in 2012. Phase 1 involved the injection of 175 tons of CO₂ from January to March 2012, while Phase 2 involved the injection of 73 tons of CO₂-H₂S gas mixture from June to August 2022, of which 55 tons were CO₂. Due to the relatively shallow depth of the target storage reservoir, injection of buoyant supercritical CO₂ into the fractured basalt reservoir was not possible. For this reason, a novel injection system of separately injecting CO₂ and H₂O at a ratio that facilitated complete solubility of CO₂ into the water at the target depth was developed (Sigfusson et al., 2015). The water for the injection was sourced from the target storage reservoir. Injectivity at the target depth of 500–800 m was high enough for the injected water to flow down the injection wellbore by gravity alone. In the injection well, CO₂ was released into the downflowing water through a sparger at a depth of 350 m, applying a CO₂ injection pressure just above 25 bars. To assure complete dissolution of the CO₂ before arriving in the target storage reservoir, the H₂O:CO₂ ratio was chosen to be greater than the CO₂ solubility at the release depth. Furthermore, the water velocity in the injection well and thus the water injection rate was critical to counteract the buoyancy of the CO₂ gas. Typical injection rates were ~260 L/s for CO₂ and ~6,800 L/s for H₂O during Phase 1 and between 38 and 190 L/s for CO₂ and 1,578 and 7,881 L/s for H₂O during Phase 2 (Matter et al., 2016).

The mineralization of the injected CO₂ was monitored by co-injecting a suite of chemical and isotopic tracers. The injected CO₂ was spiked with radiocarbon (¹⁴C) to monitor its transport and reactivity in the reservoir. The ¹⁴C concentrations of the injected fluids were 40.0 Bq/L (¹⁴C:¹²C 2.16 × 10⁻¹¹) during Phase 1 and 6 Bq/L (¹⁴C:¹³C 6.5 × 10⁻¹²) during Phase 2 (Matter et al., 2016). In addition, non-reactive but volatile sulfur hexafluoride (SF₆) and trifluoromethyl sulfur pentafluoride (SF₅CF₃) tracers were co-injected with the CO₂ to monitor injection plume migration and conservative mixing between injectate and reservoir fluid. Fluid samples for cation, anion,

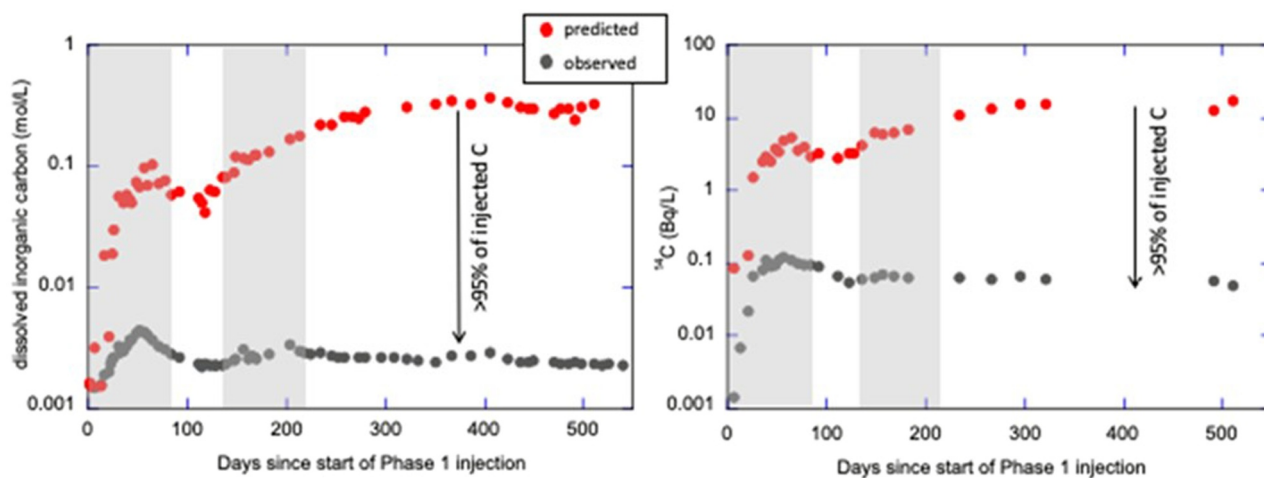


Figure 2. CarbFix1 mass balance calculations that indicate that >95% of dissolved CO₂ was mineralized along the subsurface flow path from the injection to the monitoring well within two years. The figure depicts the predicted and observed dissolved inorganic carbon concentrations and isotope ratio of ¹⁴C in water at the CarbFix1 monitoring well. Predicted values are based on conservative mixing between the injectate and reservoir fluid using non-reactive tracers such as SF₆. The differences between predicted and observed values are consistent with the loss of almost all injected CO₂ to form solid carbonate minerals along the flow path (modified from Matter et al. (2016)).

trace element, dissolved inorganic carbon, and tracer analyses were collected using an in-situ downhole sampler in the injection well, and with a submersible pump from monitoring well HN04 during and after the dissolved CO₂ injection.

CarbFix2 was designed to demonstrate the technical maturity and economic feasibility of CO₂ and H₂S capture from emission sources and permanent geologic storage via mineralization. Exhaust gas from the geothermal powerplant was dissolved in condensate in a scrubbing tower at 5–6 bar pressure (Gunnarsson et al., 2018). Subsequently, the CO₂ and H₂S-charged condensate water was pressurized to 9 bar and transported to the CarbFix2 injection wells (Gunnarsson et al., 2018). The gas-charged condensate water was injected to a depth of 750 m in separate stainless-steel tubing in the injection wells at a rate of 30–60 L/s, where it was released into the downflowing geothermal brine from the powerplant (Clark et al., 2020). The inert tracer, 1-naftalenesulfonic acid (1-ns) was co-injected with the gas-charged condensate water to monitor injection plume migration and mixing (Clark et al., 2020). Steam and water phase samples were collected at the monitoring wells during the injection for geochemical analyses. By the end of 2017, 23,200 metric tons of CO₂ and 11,800 metric tons of H₂S had been injected. Injection at the CarbFix2 site continued after 2017 and by the end of 2023, over >97,000 tons of CO₂ had been injected into the Hellisheiði geothermal reservoir (www.carbfix.com).

2.2.3. Key Findings

The injection of acidic CO₂-charged water results in the dissolution of the basalt host rocks, releasing divalent metals while consuming H⁺ ions (e.g., Oelkers et al., 2008). The consumption of H⁺ via silicate rock dissolution causes pH, HCO₃⁻ and CO₃²⁻ concentrations to increase, resulting in the precipitation of carbonate minerals at a distance from the injection well. CarbFix1 verified these reactions by following the reaction progress of the dissolved injected CO₂. Fluid samples were regularly collected and analyzed from the HN04 monitoring well. The use of non-reactive tracers (SF₆, SF₅CF₃) allowed CarbFix researchers to detect the arrival of the injection plume in HN04. The SF₆ data from Phase 1 revealed an initial breakthrough peak in HN04 56 days after injection and the bulk arrival (peak concentration) 406 days after injection (Matter et al., 2016). Similarly, the conservative SF₅CF₃ tracer co-injected with the Phase 2 CO₂-H₂S gas mixture showed an initial breakthrough 58 days after initiation of the injection. The double peak of the tracer breakthrough curves is consistent with the pre-injection tracer test results (Rezvani Khalilabad et al., 2008), suggesting a homogeneous porous media that is intersected by a low-volume but fast flow fracture. Mass balance calculations for CarbFix1 using the carbon/conservative tracer ratios and the ¹⁴C/conservative tracer ratios indicated >95% loss of the dissolved CO₂ via mineralization along the subsurface flow path from the injection to the monitoring well within 2 years (Figure 2; Matter et al., 2016). This was confirmed by corresponding mass balance calculations of dissolved Ca, Mg, Fe, and Si in the monitoring well

fluids, mineral saturation states, as well as direct evidence of precipitated carbonate minerals (Snæbjörnsdóttir et al., 2017). Measured Ca, Mg, and Fe concentrations showed an initial increase during the injections with a gradual decline in the following months, which is consistent with the initial release of these elements from the basalt and their subsequent precipitation as carbonate minerals (Snæbjörnsdóttir et al., 2017).

A similar mass balance approach to determine the mass of CO₂ and H₂S fixed in the subsurface via mineralization was applied in CarbFix2. CarbFix2 researchers observed a faster mineralization rate compared to CarbFix1, where >50% of injected CO₂ and 76% of sulfur were mineralized within just 4 to 9 months of Phase 1 (Clark et al., 2020). Furthermore, a twofold increase in the gas injection rate in CarbFix2 Phase 2, resulted in an increase in the mineralization to >60% for carbon and >85% for sulfur within 4 months (Clark et al., 2020). These calculations were based on the comparison of measured dissolved carbon and sulfur concentrations in the monitoring well fluids, with corresponding values determined by mass balance calculations based on conservative mixing (Gunnarsson et al., 2018). The enhanced rate of CO₂ mineralization at CarbFix2 is suspected to be due to accelerated mineralization reactions at higher temperature, increased acidity of the injection fluids, and occurrence of fewer secondary minerals reaching supersaturation at the conditions of the injection zone (Clark et al., 2018).

2.2.4. Next Steps

CarbFix1 and CarbFix2 successfully demonstrated subsurface mineralization of CO₂ in basalt and created a new rapid methodology for the secure and permanent storage of CO₂ through mineralization. Since the beginning of CarbFix1 in 2007, CarbFix as a subsidiary company of Reykjavik Energy further developed and upscaled this method, injecting >97,000 tons of CO₂ into the subsurface at the CarbFix2 injection site. It is estimated that the porous basaltic rocks in Iceland can store ~250 Gt of carbon as calcite (Gunnarsson et al., 2018). Additional upscaling of this methodology is, therefore, needed to accelerate mineralization as a global solution. For example, 1 million metric tons per year (a typical target of conventional sequestration) would require upscaling by a factor of about 100. Laboratory experiments using field samples to obtain critical reaction rates and thermodynamic data, and simulations aimed at optimizing CO₂ mineralization processes in basalt, will help gain a more comprehensive understanding of the coupled subsurface processes. A possible limitation of the CarbFix project is its reliance on large quantities of freshwater, which makes significant upscaling challenging (only 5% of the injected mass at CarbFix was CO₂; Gislason & Oelkers, 2014). The next planned steps for CarbFix are to address this issue by testing the feasibility of dissolving CO₂ into seawater, which is readily available at the site, before injection. Furthermore, researchers at CarbFix are working on combining direct air capture technologies with subsurface mineralization (Snæbjörnsdóttir et al., 2020).

2.3. The Wallula Basalt Pilot Demonstration Project

2.3.1. Site Description

The Wallula Basalt Sequestration pilot project was carried out in the southeastern region of Washington, USA, approximately 12 miles southeast of Pasco. Geologically, the site is hosted in the Miocene Columbia Plateau Province, a world-class set of continental flood basalt deposits, with an estimated volume of more than 220,000 km³, covering over 320,000 km² of Western Idaho, Oregon, and Washington (Reidel et al., 2002). In 2009, a borehole was drilled to a depth of 1,252 m, during which extensive surveys and hydrogeologic characterization of the flood basalts were carried out. A candidate injection zone was selected within the Grande Ronde Basalt lava flows, which is comprised of three permeable brecciated interflow zones (828–887 m) capped by an extremely low permeability member ($\sim 10^{-12}$ to 10^{-13} m/s), which acts as a natural cap rock (McGrail et al., 2014). The mineralogy within these flows is, in order of abundance, plagioclase, augite, and volcanic glass, with secondary hematite, pyrite, zeolites, and clay minerals (Caprarelli & Reidel, 2004; McGrail, Sullivan, et al., 2009; Zakharova et al., 2012). Well cuttings indicated that the primary minerals filling vesicles, fractures, and veins are calcite and quartz (McGrail et al., 2011). The groundwater within the injection zone is classified as brackish, non-potable, and sulfate-rich, with elevated concentrations of fluoride (McGrail et al., 2011). Natural tectonic fractures are abundant in the borehole and are identified easily in image logs by their high dip sinusoidal features, which represent their primary depositional surfaces, as shown in Figure 3 (McGrail, Sullivan, et al., 2009). Other fractures are commonly in the form of cooling joints and short, irregular fractures that are

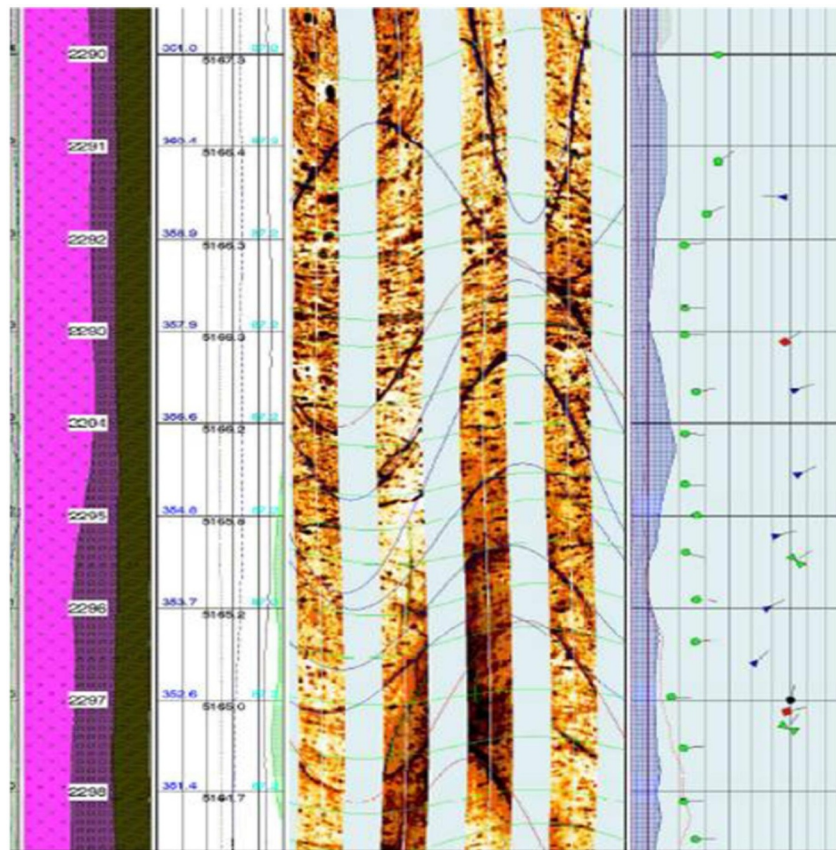


Figure 3. Fractures can be the primary flow paths for the passage and distribution of CO₂ (dissolved or supercritical) within mafic and ultramafic rocks. This figure shows an image log depicting the natural tectonic fractures that appear as sinusoidal features within the Wallula Pilot Borehole. The green sinusoidal lines are interpreted as the flow features of the basalt. Characterization of the fracture network using tools such as image logs is an essential step in determining the storage potential of a reservoir. Image from McGrail, Schaef, et al. (2009).

perceived as impermeable (McGrail, Sullivan, et al., 2009). The pre-injection reservoir conditions were ~36°C and 7.7 MPa (McGrail, Schaef, Spane, Cliff, et al., 2017; McGrail, Schaef, Spane, Horner, et al., 2017).

2.3.2. CO₂ Injection and Post-Injection Operations

In 2013, nearly one thousand metric tons (MT) of pure liquid CO₂ was injected into the Grande Ronde Basalt flows over 25 days, averaging at a rate of ~40 MT/day (McGrail, Schaef, Spane, Cliff, et al., 2017; McGrail, Schaef, Spane, Horner, et al., 2017). This carbon mineralization field demonstration was the first to inject CO₂ as a supercritical fluid into continental flood basalts, eliminating the need to dissolve CO₂ into large quantities of fresh water, as was done at CarbFix. To evaluate the extent to which the mineralization proceeded within the injection site, a suite of characterization techniques was used. Following the injection period until 2015, discrete groundwater samples were collected systematically at variable depths within the borehole for geochemical analyses (major cations, alkalinity, total dissolved solids (TDS)) to compare with pre-injection concentrations (McGrail, Schaef, Spane, Cliff, et al., 2017; McGrail, Schaef, Spane, Horner, et al., 2017). Post-injection wireline geophysical surveys and hydrologic tests were carried out to determine the extent, nature, and spatial distribution of CO₂ within the reservoir and to assess changes in the hydrologic characteristics (McGrail, Schaef, Spane, Cliff, et al., 2017; McGrail, Schaef, Spane, Horner, et al., 2017). Before decommissioning the site in 2015, more than 50 side-wall cores were collected from within the injection zone and subjected to detailed geochemical and geophysical analyses and 3D imaging to identify carbonates that precipitated from the injected CO₂ (Polites et al., 2022).

2.3.3. Key Observations

The collective results from the Wallula Basalt Pilot Project offer compelling evidence for the effectiveness of CO₂ mineralization in continental flood basalts. Concentrations of major cations (e.g., Ca and Mg), alkalinity, and TDS measured in groundwater samples increased by 1.5–3 orders of magnitude from their pre-injection formation concentrations, indicating the dissolution of CO₂ into the groundwater and its reaction with the basalt's ferromagnesian minerals (McGrail, Schaef, Spane, Cliff, et al., 2017; McGrail, Schaef, Spane, Horner, et al., 2017). Geochemical calculations using the post-injection groundwater data at reservoir conditions determined that the groundwater was supersaturated with respect to carbonate minerals such as calcite and dolomite (McGrail, Schaef, Spane, Cliff, et al., 2017; McGrail, Schaef, Spane, Horner, et al., 2017). Wireline logging characterization, including residual saturation and fluid temperature survey logging, identified highly electrically resistive free-phase supercritical CO₂ (scCO₂) within the injection zone, which was not present prior to injection. It was estimated that 75%–90% of the pore water was replaced by CO₂ in the middle layer, while ~40% of the pore water was replaced in the bottom layer of the injection zone (McGrail, Schaef, Spane, Cliff, et al., 2017; McGrail, Schaef, Spane, Horner, et al., 2017). Simulations to determine the distribution of the CO₂ within the formation yielded similar results (S. K. White et al., 2020).

While difficult to determine how CO₂ was trapped within the injection zone at the time of sampling, the examination of sidewall cores identified two distinct carbonate phases that are interpreted to be formed from the injection, suggesting that some of the injected CO₂ has already been mineralized (McGrail, Schaef, Spane, Cliff, et al., 2017; McGrail, Schaef, Spane, Horner, et al., 2017; Polites et al., 2022). The carbonate phases occurred as large nodules within the basalt vesicles and carbonate cements thinly coating the borehole wall face (McGrail, Schaef, Spane, Cliff, et al., 2017; McGrail, Schaef, Spane, Horner, et al., 2017). Analysis of the precipitates, including X-ray diffraction, X-ray microtomography (XMT), scanning electron microscopy, and energy dispersive X-ray spectroscopy were carried out, and identified the carbonate nodules as the mineral ankerite, a Ca- and Fe-rich carbonate mineral [Ca(Fe,Mg,Mn)(CO₃)₂]. These nodules were found to be chemically zoned, with a Ca-rich phase near the center and a Fe-rich phase at the surface (McGrail, Schaef, Spane, Cliff, et al., 2017; McGrail, Schaef, Spane, Horner, et al., 2017), with a minor zonation in Mn decreasing toward the surface (Polites et al., 2022). The zonation within the nodules is suspected to be due to temporary changes in the formation water's geochemistry (oxygen fugacity) due to CO₂ injection, prior to its buffering by the surrounding basaltic rock. These findings are distinct from analyses on naturally occurring calcite veins within the sidewall, which had no trends in major cations (McGrail, Schaef, Spane, Cliff, et al., 2017; McGrail, Schaef, Spane, Horner, et al., 2017). Selected samples were thin-sectioned for a more thorough investigation of the mineralogy and spatial and paragenetic relationship of the minerals (Polites et al., 2022). A fibrous texture was observed within the nodules, suggesting that the ankerite phase was a result of the pseudomorphic transformation of aragonite due to increased Mn²⁺ and Fe²⁺ (Polites et al., 2022).

Comparative isotopic characterization of the post-injection ankerite nodules, post-injection groundwater samples, preexisting natural calcite veins, and the injected CO₂ offers the most convincing evidence of CO₂ mineralization within the Columbia River basalt formation as a result of the pilot test. Using nano secondary ion mass spectrometry (nanoSIMS) to measure delta oxygen-18 (δ¹⁸O) and delta carbon-13 (δ¹³C) concentrations (McGrail, Schaef, Spane, Cliff, et al., 2017; McGrail, Schaef, Spane, Horner, et al., 2017), the measured values for the ankerite nodules (δ¹³C = −37.7 ± 2.19‰, δ¹⁸O = −22.5 ± 2.38‰), post-injection formation water (δ¹³C = −32.2 ± 0.79‰, δ¹⁸O = −22.3 ± 1.53‰), and CO₂ (δ¹³C = −36.3 ± 0.09‰, δ¹⁸O = −27.9 ± 0.51) indicate a common source, distinct from the natural calcite values (δ¹³C = 15.8 ± 1.01‰, δ¹⁸O = −20.0 ± 0.41) (McGrail, Schaef, Spane, Cliff, et al., 2017; McGrail, Schaef, Spane, Horner, et al., 2017). Based on the data derived from the multitude of tests, numerical modeling estimates that ~60% of the supercritical CO₂ was mineralized during the first two years following injection, with the carbonate precipitation encompassing ~4% of the reservoir's available pore space (S. K. White et al., 2020). Based on these calculations, the total mineral trapping capacity of the Grande Ronde Basalt is estimated at 47 kg of CO₂/m³ (Xiong et al., 2018). Assuming the carbonation rate were to remain constant, and the pore pressure was fixed at ~4%, it would, thus, take 38 years to fill the pore space in the Grande Ronde Basalt at 100°C (Xiong et al., 2018).

2.3.4. Role of Fractures

Conclusions specific to the spatial distribution of the CO₂ mineralization within the fracture network of the Wallula basalt injection zone are absent from the literature. Aside from the initial fracture characterization within

the borehole, the orientation of the fracture network within the basalt is not defined. Therefore, it is difficult to assess the role of fractures in the distribution and reaction of CO₂ within the reservoir. Furthermore, Columbia River basalt flows are highly heterogeneous and generally consist of dense flow interiors sandwiched by irregular, brecciated, and vesicular flow tops and bottoms (Burns et al., 2015). Therefore, fractures will not be the only source of fluid flow and storage volume. Nevertheless, models can shed light on the mineralization potential of a system, as exemplified in a recent simulation study, which used ensemble simulation methods to predict the geomechanical integrity of the Wallula Basalt Project reservoir (Jayne et al., 2019). This study provides a first order estimate for the potential evolution of the permeability of the reservoir during CO₂ injection at a large scale. The authors simulated the injection of CO₂ into the reservoir at a constant mass of 21.6 kg/s and variable permeability distributions. Notably, they determined that the pressure build-up near the injection site due to CO₂ injection geomechanically impacts a significantly larger radius than the injection fluid itself (Jayne et al., 2019). This pressure build-up could result in shear slip of pre-existing fractures, which can ultimately increase the total permeability of the reservoir (Jayne et al., 2019). It should be noted that this model does not consider geochemical reactions, where dissolution and precipitation could alter the aperture of the fractures. Given the heterogeneous nature of basalt reservoirs, extensive characterization is necessary to provide an accurate understanding of the storage potential and the evolution of the fracture network as CO₂ is injected and mineralized. Moreover, it is important to understand how the injection of scCO₂ versus CO₂ dissolved in water will influence the reactivity and storage potential of a fractured reservoir. Ultimately, future research should emphasize the geomechanical evolution of the reservoir, in addition to changes in the geochemistry.

2.4. Subsurface Mineralization in Peridotite—Oman Drilling Project

Peridotite is a major component of the Earth's upper mantle and is exposed at the earth's surface as ophiolite massifs, of which the largest is the Oman ophiolite in Oman and the United Arab Emirates (e.g., Kelemen & Matter, 2008). Peridotite is mainly composed of the primary minerals olivine, pyroxene, and spinel, which are commonly partially or completely altered to mixtures of serpentine, brucite, Fe-oxides, and oxyhydroxides by water-rock reactions (e.g., Kelemen et al., 2019). Extensive natural CO₂ mineralization has been observed in peridotite, with predicted rates on the order of 1,000 t CO₂/km³/yr (Kelemen et al., 2011; Mervine et al., 2014). At Oman, 5,000 tons of carbonate is estimated to form within the Oman peridotite each year (Kelemen et al., 2011; Kelemen & Matter, 2008). Listvenites—fully carbonated peridotites—are exposed at the surface of the Oman ophiolite, having formed ~90 million years ago at temperatures of ~80–130°C, depths of 10–50 km, and under elevated pressure ($P_{\text{CO}_2} \sim 1\text{--}5$ bars) (Beinlich et al., 2020; Falk & Kelemen, 2015; Kelemen, Matter, et al., 2020; Kelemen, McQueen, et al., 2020). These listvenites offer a natural analog to present-day carbon mineralization and insight into the capacity of these rocks to store CO₂.

The Oman Drilling Project (OmanDP), an International Continental Scientific Drilling Program (ICDP) project, was established to improve our quantitative understanding of processes of mass and energy transfer between the mantle, crust, hydrosphere, atmosphere, and biosphere. The project drilled a cross-section through the Oman ophiolite from 2016 to 2019, where a total of 5,400 m (15 boreholes) were drilled and 3,220 m of core collected. Included in this project was the establishment of the Multi-Borehole Observatory (MBO) to investigate the geochemical, hydrological, and geomechanical alteration of partially serpentinized peridotite and study active low-temperature alteration processes, including carbon mineralization. In contrast to the CarbFix and Wallula projects, CO₂ mineralization studies in Oman are still in their early stages. Nonetheless, a suite of fracture and geochemical parameters have been collected as an initial stage for reservoir characterization, as described below.

2.4.1. MBO

The OmanDP MBO in the Wadi Tayin massi of the Oman ophiolite, SE of the capital Muscat, includes four air-rotary-drilled boreholes and three diamond-cored boreholes. The total depth of the boreholes ranges from 300 to 400 m (Kelemen, Matter, et al., 2020; Kelemen, McQueen, et al., 2020). The boreholes penetrate two major rock sequences: fully serpentinized dunites with pyroxenite dikes and 80%–100% serpentinized harzburgite with gabbro (Kelemen, Matter, et al., 2020; Kelemen, McQueen, et al., 2020). The boreholes and rock sequences were fully characterized using wireline geophysical logging and hydrogeological testing to investigate the natural carbonation process.

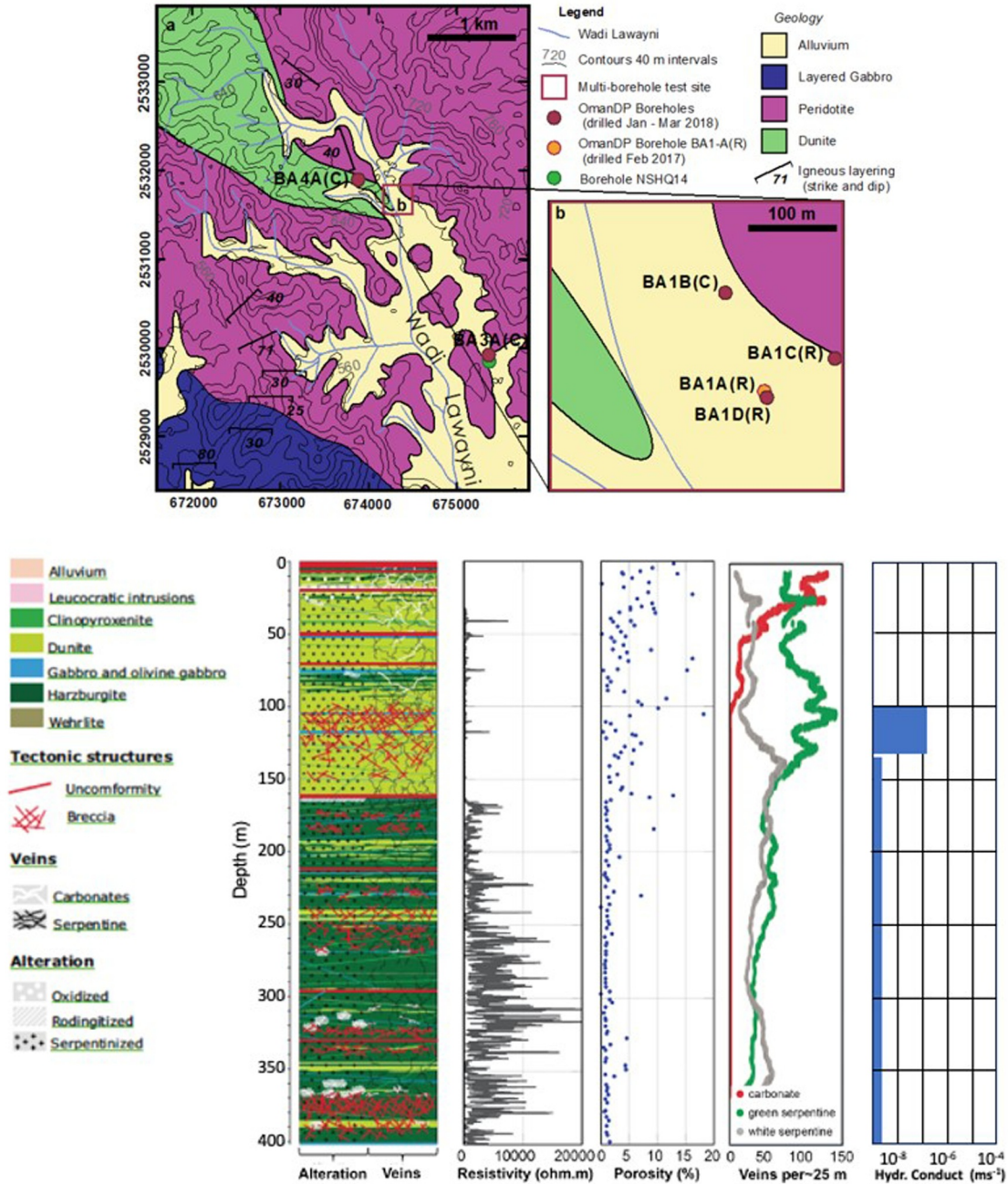


Figure 4. Geophysical borehole and core logs from the Oman Drilling Project reveal a pervasive fracture and vein network. Data collected from borehole BA1B (as shown on the map) includes a lithostratigraphy log (OmanDP Multi-Borehole Observatory), wireline borehole resistivity log, and downhole plots of discrete sample measurements of porosity and vein types (25-m average; Kelemen, Matter, et al., 2020; Kelemen, McQueen, et al., 2020) as well as a summary of the estimated hydraulic conductivity of discrete intervals based on pumping tests (Lods et al., 2020). The data shows that the permeability decreases with depth, relating to a decrease in alteration and crack/vein density (Kelemen et al., 2021).

2.4.2. Key Findings

Geophysical borehole and core logs reveal a pervasive fracture and vein network, primarily filled with secondary minerals, and a rock matrix with micro to nanopores (Kelemen, Matter, et al., 2020; Kelemen, McQueen, et al., 2020). The serpentinized dunite sequence has higher porosity, higher fracture density, and lower electrical resistivity than the serpentinized harzburgite sequence (Figure 4). Permeability decreases with depth and ranges from 10^{-12} m^2 at $<50 \text{ m}$ to $<10^{-14} \text{ m}^2$ at $<150 \text{ m}$, and $<10^{-17} \text{ m}^2$ below 150 m depth (Lods et al., 2020).

Decreasing permeability with increasing depth correlates with decreasing alteration and decreasing crack/vein density (Kelemen et al., 2021). Decreasing permeability also correlates with the type of groundwater that is present in the peridotite. A Mg-HCO₃, pH ~ 8 oxidized groundwater occurs in the highly weathered and higher permeability zone near the surface, whereas a Ca-OH-rich, pH > 11 and highly reduced groundwater is found at a greater depth, thought to be associated with more extensive and deeper interaction between peridotite and groundwater and a reduction of Mg and CO₂ due to the mineralization of carbonate minerals and serpentine (Kelemen et al., 2021). Borehole flowmeter logs and multi-level cross-hole hydraulic experiments show that complex vertical and horizontal structural heterogeneities govern fluid flow (Lods et al., 2020). However, fluid pathways in the fracture network and their interconnectivity are poorly characterized and understood.

The present-day carbonation of peridotite is driven by near-surface weathering, as indicated by the rapidly decreasing occurrence of Ca- and Mg-carbonate-filled veins with depth. No carbonate veins were found in the MBO cores below 100 m (Kelemen et al., 2021). This agrees with the proposed reaction path of infiltrating surface water and descending shallow groundwater through the upper, high-permeability aquifer with progressive interaction with peridotite along the flow paths (Dewandel et al., 2005; Paukert et al., 2012). This implies that the deeper subsurface has a greater CO₂ mineralization potential that could be utilized for engineered carbon mineralization. Indeed, the injection of CO₂-rich fluids into peridotite at depth below the weathering horizon could enable CO₂ mineralization, potentially storing 10⁵ to 10⁸ GtCO₂ (Kelemen & Matter, 2008). However, new data from the MBO site reveals that injectivity into the deeper subsurface is greatly limited by the low permeability of the peridotite. Thus, engineered carbon mineralization in peridotite will most likely require permeability enhancement via industrial hydraulic fracturing or naturally induced subcritical fracturing and reaction-driven cracking/damage due to mineralization. The latter depends on the increase in differential stress in the rock by the solid-volume increasing carbonation reaction, resulting in the generation of fractures and subsequent increase in the rock's permeability and reactive surface area (See Section 3; e.g., Jamtveit et al., 2008; Kelemen & Hirth, 2012; Uno et al., 2022; W. Zhu et al., 2016).

2.4.3. Next Steps

Experiments at different length scales from mineral grain to field scale are required to better understand the coupled thermo-hydro-mechanical-chemical (THMC) processes in fracture-dominated systems, such as peridotite (as discussed in the next section) (Plümpner & Matter, 2023). Like the CarbFix project, the technology start-up 44.01, in collaboration with industrial and academic partners, started multiple research-to-application initiatives to demonstrate the feasibility of carbon mineralization in peridotite (www.4401.earth). Project Chalk was established to test CO₂ mineralization in peridotite at the MBO site in Oman. Utilizing MBO boreholes, several hundred kilograms of CO₂ dissolved in water have been injected and the progress of mineralization is being monitored. In addition, a mineralization pilot test site in Fujairah (UAE) successfully injected 10 tonnes of air-captured CO₂ into peridotite in 2023, with plans to scale up this operation to 300 tonnes soon (www.4401.earth).

2.5. Challenges With Industrial-Scale Carbon Mineralization

Field experiments, such as the CarbFix, Wallula, and Oman projects, have successfully demonstrated the feasibility of in-situ mineral carbonation in mafic and ultramafic rocks. For mineralization to be a global solution, significant upscaling and acceleration of the deployment of mineralization field sites are needed. This will require maximizing CO₂ injection rates per borehole, sustaining long-term injection and fluid flow rates in the storage reservoir, and maximizing dissolution and carbonate precipitation rates. Challenges remain from the pilot projects, as in many cases detailed hydrological, chemical, and mechanical parameters cannot be derived from field observations. Outstanding questions include: (a) how to minimize the requirement of large volumes of fresh water for dissolved CO₂ injection; (b) the feasibility of supercritical CO₂ injection, which will require a caprock and perhaps longer retention times in the reservoir to fully mineralize the injected CO₂; (c) constraining the timescales of the different processes, including mineral dissolution and precipitation rates; and (d) defining reactive surface area, reactions and rates of reaction in fractures (advection-dominated) and in pores & matrix (diffusion-dominated). In addition to field characterization data, laboratory experiments, discussed in the next section, will be critical for addressing these outstanding questions, and deriving important parameters required for modeling CO₂ mineralization.

3. Experimental Studies on Carbon Mineralization in Fractured Systems

3.1. Introduction

Observations derived from pilot-scale carbon mineralization field tests delineate important knowledge gaps that can be better understood through controlled laboratory experiments. These knowledge gaps center on the overarching question of the scalability and feasibility of large-scale CO₂ mineralization in mafic and ultramafic rocks, which requires an understanding of reaction rates, feedbacks between geochemical and geomechanical reactions, and the influence of flow and transport, among other factors. Recent advances in experimental capabilities, such as high pressure (P)/temperature (T) systems, coupled stress, flow and reaction in geomaterials, and in situ imaging capabilities, have aided in the derivation of parameters needed to model mineralization processes and field site development. In this review, we highlight four key areas of laboratory research that are centered on bridging these knowledge gaps: (a) reactivity of mafic minerals in CO₂-rich environments (Section 3.2), (b) the dynamic interaction between fluid flow and chemical reactions in fractures (Section 3.3), (c) the coupling between fluid flow and mechanics for stimulation (Section 3.4), and (d) the coupled feedback between chemical reactions and the development of fractures (Section 3.5).

Reactivity of the minerals: CO₂ mineralization in mafic and ultramafic rocks is induced by the injection of CO₂ or CO₂-charged water, dissolution of key divalent cation-bearing minerals (olivine, pyroxene, serpentine, plagioclase, volcanic glass), and the precipitation of a variety of carbonates including magnesite (MgCO₃), calcite (CaCO₃), siderite (FeCO₃), and ankerite (Ca(Mg,Fe) (CO₃)₂) (Romanov et al., 2015). These reactions occur in an acidic aqueous medium produced by high-pressure CO₂, where the pH is controlled to first order by equilibrium between CO₂ and the precipitating carbonates. The extent of carbonation is controlled by the dissolution rates, precipitation rates, and the available surface area (Romanov et al., 2015), which are governed by many factors including hydrodynamic effects, fracture characteristics, surface passivation, and reservoir geochemistry.

Fluid flow and chemical reactions in fractures: A major challenge in optimizing in situ carbon mineralization arises from the fact that the process depends not only on the mineral distribution and geochemistry, but also on the structural properties of the fractures, and the rock matrix (aperture, reactive surface area, porosity), fluid flow conditions (flow rate), and fluid properties (density, viscosity) (Deng, Molins, et al., 2018; Deng, Steefel, et al., 2018; S. Li et al., 2007). Furthermore, dissolution and precipitation reactions can simultaneously create or destroy permeable paths of fluid flow, which are often dominated by complex fracture networks in mafic and ultramafic rocks (Jiménez-Martínez et al., 2020; Luquot & Gouze, 2009; Noiriél & Soulaire, 2021; Noiriél et al., 2013; H. Yoon et al., 2019). This fluid flow is required for the dissolution of a rock matrix and delivery of chemical species (CO₂, cations) needed to mineralize carbon; however, those mineralization products can also clog flow paths. These interconnected feedbacks demonstrate how CO₂-fluid-rock reactions under fluid flow are highly nonlinear and dynamic.

Fluid flow and mechanics for stimulation: Permeability enhancement, such as hydraulic fracturing and hydro-shearing, may be needed to artificially stimulate fracture growth in mafic and ultramafic rocks for sustained, extensive CO₂ mineralization. Two primary methods of permeability enhancement in deep subsurface rocks include hydraulic fracturing, which requires fast-rate fluid injection to create new fractures, and hydro-shearing, which involves moderate-rate fluid injection to reactivate pre-existing geological discontinuities. Both hydraulic fracturing and hydro-shearing have been extensively studied in hydrocarbon-bearing sedimentary rocks (Bunger et al., 2005; Detournay, 2016; Fisher & Warpinski, 2012; W. Li et al., 2021) and geothermal rocks (Meng et al., 2022; Rinaldi & Rutqvist, 2019; Yuan et al., 2020), but rarely in CO₂-reactive mafic and ultramafic rocks (Nicolas & Jackson, 1982).

Coupled feedback of chemical reactions and fracture development: Efficient carbonation of basalt and peridotite requires widespread porosity and/or an extensive fracture network through which the injected CO₂ can flow and react with the host rock. Basalt formations naturally contain more porosity and fractures than peridotite due to porous inter-flow regions and thermally fractured flow boundaries (McGrail et al., 2006). However, carbonating a large mass of impermeable basalt in flow centers or impermeable peridotite with a porosity of about 1% (Kelemen et al., 2011) requires some form of anthropogenically- or tectonically-induced fracturing. It is possible that mineral carbonation itself may provide the means to access more reactive surfaces, either through reaction-driven fracturing or subcritical fracturing. These dynamics must be better understood to determine the long-term feasibility of carbon storage in mafic and ultramafic rock.

Whether experimental observations hold in the field (Section 3.6) is of critical importance for furthering field site testing and providing realistic parameters for modeling studies. Although experiments cannot inform large-scale processes, they play an important role in constraining kinetic rates, thermodynamic data, and small-scale fracture properties. While carbonation beyond a fracture surface has been shown to occur in nature (Kelemen et al., 2011), as discussed in previous sections, it is critical to demonstrate that this process can be engineered for large-scale, long-term anthropogenic CO₂ mineralization operations. Here we review the experimental evidence that can provide insight into the key processes that occurred (and cannot be directly observed) during the CO₂ mineralization operations discussed above. Findings from these studies, such as mechanisms and timescales, are critical to constrain models (as discussed in the next section) and provide insights that will aid in optimizing anthropogenic CO₂ injection into mafic and ultramafic rocks.

3.2. Reactivity of Mafic Minerals

Field-scale carbonation efficiency is in large part defined by the individual reactivities of constituent rocks and minerals toward carbon mineralization, which are typically determined using batch experimental studies. The work of Gadikota et al. (2020) measured the reactivity of common mafic minerals and rocks in NaCl- and NaHCO₃-bearing solutions including Mg-rich olivine, labradorite plagioclase, and basalt, and found that the extents of carbonation were 85%, 35%, and 9%, respectively, under optimized conditions. This finding has important implications for assessing the relative advantages of peridotite and basalt: peridotites are rich in olivine, which has the most favorable carbonation kinetics; and basalts are rich in labradorite plagioclase with less favorable kinetics and the additional potential to leave greater residual barriers (clay) to continued carbonation.

The overall extent of mineralization will depend on (a) the dissolution of mafic minerals, which promotes the release of divalent cations and (b) the rate of carbonate mineral precipitation. Dissolution is thus an essential first step in the mineralization process. Of the possible reactant minerals, the dissolution rate of olivine has received extensive consideration due to its higher reactivity (Oelkers et al., 2018; Rashid et al., 2022). The review of Oelkers et al. (2018) concluded that the primary factors that control olivine dissolution rates are temperature, pH, water activity, and surface area. In addition, the degree of serpentinization of olivine is also expected to affect the rates (Klein & Garrido, 2011; Klein & McCollom, 2013). The dissolution rates of other key minerals such as plagioclase (De Obeso et al., 2023; Gudbrandsson et al., 2014; Min et al., 2015), pyroxene (Golubev et al., 2005; Knauss et al., 1993), and serpentine (Thom et al., 2013) are also reported in the literature and summarized in Kelemen et al. (2019). However, the dissolution rates for olivine and other mafic minerals vary significantly among experimental studies (Oelkers et al., 2018), and thus, further research is required to more tightly constrain realistic dissolution rates.

In contrast to dissolution rates, few experimental efforts to constrain precipitation rates have been conducted. There is a framework for calculating rates of precipitation by extrapolating dissolution data (transition-state-theory; e.g., Lasaga, 1981). However, many experiments show precipitation rates that are a complex function of supersaturation and pH conditions, with particular sensitivity to other solution components (Shiraki & Brantley, 1995; Teng et al., 2000; Y. Zhang & Dawe, 2000). Furthermore, while calcite precipitation is relatively well understood (Dreybrodt et al., 1997; Inskeep & Bloom, 1985; Y. Zhang & Dawe, 2000), magnesite precipitation is more complicated, with different controls and greater kinetic barriers (Giammar et al., 2005; Hellevang et al., 2013), usually attributed to freeing magnesium ions from a strong hydration shell (Power et al., 2017). Giammar et al. (2005) determined that supersaturation indices of 0.25–1.14 were required to induce magnesite precipitation and growth. Moreover, experimental studies have shown that the rate of magnesite precipitation from olivine dissolution is quite slow at temperatures $\leq 90^{\circ}\text{C}$ (Gadikota et al., 2014), and that magnesite is unlikely to form at temperatures $\leq 75^{\circ}\text{C}$ (Oelkers et al., 2018). The surface area on which precipitation may occur is even more poorly constrained, as precipitation on solid surfaces (heterogeneously), in solution (homogeneously), and/or only on particular faces of certain crystals are all possible options. Therefore, case-specific measurements of precipitation rates are needed at various conditions relevant to reservoirs proposed for CO₂ storage. At this time, there is not a well-accepted kinetic model that predicts the rate of magnesite or other carbonate precipitation from olivine or other mafic minerals.

As previously mentioned, when comparing the carbonation potential of peridotites and basalts, it is important to consider the overall geochemical makeup. Peridotites are composed of more than 90% Mg compared to Ca and Fe (Kelemen et al., 2011), while basalts contain subequal amounts of Mg, Ca, and Fe, generally with $\text{Fe} > \text{Ca} > \text{Mg}$

(Schaefer et al., 2009). Experiments by Schaefer et al. (2009) demonstrated that carbonate precipitation in basalt had complex zonation that generally varied from dominantly Ca-rich to Fe-rich, with less than 20% Mg. This suggests that the carbonation of basalt does not suffer from the same kinetic limitations of magnesite precipitation, as seen in peridotite, thanks to the presence of Ca and Fe as alternative divalent cation reactants. While these findings may appear contradictory to those of Gadikota et al. (2020), which showed that the extent of carbonation of olivine was significantly greater than that of basalt, the basalt reactivity experiments in Schaefer et al. (2009) were conducted at lower temperatures and CO₂ pressures (60–100 °C, 10.34 MPa CO₂). Additional comprehensive studies comparing the mineralization potential of basalt versus peridotite at lower temperatures are needed to determine whether high-temperature trends hold. Other factors contributing to the reactivity differences between these two rocks include the potential for higher divalent cation concentrations in peridotite due to its high olivine content and the generally higher porosity and permeability of basalt, which may aid in more widespread mineralization under fluid flow conditions.

Despite variable results of laboratory-based dissolution measurements, the principal uncertainty in the field is likely to be the available surface area where the chemical reactions take place. For a fracture system in an impermeable rock, a conservative assumption would be the geometric fracture surface area. However, Van Noort et al. (2013) provided experimental evidence to suggest that the effective reactive surface area could be 100 times greater than the geometric fracture surface due to grain-scale structure, even in nominally impermeable peridotite. Whether this apparent surface area would persist as the reaction front penetrates deeper into the peridotite is unknown. Nonetheless, compared with the mass of the bulk rock and considering reaction rates determined on fine-grained powders, this is a relatively small surface area that will limit the net production of divalent cations needed for carbonation.

Even with the uncertainties in dissolution and precipitation rates, basalts and peridotites possess enormous theoretical carbonation capacities (Matter & Kelemen, 2009; McGrail et al., 2006). As discussed, batch experimental studies of dissolution and precipitation show that reaction rates are relatively slow, meaning that uncertainty in kinetic data plays a significant role in constraining the timescale of mineralizing CO₂ in basalt and peridotite sequestration projects. Further experimental studies must be designed to better constrain rates and extents of carbonation of whole rock samples. In the following two sections, we examine our current understanding of the potential role of coupled processes in accelerating mineralization, including the coupling of fluid flow and reaction and the coupling of flow, reaction, and mechanical processes as important considerations in mineralization efficiency.

3.3. Coupling Between Fluid Flow and CO₂ Mineralization Reactions

For successful prediction and optimization of mineralization, it is necessary to identify the key regimes of coupled dissolution and precipitation behavior as a function of the main parameters of geochemistry, flow, and rock structure. Carefully designed laboratory experiments play an essential role in understanding mineralization because they allow for the isolation of key processes of interest and enable the detailed characterization of rocks undergoing carbonation.

Experimental studies have elucidated important interface-coupled dissolution and precipitation processes that are relevant to carbon mineralization (Cubillas et al., 2005; Raza et al., 2022; Ruiz-Agudo et al., 2014). Multiple coupled dissolution and precipitation regimes exist: at one extreme is surface passivation, where mineral precipitation results in coatings that limit reactive surface area and inhibit reactions, while at the other extreme, complete mineralization occurs, resulting from net increases in porosity and sustained reaction (Forjanés et al., 2020). A main challenge, however, is that most studies are conducted under well-mixed batch conditions (Løge et al., 2023; Xiong & Giammar, 2014; Xiong, Wells, Menefee, et al., 2017), with limited studies that honor realistic fluid flow conditions (Baek et al., 2019; Menefee et al., 2017, 2018). It is well established that hydrodynamic conditions strongly impact reaction kinetics and dissolution and precipitation patterns (Arvidson et al., 2003; Colombani, 2008; Osselin et al., 2016; Qin & Beckingham, 2021; Yang et al., 2024), but there remain open questions on how best to utilize the parameters derived from batch experiments in carbon mineralization. In geologic fractured porous media systems, variations in reaction rates and reactive surface areas lead to highly heterogeneous dissolution and precipitation patterns and mineralization rates that are significantly different from batch conditions (L. Li et al., 2008; M. Liu et al., 2022). For example, studies of dissolution under flow have demonstrated how the relative rates of reaction and transport, codified by the Damköhler number, dramatically

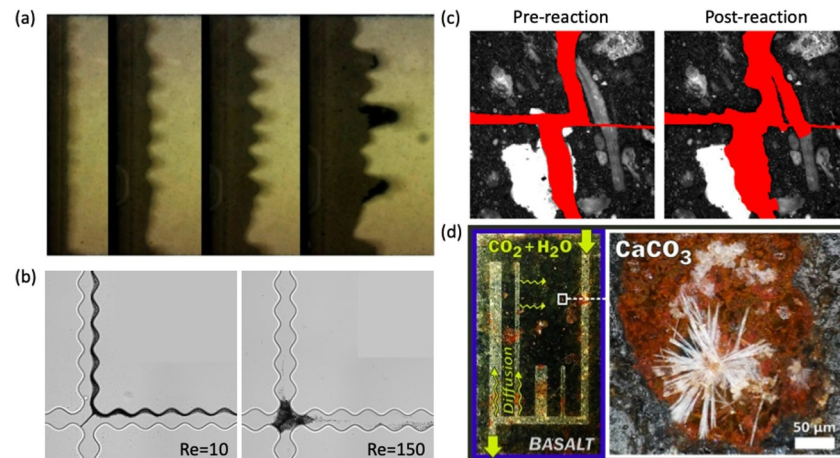


Figure 5. Laboratory experiments can help visualize fluid flow and reaction and identify key processes that govern carbon mineralization. Some recent examples include: (a) Investigating reactive-infiltration instability to understand advection, diffusion, and reaction in an analog fracture. The direction of water infiltration into gypsum chips is from the left to right. The dissolved portion of the chip is indicated by a dark color, while the undissolved portion is shown in a light color (Osselein et al., 2016). (b) Visualization of fluid inertia effects on mineral precipitation patterns in microfluidics experiments. Barium and sulfate solutions are co-injected into the intersection, where they are subsequently mixed and precipitates are formed. The barite precipitates are indicated in black (Yang et al., 2024). (c) Characterizing mineral mechanistic processes during the dissolution of natural rock samples embedded in microfluidic cells. The fracture space is indicated in red, while the surrounding rocks are depicted in black and white (Ling et al., 2022). (d) Understanding how temperature, chemistry, and transport limitations affect mineral dissolution and precipitation in flow-through rock core experiments. Carbonation occurs within the diffusion-limited zone when CO₂-charged water is injected into a fractured basalt rock sample (Menefee et al., 2018).

alter spatiotemporal trends of dissolution and effective dissolution rates (Fredd & Fogler, 1998; Golfier et al., 2002). These trends should also manifest in coupled dissolution-precipitation systems. As a result, we cannot currently predict CO₂ mineralization rates under relevant flow conditions.

Recent laboratory core flow studies conducted under reservoir pressures and temperatures have provided valuable insights into the interplay of flow, transport, and geochemistry on CO₂ mineralization (Adeoye et al., 2017; Andreani et al., 2009; Luhmann, Tutolo, Bagley, et al., 2017; Luhmann, Tutolo, Tan, et al., 2017). For example, Luhmann, Tutolo, Bagley, et al. (2017) and Luhmann, Tutolo, Tan, et al. (2017) found that lower flow led to greater secondary mineralization and consequently lowered the rock permeability. Andreani et al. (2009) found similar results and concluded that moderate injection rates are optimal, ensuring partial carbonation while maintaining the permeability of the reservoir. The pH level of the fluid has also emerged as a pivotal factor influencing the dissolution-precipitation dynamics and carbonation efficiency (Luhmann, Tutolo, Tan, et al., 2017; Menefee et al., 2018; Xiong, Wells, & Giammar, 2017; Xiong, Wells, Menefee, et al., 2017). Lower pH values favor dissolution over precipitation, resulting in a net increase in porosity. In contrast, higher pH fluids suppress dissolution and promote rapid carbonate precipitation. The role of fluid flow further influences these dynamics (Menefee et al., 2018; Phukan et al., 2021). Elevated flow rates, typically observed in fractures, result in enhanced dissolution due to the high flux of low pH fluid that creates slow precipitation kinetics compared to transport (i.e., low Damköhler number). Conversely, stagnant zones, where diffusion controls transport, have a low flux of acidic fluid, resulting in higher pH values and rapid precipitation. While these overall trends in precipitation and dissolution regimes in carbon mineralization are understood, many questions remain in constraining the dominant regimes as a function of flow and geochemical parameters.

Laboratory experiments that visualize fluid flow and mineral dissolution and precipitation shed light on key interacting processes governing carbon mineralization (Figure 5). In particular, experiments using lab-on-a-chip (LoC), a microfluidic platform that allows detailed spatiotemporal characterization of micro-scale phenomena, show great promise (Datta et al., 2023). These experiments effectively reproduce complex features of fractured porous media structures that are central to efficient mineralization, such as fractures and the surrounding rock

matrix, which are needed to sustain both flow and mineralization (Cardona & Santamarina, 2023; Ghassemi & Suresh Kumar, 2007; Kong et al., 2023; Porter et al., 2015; Steefel & Lichtner, 1994; Q. Zhang et al., 2022). The LoC approach can also realize and characterize a wide range of fluid flow conditions. For example, this platform can visualize often-neglected inertial laminar flows that readily occur in fractured media. Inertial laminar flows fall between the well-known extremes of creeping (Stokes) and turbulent flow regimes. They are distinct in that they have more complex steady flow structures, such as helical flows and recirculating flows (weak inertia), or periodic flow structures, like vortex shedding (strong inertia), which are not observed in creeping flows. However, they do not exhibit the chaotic behavior that is characteristic of turbulent flows (Wood, 2007; Wood et al., 2020). Recent studies, including LoC experiments, have shown that inertial laminar flow regimes, even comparatively weak ones, strongly affect reactive transport and the patterns of mineralization and dissolution, and may contribute to the variation in observed reaction rates (Figure 5b) (Crevacore et al., 2016; Deng, Molins, et al., 2018; Deng, Steefel, et al., 2018; Lee & Kang, 2020; M. Liu et al., 2020; Ma et al., 2021; Moosavi et al., 2019; Yang et al., 2024; S. Yoon & Kang, 2023). In another example, density-driven flows are also expected to occur during carbon mineralization due to density contrasts arising from the injection of higher-density CO₂-charged water into groundwaters (Snæbjörnsdóttir et al., 2020; Z. Xu et al., 2023) or mineral dissolution, which will cause unexpected instabilities and distinctive fracture permeability scaling laws (Ahoulou et al., 2020; H. Cao et al., 2023; Huang et al., 2020; J. Zhu & Cheng, 2018). Laboratory experiments, especially those using the LoC approach to visualize these complex fluid flow and transport processes in fractured porous media, have great potential to interrogate these interlinked flow and geochemical processes.

More advanced experiments coupling fluid dynamics and geochemical processes are required to address questions relevant to carbon mineralization. In particular, the geochemical properties of geologic media must be captured to investigate coupled dissolution and precipitation processes (Figures 5c and 5d). There are two major directions in this effort: experiments in rock-analog systems (Jones & Detwiler, 2019; Neuville et al., 2017; Osselin et al., 2016; Park et al., 2021; Poonosamy et al., 2020; H. Yoon et al., 2019) and embedding real rock samples into microfluidics or other flow-through setups (Deng et al., 2020; Fazeli et al., 2020; Ling et al., 2022; Neil et al., 2024; Singh et al., 2017). Using rock-analog systems (Figure 5a), one can efficiently explore wide ranges of fluid flow and reaction regimes with direct visualization at more feasible time scales. Such experiments enable the identification of the various regimes of dissolution-precipitation reactions that occur during mineralization, including a coupled regime, where co-located dissolution and precipitation result in sustained mineralization, a passivation regime, where precipitation rates are so fast that the reaction shuts down, and a decoupled regime, where precipitation occurs in a location far from the initial dissolution. Recent advancements have also enabled high-pressure-high-temperature microfluidics and core flooding systems, which are important for realizing in situ reservoir conditions during carbon mineralization of mafic/ultramafic rocks with direct visualization (Jiménez-Martínez et al., 2020; Menefee et al., 2018; Porter et al., 2015). Despite these advances, the slow dissolution kinetics of mafic and ultramafic rocks have resulted in either dissolution-dominated or precipitation-dominated processes depending on the injection fluid chemistry (Luhmann, Tutolo, Tan, et al., 2017). For the purposes of capturing the spatial and temporal evolution of both dissolution and precipitation processes, microfluidic and core flooding experiments must be carried out under high pressure and temperature conditions with carefully tuned experimental parameters, including fluid chemistry and residence time of fluids injected.

By combining these systematic laboratory experiments with validated models and reactive transport simulations (Section 4.5), key dimensionless numbers that can help delineate major carbon mineralization regimes may be identified. These include Damköhler numbers that compare reaction rates with transport rates, Peclet numbers that compare advective and diffusive mass transfer, and Reynolds and Rayleigh numbers that quantify inertia and density-driven flow, respectively. Dissolution-precipitation reactions are largely influenced by the dominant minerals, such as olivine in peridotite and plagioclase feldspars in basalt (Kelemen et al., 2019). The kinetics of these reactions have been extensively characterized in batch experiments (Pokrovsky & Schott, 2000; Schaef & McGrail, 2009). Consequently, the controlling Damköhler values can be determined based on the representative minerals for dissolution and precipitation. Regarding nucleation, it typically governs the early stages of mineral precipitation. Therefore, the overall precipitation kinetics are primarily controlled by crystal growth (Lasaga, 2014). However, depending on the distribution of minerals, spatially heterogeneous nucleation sites could significantly influence precipitation patterns and clogging. Therefore, studying the effects of nucleation on mineral precipitation is an important area of research.

The improved understanding of mineralization processes under fluid flow conditions could lead to improved engineering strategies to overcome reaction slowdowns, such as creating new fracture surfaces and flow paths by controlling injection strategies. Additional well-controlled core flooding experiments of real rock at high-pressure-high-temperature conditions and nanoscale characterization of dissolution and precipitation phenomena (e.g., etch-pits, nucleation) are needed to verify results obtained from LoC experiments (Kim et al., 2021; Luhmann, Tutolo, Tan, et al., 2017; Noiriél et al., 2020). Ultimately, a major goal of experimental studies should be to inform THMC models for improved prediction of carbon mineralization at the field scale.

3.4. Coupled Fluid Flow and Mechanics for Stimulation

The existence or creation of a complex fracture network is needed to unlock the full carbon sequestration potential of subsurface mafic and ultramafic formations, especially considering the relatively low porosity and permeability of the rock matrix. Natural fractures are ubiquitous in the subsurface, but most of them are cemented or mineralized due to geological diagenesis at subsurface temperature and pressure conditions, suggesting low apparent permeability (Fu et al., 2021; Gale et al., 2014, 2018; Kostenko et al., 2002). As a result, methods of permeability enhancement, such as hydraulic fracturing and hydro-shearing, may be needed to enhance the permeability of mafic and ultramafic rocks for sustained, extensive CO₂ mineralization. Controlled laboratory experiments are essential to understanding permeability enhancement approaches because they allow for the identification of key mechanisms and the evaluation of optimization strategies. Here, we summarize key lessons learned from the permeability enhancement approaches used in the unconventional oil and gas revolution and enhanced geothermal system (EGS) development. We then identify the important knowledge gaps and future research topics to adapt the technologies for carbon mineralization in subsurface mafic and ultramafic rocks.

Extensive laboratory studies of hydraulic fracturing have been conducted on sedimentary, metamorphic, and igneous rocks, including shale (Tan et al., 2017), sandstone (Zoback et al., 1977), carbonate (Hou et al., 2018), phyllite (Oldenburg et al., 2020), schist (Farkas et al., 2019), gneiss (Boese et al., 2022), granite (Zhuang & Zang, 2021), and gabbro (D. Liu & Lecampion, 2022). The key experimentally identified parameters that affect hydraulic fracture initiation and propagation include rock microstructures, fluid viscosity, injection rate, stress conditions, and rock matrix permeability. Theoretical work also demonstrates several key physical processes strongly influencing hydraulic fracturing, such as borehole pressure diffusion, viscous fluid flow, creation of new solid surfaces, and leak-off of fracturing fluid into porous fracture walls (Bunger et al., 2005; Detournay, 2016; Haimson & Fairhurst, 1967). These findings are mainly developed based on the coupling between fluid flow and rock deformation/fracturing. However, hydraulic fracturing of mafic and ultramafic rocks may involve additional physics—thermal effects and solid volume expansion—largely because certain minerals, such as olivine, will undergo hydration reactions upon contact with water-based fracturing fluids that form volume-expansion product minerals and generate significant heat (McCollom & Bach, 2009; Scott et al., 2017). Future studies are needed to explore the impact of thermal effect and solid volume expansion on hydraulic fracturing of mafic and ultramafic rocks.

There is an increasing interest in managing the complexity of hydraulic fractures in hydrocarbon-bearing formations for enhanced oil and gas recovery, which can also benefit carbon mineralization in mafic and ultramafic rocks because a complex hydraulic fracture network will provide more reactive surface area for carbonation than simple fracture structures. Multiple hypotheses have been proposed to predict and manage hydraulic fracture complexity in hydrocarbon-bearing formations. One popular hypothesis, pioneered by Renshaw and Pollard (1995), suggests that hydraulic fractures activate pre-existing natural fractures, leading to a fracture network under weak horizontal stress anisotropy (Weng et al., 2011). Other studies suggest that the damage-dependent Biot coefficient and its tensorial anisotropy can either promote or suppress the localization of multiple hydraulic fractures (W. Li et al., 2022; Rahimi-Aghdam et al., 2019). The Biot coefficient governs the change of stress in the solid phase due to a change in fluid pressure with no change in the overall strain. Another recent experimental study indicates that the so-called T-stress, that is, the parallel stress near the crack tip, can cause fracture path curvature and strong localized stress concentration, eventually leading to fracture branching in homogeneous analog rocks (W. Li et al., 2022). Injection rate, fluid viscosity, and fluid chemistry have also been observed to strongly affect hydraulic fracture complexity (Barati & Liang, 2014; Ishida et al., 2004; W. Li et al., 2021). Future experimental studies are needed to investigate the mechanisms controlling hydraulic fracture complexity in mafic and ultramafic rocks, particularly accounting for the unique hydration and exothermic (heat releasing) reactions when water is in contact with olivine—one major constituent mineral in these rocks.

Hydro-shearing is another means for permeability enhancement, often in EGS development. Hydro-shearing involves the injection of fluid at pressures below or close to the minimum principal stresses in the reservoir to induce the shear slip of pre-existing fractures. Shear slip of the pre-existing fractures can cause self-propping, hence permeability enhancement, due to the rough surfaces of the fracture walls. Numerous laboratory hydro-shearing studies have been conducted on shale, granite, schist, amphibolite, and rhyolite, suggesting that in-situ natural fractures must be permeable, weak, and favorably oriented to be hydro-sheared (French et al., 2016; Kc & Ghazanfari, 2021; Meng et al., 2022; W. Wu et al., 2017; Ye & Ghassemi, 2018). After shearing, permeability enhancement differs significantly among different rock types, and in some cases, shear slip even causes decreasing fracture permeability (Z. Lei et al., 2023; Meng et al., 2022). It is currently unknown whether these findings apply to hydro-shearing of fractures in mafic and ultramafic rocks, mainly because complex hydration, carbonation, and exothermic reactions can simultaneously occur during and after hydro-shearing in these rocks. Laboratory experiments are needed to investigate these open questions because hydro-shearing could provide a potential mechanism for enhancing CO₂ storage potential in low-permeability reservoirs during large-scale CO₂ mineralization operations.

Laboratory studies of hydraulic fracturing and hydro-shearing on mafic and ultramafic rocks are crucial to identifying the key mechanisms for permeability enhancement to provide large reactive surface areas for CO₂ mineralization. Furthermore, data collected from the controlled laboratory experiments will facilitate the development and validation of numerical models, with the ultimate goal of effectively predicting carbon mineralization at the field scale. However, it must be emphasized that hydraulic fracturing and hydro-shearing, even when generating complex fracture networks, are expected to only provide initial surface areas for carbonation reactions. Sustained CO₂ mineralization at scales will require significant fluid access to the rock matrix, which calls for an improved understanding of reaction-driven damage/cracking, as discussed in the next section.

3.5. Coupled Flow-Reaction-Mechanics of Mineralization (HMC)

For low porosity and low permeability mafic and ultramafic rocks, CO₂ storage volumes and reactive surface areas are limited to the pre-existing fracture network. Thus, promoting storage in the long term requires processes that continually expand this network. Here, we review three coupled geochemical and geomechanical processes that could play a role in the evolution of fractures and reservoir reactivity during CO₂ injection: (a) Reaction-driven fracturing; (b) Sub-critical fracture propagation; and (c) Enhanced reactivity of fracture systems.

3.5.1. Reaction-Driven Fracturing

The hydration of olivine and the carbonation of silicate minerals in mafic and ultramafic rocks results in a significant increase in volume, with the corresponding crystallization pressure estimated to be sufficiently large to fracture mafic and ultramafic rocks in the subsurface (e.g., Van Noort et al., 2017). For example, the reaction of olivine to magnesite and quartz yields a solid volume increase of 80%. However, the theoretical estimates of the crystallization pressure are an upper bound of the actual pressure exerted by the growing crystal, as it is calculated under the conditions of thermodynamic equilibrium. Without knowledge of the kinetics of the different reactions, it is not possible to assess the time it will take to cause microcracking of the rock and which reaction, hydration or carbonation, is mainly responsible for reaction-driven cracking (Correns, 1949). For differential volumetric changes to work, carbonates must precipitate non-uniformly (Xing et al., 2018); for crystallization pressure to work, carbonates must precipitate in interstices (grain boundaries, crystal defects) and have access to sufficient supersaturated fluids to grow and eventually crack the rock aggregate. Relevant field evidence for reaction-driven fracturing exists in the spheroidal weathering of granite (Fletcher et al., 2006), basalt, and the serpentinization of peridotite (Jamtveit et al., 2009; Renard, 2021). Extensive carbonation of the Oman peridotite has been proposed as possible evidence of carbonation-driven fracturing (Beinlich et al., 2020; Kelemen et al., 2011, 2018). Abundant listvenite outcrops—peridotite rocks that have been completely carbonated, exhibit brecciated textures with hierarchical fracture networks that are reflective of coupled carbonate deposition and fracture propagation (Beinlich et al., 2020; Falk & Kelemen, 2015; Kelemen et al., 2011). However, Menzel et al. (2022) argue that, based on observation of the core, the creation of persistent fluid pathways is primarily a function of tectonic stress and fluid over-pressure rather than reaction-driven cracking.

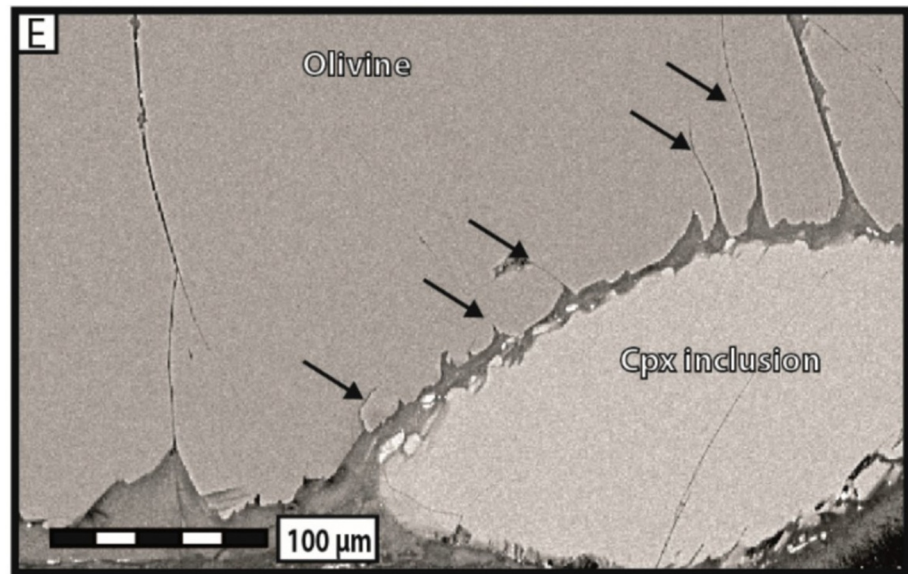


Figure 6. Volume-increasing reactions under confining pressure could result in reaction-driven fracturing during carbon mineralization operations. It is hypothesized that the induced fracturing could lead to increased permeability of the rock, and subsequently, a greater storage capacity. This figure shows experimental evidence of reaction-driven fracturing of olivine by hydration and serpentine formation (Lafay et al., 2018).

Laboratory studies provide evidence of reaction-driven fracturing during the evaporative precipitation of salt (Scherer, 2004), hydration of periclase (MgO) (Kuleci et al., 2017; Uno et al., 2022; Zheng et al., 2018), and the serpentinization of olivine, shown in Figure 6 (Lafay et al., 2018). However, experimental evidence for carbonation-driven fracturing in mafic minerals is limited. While Lafay et al. (2018) observed clear evidence for hydration-induced fracture propagation in olivine, they found no evidence for carbonate-driven fracturing, possibly because carbonate reaction products were “delocalized” (i.e., did not concentrate on defects). Rather than searching for individual fractures, Van Noort et al. (2017) assessed the volumetric expansion of olivine aggregates exposed to high-pressure CO₂ and found limited evidence (only 1 of 17 triaxial experiments) for expansion, which they suggested was the result of precipitation clogging transport pathways, limiting continued reaction. W. Zhu et al. (2016) observed an increase in porosity in experiments on sintered olivine cups possibly due to reaction-driven fracturing, but the deformation of the complex cup geometry created ambiguity in the interpretation. Xing et al. (2018) extended the work of W. Zhu et al. (2016) and argued that they observed reaction-driven fracturing generated by non-uniform distribution of precipitation and dissolution.

Whether or not reaction-induced fracturing can occur depends on pore-scale processes, including where carbonate crystals precipitate (on surfaces, in the solution, or focused on defects). The relative rates of growth and access to reactants are critical (Kelemen et al., 2019), as is the role of passivation and permeability reduction or enhancement. Different carbonation experiments have resulted in both the reduction in permeability of olivine-rich peridotite (Lisabeth et al., 2017) and the increase in permeability at higher CO₂ pressures (Andreani et al., 2009). It is unknown whether reaction-driven processes occur in mafic rock such as basalt. Further investigation into reaction-driven fracturing is needed to establish whether this process will play an important role during large-scale industrial CO₂ storage in mafic and ultramafic reservoirs.

3.5.2. Subcritical Fracture Propagation

Chemical reactions have the potential to modify fracture toughness or the ease of fracture propagation (Atkinson, 1984; Eppes & Keanini, 2017). Because the subsurface is in many places “critically stressed” (Townend & Zoback, 2000), chemical reactions that weaken existing fractures can lead to spontaneous fracture initiation and propagation, called subcritical cracking (Brantut et al., 2013; Laubach et al., 2019). Although subcritical cracking is a localized failure, its occurrence will provide new fluid flow conduits for access to additional rock volumes, which may benefit the volumetric process of reaction-driven cracking. There has been relatively little work

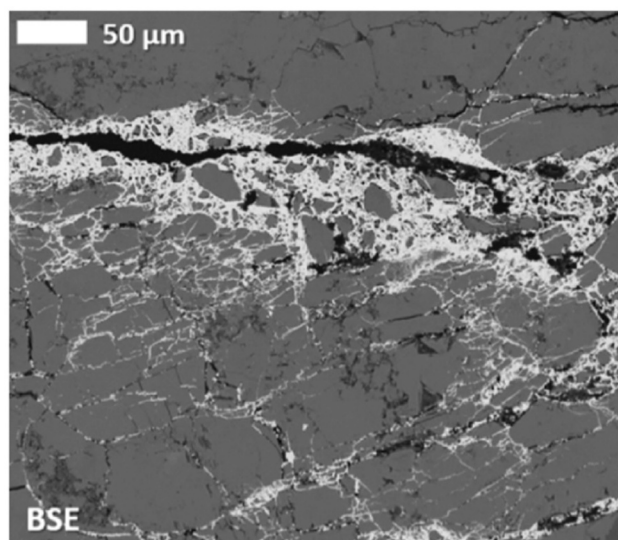


Figure 7. Fractured rock is expected to be more reactive with CO₂ due to the generation of fine-grained rock material, called fracture gouge, and the exposure of fresh mineral surfaces. This higher reactivity is demonstrated in this backscattered electron image of an experimentally shear-fractured carbonate-rich shale. The injected barium chloride solution resulted in the rapid (1 hr) precipitation of barium carbonate (bright-white material; Menefee et al. (2020)).

conducted on the impacts of CO₂-induced reactions on rock strength and fracture propagation (Vafaie et al., 2023). Most of the existing work has been done on sandstone, showing variable but generally weakening impacts on rock strength, creep, and fracture behavior (Otu et al., 2023; Rinehart et al., 2016; Z. Wu et al., 2020; G. Zhang et al., 2020). An experiment on olivine-rich peridotite (Lisabeth et al., 2017) found reduced strength, which they suggest may have involved sub-critical fracturing during triaxial loading as a possible experimental demonstration of this behavior. However, much more work is needed on basalt and peridotite reactions with CO₂ to assess the potential of subcritical fracture propagation to enhance carbonation.

3.5.3. Enhanced Reactivity of Fracture Systems and Fracture Branching

Fracturing rock generates fresh mineral surfaces and comminuted material called fracture gouge (Reches & Dewers, 2005), which are likely to be more reactive with CO₂-bearing fluids. The gouge can include very fine-grained and potentially strained or damaged material that has a greater reactive surface area (Tenthorey & Cox, 2006; Vrolijk & van der Pluijm, 1999). Additionally, newly-exposed mineral surfaces lack thin, passivating layers (e.g., formation of nano-scale hydration products) that can slow chemical reactions (e.g., Eisenlohr et al., 1999; Olsson et al., 2012). This higher reactivity has been demonstrated experimentally by Menefee et al. (2020), who provided evidence of enhanced carbonation within a fractured shale under dynamic fracturing experiments, in which a reactive solution was injected into newly created shear fractures (Figure 7). It is thus suspected that the natural or engineered activation of fractures in impermeable basalt or peridotite could be

a possible mechanism to expose freshly formed and pre-existing fractures to reactive fluids, maximizing the rate and amount of CO₂ that can be stored. In addition, changes in stress induced by injection may reactivate existing shear fractures, producing more fracture gouge.

3.6. Challenges: Realistic Systems

One of the greatest challenges in predicting the long-term viability of carbon mineralization in the field is connecting experimental studies to field observations. In this section, we review the mismatches between experimental and field results and the potential for reconciliation between the two. We focus on three potential areas of mismatch: (a) time- and length-scale of reaction, (b) reactive surface area, and (c) differences in reaction conditions.

Regarding the time- and length-scale of reaction, laboratory experiments are understandably conducted over limited time periods and spatial areas compared with field operations. Many reported experimental studies occur over weeks (Ennis-King & Paterson, 2007; Raza et al., 2023; Romanov et al., 2015) to months (Gysi & Stefánsson, 2012; McGrail, Schaef, et al., 2009; McGrail, Sullivan, et al., 2009; Raza et al., 2023; Shibuya et al., 2013; Voigt et al., 2021), challenging their applicability to field sites. Even in the case of the rapid mineralization recently observed at CarbFix (Pogge von Strandmann et al., 2019) and Wallula (S. K. White et al., 2020), differences in the time scale of comparable experiments can result in overlooking mechanisms critical to predicting the long-term viability of carbon storage, such as the passivation of reactive mineral surfaces (Kelemen et al., 2019). There are also challenges associated with scaling up pore- to column-scale laboratory results. Mixing behavior is known to differ between the column- and field-scale (Schincariol & Schwartz, 1990) and the field-scale is likely to have much more spatial variability in reactive mineral facies (Deng et al., 2010).

Another source of mismatch between field and laboratory observations is the size of mineral reactants used in experiments. While increasing the reactive surface area through the use of fine-grained powders can increase carbon sequestration per unit mass (Xiong, Wells, & Giammar, 2017), this is not representative of the nature of reacting surfaces during in situ geologic storage, which likely exists as consolidated rock (L. Li et al., 2008; M. Liu et al., 2022). Additionally, the use of powder samples cannot capture preferential precipitation on different mineral crystal faces, which has been observed for olivine (Olsson et al., 2012).

Finally, replicating the conditions of the subsurface field tests remains a challenge in the laboratory, due to the relatively slow kinetics of carbon mineralization of mafic and ultramafic rocks on a laboratory time scale. Therefore, elevated temperatures and solution compositions unrealistic of subsurface conditions in the field are frequently used in experiments to increase the rate of reaction, including temperatures exceeding 150°C (Z.-Y. Chen et al., 2006; Garcia et al., 2010; Miller et al., 2019) and high concentrations of sodium bicarbonate (Z.-Y. Chen et al., 2006; Gadikota et al., 2014; F. Wang et al., 2019). While these studies offer valuable insight into the mineralization process, the extreme conditions could potentially impact the saturation index with respect to carbonate mineral precipitation, and can therefore further impact the size (Q. Li et al., 2014), polymorphism (De Choudens-Sánchez & Gonzalez, 2009), and location (e.g., homogeneous vs. heterogeneous precipitation; Amor et al., 2004) of secondary mineral precipitates.

Moving forward, a multi-pronged approach is likely needed to advance our scientific knowledge in this area. While it remains necessary to tune experimental conditions to achieve reaction on a timescale observable in a laboratory setting, complementary experiments at natural conditions are necessary to distinguish differences in the reaction mechanism. Another promising approach is to conduct experiments using rock-analog systems that can facilitate reactions while still capturing key aspects of the mineralization process (Osselin et al., 2016). These experimental insights are critical in identifying first-order processes needed for developing realistic field-scale simulations that can make actionable predictions of mineralization and capture the complex, coupled geochemical–geomechanical processes occurring in the subsurface.

4. Modeling and Simulation Studies Related to Carbon Mineralization

4.1. Introduction

The use and development of mathematical models and computational tools, guided by field and experimental data, is a necessary practical step if CO₂ mineralization is to be predicted and realized at the field scale. Given our currently available computational tools, it is relatively infeasible to accurately predict the amount of CO₂ mineralized as a function of time within a complex fractured system. Therefore, this section is dedicated to noting what models are available to initiate studies on CO₂ mineralization in mafic and ultramafic rock. In addition, we describe the knowledge gaps of current modeling techniques and propose methods to fill these gaps.

CO₂ mineralization within mafic and ultramafic rocks includes coupled THMC processes, which are poorly understood and not fully represented by current models. Temperature (T) has a critical effect on chemical reaction rates and mechanical properties. Hydrologic processes (H) control the transport of CO₂ and chemical species necessary to dissolve rock and precipitate carbonates. Mechanics (M) determines the growth and closure of fractures that provide pathways for fluid to interact with fresh rock. Finally, chemical reactions (C) govern the kinetics of carbon mineralization in the system.

Experiments alone cannot provide sufficient information for models because key THMC parameter values require scale-appropriate benchmark data to develop and validate the coupled models. Thus, there needs to be an integration of experiments and field data (both short-term injections like CarbFix and natural analogs) to develop and validate models of the coupled processes involved in fracturing, injecting, and mineralizing CO₂ in mafic and ultramafic rocks. We note that although models of some physical processes in the uncoupled endmembers of THMC are reasonably complete (e.g., flow in fractures, dissolution of minerals, strength of rocks), there are important processes that aren't adequately captured, such as passivation, sub-critical cracking, reaction-driven fracturing, and precipitation in fracture networks.

In many cases, separate thermo-hydro-mechanical (THM) and thermo-hydro-chemical (THC) models can be used to gain an understanding of mineralization in mafic and ultramafic rocks. THM models can help elucidate how the fracture network is created and THC models, including reactive transport models, can be used to predict how dissolution and precipitation affect flow and transport in the fractured system (Viswanathan et al., 2022). Combining these model types through the development of coupled thermo-hydro-mechanical-chemical models is necessary for cases when there is strong feedback between mechanical and chemical processes. A major challenge will be to simulate THMC processes in complex fracture networks since THM and THC often operate at disparate time and length scales.

To move toward this objective, reduced complexity modeling (RCM) (Section 4.2) and Uncertainty Quantification (UQ) (Section 4.3) will be imperative first steps. RCM, which is based on models with first-order couplings

in simplified domains, can provide baseline insights into carbon mineralization processes and phenomena. This systematic approach to increasing complexity provides an initial step to coupling THMC phenomena in a single model. On the other hand, UQ can be implemented to account for poorly constrained input parameters in models, including inaccurate thermodynamic data, reaction rates, fracture parameters (e.g., fracture density, orientation, connectivity, etc.), and estimates of reactive surface area that may lead to grossly inflated mineralization rates in modeling studies. Once the key processes and uncertainties are defined, existing THM (Section 4.4) and THC (Section 4.5) models can be used for more detailed analyses of carbon mineralization. To arrive at a fully coupled THMC model of CO₂ mineralization (Section 4.6), constrained by field and laboratory observations, it is imperative to overcome the key challenges outlined in Section 4.7.

4.2. Reduced Complexity Models

To unravel and understand the inner workings and couplings of key carbon mineralization phenomena, reduced complexity models can provide critical insight. Examples of how these models can be applied include: (a) classic scaling analysis (Barenblatt, 1996) focused on determining appropriate definitions of governing dimensionless groups (e.g., the Damköhler number) that control the transport and reaction of CO₂-charged fluids in the subsurface and (b) the development of models that capture and couple the first-order phenomena in carbon mineralization. These efforts should incorporate models of transport, geomechanics, and geochemistry in one-dimensional domains that consider the competing roles of phenomena such as dissolution and precipitation reactions, the impacts of dissolution- and precipitation-induced porosity modifications on fluid flow, and the physical components of reaction-driven fracturing. Ultimately, RCM models could build our understanding of key carbon mineralization phenomena and their interaction, identify the underlying time and space scales of carbon mineralization processes, prioritize the order of carbon mineralization phenomena, guide the effective design of laboratory experiments to provide key parameters for larger-scale models, and determine which processes must be considered in the physics-based models described in the forthcoming sections.

4.2.1. Examples of RCMs to Provide Insight on THMC Processes

RCMs have been used in several efforts to better understand carbon mineralization. A recent study by Ratouis et al. (2022) was conducted to investigate CO₂ mineralization during the CarbFix2 project in Iceland. The model considered non-reactive solute transport and thermal effects while using a dual-porosity type of model to represent the fractured basaltic reservoir, which covers an area of 42 km². The tracer data measured to monitor the movement of the injected CO₂ in the reservoir and the thermal data collected from the monitoring wells in the field were in agreement with the results of the numerical model, suggesting that, in certain cases, a non-reactive simulation scheme can be used to monitor in-situ mineralization, CO₂ containment, and long-term storage security in the reservoir. In addition, complementary geochemistry studies (Clark et al., 2020) showed that the processes of carbon and sulfur mineralization occurred fairly rapidly in CarbFix and CarbFix2 over timescales of months to years. The Carbfix and CarbFix2 pilot tests indicate that the permeability of the basaltic reservoir was barely affected by mineralization reactions over multiple years (Clark et al., 2020). This was attributed to the overall low volume percentage of mineral precipitation in the reservoir and the injected acidic fluids' tendency to dissolve the host rock close to injection well while precipitating minerals further away (Clark et al., 2020). The observation of mineral dissolution and thermally induced fracture growth near the borehole argues that coupling of mechanical deformation with reactive transport in a highly fractured basaltic reservoir is relatively weak. This is likely not the case in low-permeability rocks such as peridotite, where permeability is expected to be affected by mineralization.

Evans et al. (2020) considered reaction-driven cracking during the serpentinization of olivine with a model that combined reaction, deformation, and fluid flow. This model accounts for the presence and growth of cracks, which are described by a phase-field model. Although phase-field models are computationally expensive, they are used in this study to determine first-order processes controlling reaction-driven cracking. The model simulates the effect of the competition between cracking and porosity clogging on fluid pathway evolution. Although the study does not rigorously simulate coupled reactions, it demonstrates the positive feedback between an effective precipitation reaction and cracking, which leads to a self-sustaining process. Notably, after introducing water diffusion due to chemical potential gradient into the numerical model, a crack pattern consisting of a primary path intersected by an orthogonal secondary set was reproduced, as has been observed in nature. Such a pattern

resembles the so-called “Frankenstein” crack frequently observed in peridotite outcrops in Oman (Evans et al., 2020).

4.3. UQ for Carbon Mineralization Applications

Uncertainty quantification is another critical tool needed to characterize CO₂ mineralization, as both fracture and reaction parameters are difficult to constrain. Even if a fully coupled THMC model for CO₂ mineralization in fractured mafic and ultramafic rocks were to exist, it could not be used to definitively predict the quantity of interest (QOI), that is, the temporal and spatial evolution of CO₂ mineralization in mafic and ultramafic rocks. Rather, the model could be used to prescribe bounds on the QOI. This is due to the highly heterogeneous and uncertain nature of the fractured systems and the processes driving mineralization.

When considering engineering actions that could significantly increase CO₂ mineralization rates, the following mechanisms are proposed: (a) Maximizing the reaction kinetics by dissolving CO₂ in water (Sigfusson et al., 2015; Snæbjörnsdóttir et al., 2020) and adjusting pressure and temperature (Kelemen & Matter, 2008); (b) Increasing the rock surface available for reaction by pumping (injecting) the CO₂ mixture through the fracture networks—natural or engineered—in the subsurface rock mass; (c) Creating self-sustaining, reaction-driven fracturing pathways by which the CO₂ mixture can progressively advance from the fracture network into and through the bulk of the rock mass; and (d) Monitoring mineralization progress via remote sensing, for example, seismic imaging so that operational parameters can be adjusted as a function of time to maximize mineralization. The major caveat is that many of these processes are not well understood or characterized for mafic and ultramafic rocks. Key knowledge gaps revolve around a lack of a fundamental understanding of fluid flow and reactive transport in a fractured multi-scale system, where the permeability, porosity, pore space geometry, and available surface area are continually changing through time. The primary uncertainties to consider are processes and parameters. The first uncertainty focuses on delineating the most important processes that influence the bounds of the QOI and the uncertainties in representing those with mechanistic models. The second uncertainty is centered on the parameters that play a role in the first-order processes. These two aspects cannot be decoupled, since the uncertainty in model and parameter space has a significant influence on determining the most sensitive processes.

Identifying which processes have the most significant effects on carbon mineralization can be difficult because it is rare that one can observe the effects of a single process at the field scale. Often there are complementary or competing processes that make it impossible to isolate and quantify the impacts of a given process. Previous work has focused on the coupled effects of reactions and flow on the fate of solute transport through varying parameters such as the Damköhler number (Severino et al., 2012). As the mineralization of CO₂ will depend upon the rates of precipitation and dissolution reactions as a function of the flow field, these parameters offer valuable insights into the behavior of dead-end fractures, flow channeling, and other relevant phenomena. However, reaction rate constants utilized in these models are typically measured through batch laboratory experiments, which have shown significant variation compared to those observed in the field (Viswanathan et al., 1998). Attempts have been made to quantify the effects of such variations in key QOI such as solute-to-precipitate ratios (Srinivasan et al., 2007), where smaller laboratory-scale experiments can provide invaluable information to make direct comparisons. For example, controlled laboratory experiments at reservoir temperatures, pressures, and stresses can mimic subsurface conditions to guide the optimization of mineralization at reservoir conditions. Experiments can also be designed to establish how to maximize reaction kinetics and create positive feedbacks to stimulate fracture branching and growth to access larger volumes of the reservoir rock. There will always be issues of scaling when applying models and parameters identified at the laboratory scale to field-scale operations, however, significant insight can be gained from first-order effects and associated uncertainties by this approach.

Recently, the use of Machine Learning (ML) algorithms in UQ has gained a lot of traction since these algorithms offer the ability to explore large dimensional models and parameter spaces very efficiently through the development of surrogate models. ML algorithms can also be used to query the sensitivity of processes relative to one another. Random Forest algorithms are perhaps one of the simplest ML techniques that have proven very powerful in their ability to identify the relative importance of models and parameters in various fields including geosciences (M. Liu et al., 2022; Srinivasan et al., 2018). As an example, a Random Forest algorithm can be used to infer whether rates for precipitation/dissolution reactions affect mineralization more than hydrogeological parameters like flow rate or fracture aperture, and how the topology or the fracture connectivity affects the amount mineralized.

Another popular use of ML algorithms is their ability, once trained, to accurately mimic complex multi-physics problems at a fraction of the speed that it would take to run the original physics-based models. As previously mentioned, mechanistic models of THMC processes in complex fracture networks would take several hours on High-Performance computers, even when run in parallel. Since UQ requires several thousands, if not millions of runs to bound uncertainties in processes and parameters, this task becomes prohibitively expensive. For this reason, multi-fidelity Monte Carlo models (Ng & Willcox, 2014; O'Malley et al., 2018; Peherstorfer et al., 2016) have been used very successfully to optimize available computational resources by utilizing a small number of high-fidelity runs for learning the systematic biases between pairs of high and lower-fidelity models.

Uncertainty quantification techniques can be used to characterize the relative uncertainties in reaction parameters and fracture/host rock properties and their impact on key quantities of interest such as carbon mineralized as a function of time. Parameters we have identified as uncertain include reactive surface area, reaction kinetics, thermodynamic data, fracture connectivity, fracture permeability, and matrix permeability. Therefore, we recommend that UQ techniques permeate all facets of carbon mineralization research including field observations, laboratory experiments, and computer simulation.

4.4. Thermo-Hydro-Mechanical (THM) Modeling of Fractures

Thermo-hydro-mechanical (THM) models have been used extensively to explore the physical processes involved in complex subsurface systems, including geothermal systems and unconventional reservoirs, at the pore and reservoir scale. Carbon mineralization has many commonalities to these systems with the exception that chemical reactions play an even more important role. Nevertheless, THM models can provide important information for understanding the structure of the fracture network and mechanical changes in fractures induced by fluid injection. THM models are generally categorized as discrete or continuum. In discrete models, the fracture is explicitly represented in the model. As a result, these models have been developed to simulate and predict complex fracturing processes such as fracture growth and branching. Continuum models use effective properties to consider existing fractures and do not consider fracture growth, but can model larger and more complex systems. Both continuum and discrete models have been applied at the pore and reservoir scale and will be discussed here. Given the wealth of existing studies and reviews on both thermo-mechanical (TM; e.g., English, 2012; Ghassemi, 2012) and hydro-mechanical (HM; e.g., Q. Lei et al., 2017) models and effects in fractured systems, we will focus our attention solely on thermo-hydro-mechanical (THM) models in this section, which are relatively few compared to TM, HM, and thermo-hydro-chemical (THC) models, the latter of which are discussed in the following section.

4.4.1. Pore-Scale THM Modeling

Carbon mineralization in mafic and ultramafic rocks involves important pore-scale mechanisms that can alter the permeability, mechanical properties, and storage volume of the reservoir. Crucial micromechanical processes during CO₂ injection include the interplay between reaction-induced volume change, distributed microcracking, crack coalescence, and, ultimately, changes in bulk and/or fracture permeability (Figure 8). A promising avenue to accommodate these interactions is the incorporation of micromechanics theories into chemo-poro-mechanics constitutive frameworks. These efforts can benefit from analytical results by linking bulk mechanical properties to the microstructure of a solid matrix, such as the classic upper bound proposed by Hashin and Shtrikman (1963). Initial results in this area have recently been obtained in the context of micro-poromechanics for water-saturated geomaterials (e.g., Dormieux, 2006; Dormieux & Kondo, 2016; Kachanov & Sevostianov, 2018; Zaoui, 2002), providing a favorable avenue for future models focused on carbon mineralization.

Various other pore-scale models that have been developed to simulate coupled THM processes include Discrete Element Method Pore Network Model (DEM-PNM) (Al-Busaidi et al., 2005; Shimizu et al., 2011), Discrete Element Method Computational Fluid Dynamics (DEM-CFD) (Xiao-Dong et al., 2015), and Lattice Boltzmann Method Discrete Element Method (LBM-DEM) (Boutt et al., 2011; Z. Chen, Jin, & Wang, 2018; Z. Chen & Wang, 2017). In these models, mechanical interactions are solved by the discrete element method while the fluid flow equation is solved by either a pore network model, computational fluid dynamics, or lattice Boltzmann method. All three models have been applied to simulate hydraulic fracturing and achieved some success. Particularly, the coupled LBM-DEM model has been used to study the effect of strength heterogeneity on fracturing patterns and microfailure mechanisms (Z. Chen & Wang, 2017). It has also been used to investigate

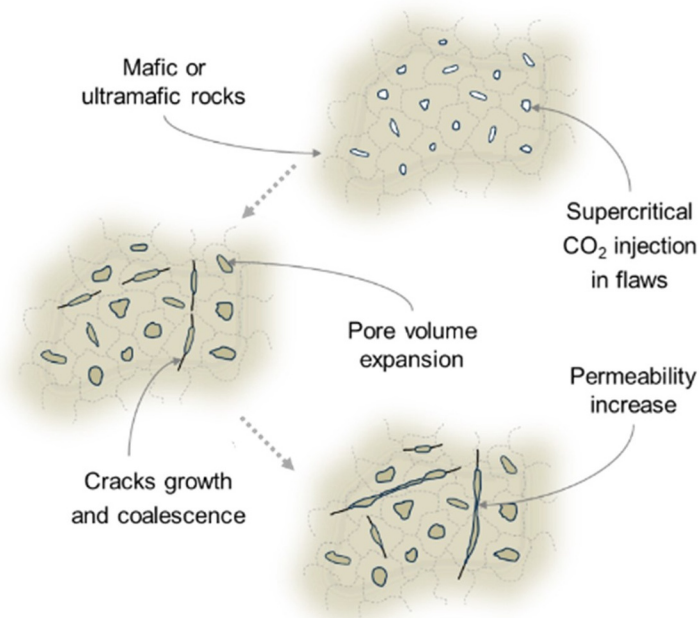


Figure 8. Schematic of crucial micro-scale mechanisms responsible for the change of rock volume and fracture connectivity during carbon mineralization that require the formulation of multiscale chemo-mechanical constitutive laws to be deployed within coupled HCM frameworks.

hydraulic fracture propagation in rocks with cemented natural fractures (Z. Chen, Yang, & Wang, 2018). The numerical results show that both the strength ratio (between cemented natural fractures and the host rock) and the approach angle (between hydraulic and cemented natural fractures) significantly affect hydraulic fracture propagation. These pore-scale coupled hydro-mechanical models have provided important insight into rock failure and fracture initiation and propagation mechanisms. These mechanisms may be important to consider during the injection of CO₂ into low-permeability rocks such as peridotite.

4.4.2. Reservoir-Scale THM Modeling

To predict CO₂ mineralization in mafic and ultramafic rocks, it is necessary to consider THM processes and responses in fractured systems at the reservoir scale to changes in effective stresses, flow conditions, and temperatures as part of the modeling framework (Stephanson et al., 1997). For instance, fracture growth due to imposed hydro-mechanical processes (e.g., hydraulic fracturing) would create additional surface area for CO₂ mineralization, whereas fracture sealing due to lithostatic load/stress changes would decrease surface area. Combining the potential thermal effects, such as the geothermal gradient in the crust or temperature changes due to reactions, with such mechanical aspects would also need to be considered because of the known feedbacks between thermal and mechanical effects.

In general, reservoir scale THM models operate by simulating fracture growth due to stress and thermal effects (discrete) or use discrete fracture networks and impose an external stress field on a pre-existing network of fractures to determine which fractures open and close as a function of time (continuum). A discrete mechanistic model for fracture growth is the combined finite-discrete element model (FDEM). FDEM is an appealing THM model for mineralization since it can simulate fracture growth due to stress and fluid effects. Details of FDEM can be found in Munjiza (2004). FDEM can effectively simulate fracture processes because underlying mechanisms of crack initiation, propagation, and coalescence in geologic materials can all be captured (Knight et al., 2020). These fracture processes are critical for predicting geologic carbon storage since subcritical and reaction-driven cracking may play an important role in accessing enough host rock for scalable carbon mineralization. Wide ranges of length and time scales can be simulated with FDEM-based models, from sub-mm to km, and ns to months, respectively. However, in practice, it is nearly impossible to use pure FDEM models for extended time period 3D simulations (>hours) due to time-stepping issues, which are discussed below. For this reason, the

mechanics of fracture growth, which tends to be a shorter time scale process, has historically been treated separately from chemical reaction, which is a long-time scale process. This separation of time scales enables a simplification of the analysis by uncoupling the fracture propagation from the chemical reactions. However, in other problems such as reaction-driven cracking, such simplification is not possible as it is the chemical processes that are driving the mechanical damage.

There are only a few examples of THM FDEM models in the literature and even fewer are capable of modeling 3D systems. Yan et al. (2022) developed a 2D THM FDEM model within the MultiFrac FDEM software that can simulate fluid and heat transport in complex fracture networks, as well as crack initiation, propagation, intersection, and closure due to THM effects. Sharafisafa et al. (2023) also developed a 2D THM FDEM model within the Irazu geomechanical software that can model both fracture creation/growth and pre-existing discrete fractures. Another example is the Hybrid Optimization Software Suite (HOSS), which is a hybrid multi-physics platform based on FDEM. HOSS allows for preexisting discrete fractures in the rock to be explicitly modeled and used in both solid and fluid domains. One of the limitations of the applications of FDEM models to carbon mineralization is the restrictions placed upon the maximum allowable time step size because a fracture aperture tends to be much smaller than the rock element sizes. The small length scales require small FDEM timesteps, limiting their applicability at the reservoir scale. That being said, FDEM models have been used recently to simulate fracture propagation and flow in fractures, both key processes for carbon mineralization at the meter to 10 m scale (Z. Lei et al., 2019).

Discrete fracture network (DFN) and discrete fracture matrix (DFM) models differ from the FDEM models previously described in the sense that they do not consider fracture growth or coalescence. Instead, they assume the majority of fractures already exist, and external stresses simply open and close these fractures. The advantage is that more complicated physics at larger scales can be more easily simulated, often using existing software. THM models coupled to DFNs are prevalent in the literature for a range of application spaces that involve subsurface fractured systems (Birkholzer et al., 2021; Cui & Wong, 2021; Garipov & Hui, 2019; Z. Lei et al., 2023; S. Li et al., 2019; Liao et al., 2023; Pandey et al., 2017; Stefansson et al., 2021; F. Wang et al., 2019; Yao et al., 2018). THM DFN models can also capture key feedback between aperture changes related to heat and changes in fluid pressure and/or in situ stress conditions. These processes are particularly important during the injection phase of an operation such as CO₂ injection or geothermal energy production. An example of their application is described by Nadimi et al. (2020), who developed a 3-D DFN model to simulate an optimum hydraulic fracture network for Phase 3 injection and production wells at the Frontier Observatory for Research in Geothermal Energy (FORGE) site in Utah. Using this method, the authors identified optimal operating conditions and principal parameters (injection temperature and flow rate) that govern production quality.

FDEM with a coupled fluid solver can aid in understanding the fracture network structure, geometry, and topology created by fluid-driven cracks within the rock, with the key drawback that likely only short timescales can be modeled. On the other hand, continuum models, such as DFN and DFM models coupled to THM simulators, can capture more complex fracture networks but are not capable of generating new fractures, which could prove critical under certain mineralization conditions. Both of these coupled models can capture more complex fracture networks and can account for changing fracture permeabilities and porosities using Barton-Bandis-type analytical equations or fully coupled physics models. Results from these models can give one an estimate of the available surface area for mineralization and garner information needed to predict how much CO₂ can be mineralized in a fractured system.

To overcome the limitations of each model, a possible solution is to employ both models and leverage the strengths of each. An excellent example of this is provided by Birkholzer et al. (2021), whose authors used this integrated modeling framework to predict fracture network evolution during the initiation of hydraulic fracturing at the Hydraulic Fracturing Field Test (HFTS) in the Permian Basin (USA). The authors coupled two high-performance simulators; GEOS, a FDEM-type geomechanical code designed to model hydromechanical variations during hydraulic fracturing initiation; and TOUGH+, a continuum code used for multi-phase flow for production, to arrive at a reservoir-scale model (Birkholzer et al., 2021). This example provides promising advancement in the application of THM models to complex reservoir-scale processes. Since TOUGH+ also has reactive transport capabilities, geochemical modeling can also be conducted, making these models quite useful for carbon mineralization calculations. The main feature lacking in these models is a mechanistic representation of

fracture growth, which could be important during the injection phase if hydraulic fracturing is creating new fractures or if reaction-driven cracking is a dominant mechanism.

4.5. Thermo-Hydro-Chemical (THC) Modeling of Fractures

As fluids pass through fractures, which are the primary pathways through low-permeability rock in the Earth's subsurface (Bonnet et al., 2001; Deng & Spycher, 2019; National Research Council, 1996; Neuman, 2005; The National Academies of Sciences, Engineering, and Medicine, 2021; Viswanathan et al., 2022), they are commonly out of equilibrium with the resident minerals and a variety of chemical reactions, for example, dissolution and precipitation, will occur (Deng & Spycher, 2019; Laubach et al., 2019). These reactions control carbon mineralization rates in mafic and ultramafic rock and can alter the passage of fluid by changing the permeability of the system. Incorporating these chemical reactions into simulations is, thus, an effective tool for identifying key parameters that can hinder or optimize mineralization rates.

In contrast to THM modeling, a large amount of literature exists on THC modeling (e.g., reactive transport modeling) that is relevant to carbon mineralization in fractured systems. This class of model is capable of estimating relevant mineralization timescales if the input parameters can be constrained and adequate benchmark data can be provided. There are a variety of THC simulator options that differ in terms of spatial dimensions, discretization schemes, time integration methods, governing equations, flow simulator capabilities (single-phase Darcy flow, variable saturation Richards flow, multi-phase flow, variable density, non-isothermal, and heterogeneous permeability), transport formulations (advection, mechanical dispersion, molecular diffusion, multi-continuum), and geochemistry options (surface complexation, kinetic mineral precipitation-dissolution, aqueous kinetics, mineral nucleation, mineral solid-solutions). The most common simulators used today are PHREEQC (Parkhurst & Appelo, 2013) which is the geochemistry engine for HPx (Jacques et al., 2018), PHT3D (Prommer et al., 2003), OpenGeoSys (Kolditz et al., 2012), HYTEC (van Der Lee et al., 2003), ORCHESTRA (Meeussen, 2003), TOUGHREACT (T. Xu et al., 2011), eSTOMP (M. D. White & Oostrom, 2003), HYDROGEOCHEM (Yeh & Tripathi, 1990), CrunchFlow (Steeffel, 2009), MIN3P (Su et al., 2021), and PFLOTRAN (Lichtner et al., 2015). A comparison of strengths and weaknesses between the codes is provided by Steefel et al. (2015).

Recently, partially complete, coupled models that include thermo-hydro-chemical (THC) processes in fractured porous media have been used to simulate geochemical reactions during carbon sequestration (Dai et al., 2020 and references therein). In this section, we present an overview of currently available flow and reactive transport simulation codes in the context of subsurface porous and fractured media with a specific focus on their utility in modeling carbon mineralization at the pore and reservoir scale.

4.5.1. Pore-Scale THC Models

In recent decades, pore-scale models have been increasingly developed and utilized due to rapid advancement in imaging techniques, which provide detailed pore structures for numerical simulations, and rapid advancement in supercomputer architectures, which enable pore-scale simulation of rather large systems, sometimes allowing direct comparison between pore-scale simulations and experiments (L. Chen et al., 2022). Pore-scale models directly solve governing equations using fully resolved pore structures. Many studies have been focused on mineral dissolution in fractured porous media considering the resultant pore-structure change (L. Chen, Kang, Carey, & Tao, 2014; L. Chen, Kang, Viswanathan, & Tao, 2014; Q. Kang et al., 2002, 2014; M. Liu & Mostaghimi, 2017; Rasoulzadeh et al., 2020; Starchenko et al., 2016; Verberg & Ladd, 2002; Verhaeghe et al., 2005, 2006). These studies identified different dissolution regimes (e.g., uniform dissolution, face dissolution, wormholing) based on the combination of Peclet and Damköhler numbers, as well as conditions for transition between different regimes (Q. Kang et al., 2014). Further investigation of coupled dissolution and precipitation in two-dimensional (2D) domains has been carried out, where the effect of precipitation of a secondary solid phase on the dissolution of the primary solid phase is investigated under varying reaction kinetics, molar volume, surface roughness, and nucleation and crystal growth mechanisms (L. Chen, Kang, Carey, & Tao, 2014; L. Chen, Kang, Viswanathan, & Tao, 2014; Q. Kang et al., 2010). More recently, these models have evolved to 3D-space, where dissolution and precipitation in 3D fractures was simulated with evolving fracture geometry (Q. Kang et al., 2023). These collective pore-scale studies have improved our understanding of the complex coupling between fluid flow, solute transport, dissolution/precipitation, and evolution of pore structures and provided physics-based constitutive parameters for large-scale models of coupled THC processes.

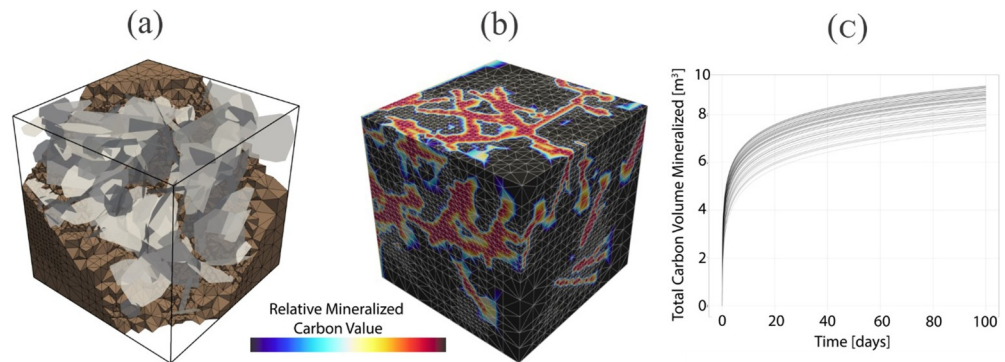


Figure 9. An example of a discrete fracture network inserted into a rock mass, allowing for a standard finite volume THC code to simulate mineralization reactions within heterogeneous flow fields. (a) A discrete fracture-matrix representative fracture network in a mafic rock. Fractures are gray discs and the rock matrix is shown in brown. (b) Results of simulating dissolution and precipitation reactions in the fracture network and rock matrix. Here we see the spatial variability in the mineralized carbon due to the heterogeneity created by the inclusion of the fracture network. (c) Estimates of the volume of CO₂ mineralized under different geochemical conditions with varying rock and fracture properties. These models allow researchers to test the relative importance of hydrological, geological, and geochemical properties on the total volume of carbon that can be mineralized.

4.5.2. Reservoir-Scale THC Models

THC reservoir-scale models are highly relevant for studying carbon mineralization in fractured systems since they capture the interplay between dissolution, precipitation, and fluid flow at a representative scale. In contrast to the pore-scale models described in the previous section, these models make continuum approximations to simulate larger scales. Specifically, continuum models do not explicitly consider features such as surface roughness in fractures but instead, use effective properties such as heterogeneous porosity and permeability to capture the effects of roughness. These models simulate key chemical reactions, such as dissolution and precipitation, by modifying the permeability and porosity within each computational cell. The modification of the porosity is used to update the rock's permeability using a constitutive relationship between permeability and porosity. The most common constitutive relation used in THC models is Kozeny/Kozeny-Carmen-like equations (Bear, 1988; Carman, 1939, 1956; Kozeny, 1927). However, further study is needed to determine if a more rigorous pore-scale relationship between reaction and permeability/porosity warrants modification of Kozeny-Carmen-like equations to treat mineralization.

Characterizing the feedback between the network structure, flow field, and associated reactive transport during carbon mineralization requires a coupled THC simulator capable of dynamically modifying flow resistance (hydraulic aperture/permeability) within a three-dimensional fracture network. The addition of fractures, however, adds a unique element of complexity to THC modeling. Within these models, fractures are mostly treated indirectly using effective parameters, where the fracture walls are not explicitly represented. Rather, most models retain a continuum formulation where the porosity and permeability of the cell capture the higher permeability of the fracture. To date, the inclusion of fractures into THC simulations has largely been carried out in a single fracture, small two-dimensional networks, or in upscaled/equivalent continuum models (Andrews & Navarre-Sitchler, 2021; Andrews et al., 2023; Deng, Molins, et al., 2018; Deng, Steefel, et al., 2018; Feng et al., 2019; Jones & Detwiler, 2019; Lebedeva & Brantley, 2017; Molins et al., 2019; Noiriel et al., 2021; Pandey & Rajaram, 2016; Steefel & Hu, 2022; Steefel & Lasaga, 1994; Steefel & Lichtner, 1998). Recently, however, THC modeling in 2D/3D DFN and DFM models has begun to take place, cf., Y. Tsang et al. (1996), Jackson et al. (2000), Lichtner (2000), Berkowitz (2002), MacQuarrie and Mayer (2005), Neuman (2005), Hartley and Joyce (2013), Hadgu et al. (2017), Steefel and MacQuarrie (2018), Iraola et al. (2019), Sweeney et al. (2020), Andrews and Navarre-Sitchler (2021), Pachaliev et al. (2023), Andrews et al. (2023), and references therein.

Three-dimensional high-fidelity simulations, although heavily sought after, have been relatively infeasible due to computational limitations. However, recent developments in high-performance computing now allow for the exploration of flow and reactive transport properties in 3-D fractured media (Hyman, Navarre-Sitchler, et al., 2022; Hyman, Sweeney, et al., 2022). Figure 9 shows the results of a reactive transport simulation in

fractured media using the dfnWorks software suite (Hyman et al., 2015). The fractures have a permeability that is multiple orders of magnitude times higher than that of the surrounding matrix. As fluid out of equilibrium is injected into the domain, carbon is mineralized. Note that these simulations only capture thermo-hydro-chemical coupling, not mechanical changes. Figure 9a shows the fracture network and rock matrix, Figure 9b shows the spatial variability of mineralized carbon at the end of the simulation, and Figure 9c shows the total volume of mineralized carbon for different realizations of the network but under the same hydro-chemical scenarios. These recently developed 3-D simulations offer a promising technique for estimating the amount of CO₂ that can be mineralized in a fracture network.

The most physically representative simulation tools for carbon mineralization systems are DFM methods where the matrix surrounding the fracture network is included in the model (Berre et al., 2019; Hyman, Navarre-Sitchler, et al., 2022; Hyman, Sweeney, et al., 2022). Because CO₂ could mineralize in both the fractures and rock matrix, the inclusion of both is warranted. Special numerical formulations, such as mimetic finite difference, are required for DFM models (Lipnikov et al., 2014). Chemistry is simulated using codes such as Alquimia, which allow for RTM to be performed (Andre et al., 2013; Hyman, Navarre-Sitchler, et al., 2022; Hyman, Sweeney, et al., 2022). Fracture software such as dfnWorks (Hyman et al., 2015) can be used with RTM models such as PFLOTRAN, FEHM (Zyvoloski, 2007), and AMANZI (Moulton et al., 2012). The large number of THC models and fracture software allow for a comprehensive study of THC mineralization processes at the reservoir scale.

A challenge for simulating field scale mineralization is that the apparent mineral dissolution rate can be orders of magnitude lower than the laboratory-measured rates (Andrews & Navarre-Sitchler, 2021; Atchley et al., 2013; Beisman et al., 2015; Jung & Navarre-Sitchler, 2018a; A. F. White & Brantley, 2003). In turn, many of these systems are transport-controlled and are not solely a function of the kinetic parameters used in standard geochemical models. These slow apparent dissolution rates are more common in fracture networks than homogeneous porous media due to the heterogeneous flow field induced by the fracture network (Andrews & Navarre-Sitchler, 2021; Andrews et al., 2023; Becker & Shapiro, 2000; Berkowitz & Scher, 1997; Ederly et al., 2016; Geiger et al., 2010; Haggerty et al., 2001; Huseby et al., 2001; Hyman et al., 2019; Jung & Navarre-Sitchler, 2018a, 2018b; P. Kang et al., 2020; Meigs & Beauheim, 2001; Painter et al., 2002; Pandey & Rajaram, 2016; Wen & Li, 2018). However, since these models do not incorporate mechanical effects, they cannot simulate coupled geochemical-mechanical processes such as reaction-driven cracking, subcritical cracking, or fracture reactivation/closure due to mineralization, which are likely critical for accessing sufficient host rock to make mineralization feasible. As with the THM models, pore-scale processes need to be abstracted and included in reservoir models. This is more straightforward for THC models since the reactive models employed at each spatial location are often the same in pore and reservoir scale models.

4.6. Thermo-Hydro-Mechanical-Chemical (THMC) Modeling

Developing a fully coupled THMC model is a challenging task due to the disparate timescales of THC and THM processes. Geochemical processes modify the fracture's hydraulic resistance (Ellis et al., 2013) and can drive or inhibit fracture propagation (Detwiler & Morris, 2018; Shovkun & Espinoza, 2019). For example, reaction-driven cracking, which may be an important process during carbon mineralization in low permeability rocks such as peridotite, would need a model that couples the chemical effects of dissolution and precipitation with mechanical effects that lead to fracturing of the rock. Alternatively, chemical reactions in fractured rock may lead to subcritical cracking by weakening the rock, resulting in fracturing due to existing or induced stress. Evidently, to arrive at a comprehensive multi-scale model that can capture critical carbon mineralization processes, THC and THM models need to be integrated.

To date, very few THMC studies related to carbon mineralization have been published. That being said, attempts have been made at the pore-scale in areas such as serpentinization and retrograde metamorphism, and thus, similar efforts could be applied to carbon mineralization in mafic and ultramafic rocks. Although not a fully coupled model, M. Liu and Mostaghimi (2017) investigated the impact of dissolution on the mechanical properties of porous media through pore-scale simulations. In their study, pore structures of sandstone and carbonate rocks before and after dissolution were used to predict their mechanical properties (effective Young's modulus and Poisson's ratio). Their simulation results showed a strong dependency of mechanical properties on the dissolution regime characterized by the Peclet and Damköhler numbers. Nonetheless, their simulations of HC and mechanical processes are not coupled. Malvoisin et al. (2017) used a pore-scale fracture mechanics method to compute the

serpentinization-induced propagation of a Mode I fracture from an initial etch pit in an olivine grain. The authors observed an increase in reactive surface area due to micro-cracking and found that the related evolution of bulk reaction rates compared well with experimental data on olivine powders. Other THMC-relevant examples are found in Jamtveit et al. (2008), L. Zhang et al. (2019), and Y. Zhang et al. (2019). Jamtveit et al. (2008) used a 2D spring-network model of a rock undergoing a retrograde metamorphic reaction. The model shows that the network of micro-cracks resulting from the induced stress heterogeneity assists the migration of fluid in a rock that has a negligible initial permeability. It supports the hypothesis that the increase of solid volume accompanying retrograde metamorphic reaction is critical for ensuring a self-sustaining process. L. Zhang et al. (2019) and Y. Zhang et al. (2019) utilized a 3D FDEM to analyze the fracturing induced by volumetric expansion during a metamorphic reaction. The model is capable of reproducing many features observed in the periclase hydration experiment reported by Zheng et al. (2018), such as the existence of a porosity pulse accompanying the moving reaction front.

At the reservoir scale, the feasibility of using scCO₂ as a working fluid in geothermal reservoirs was assessed by Gan et al. (2021). The THMC model incorporated changes in mineral dissolution and precipitation during the injection of scCO₂ and the resultant evolution of the permeability and porosity of the reservoir. The authors determined that injecting CO₂ could be a favorable option as it increases the permeability and porosity of the aquifer more effectively than water-based circulation and is more capable of extracting heat energy from the rock.

These studies show that some progress has been made on fully coupled THMC at the pore and reservoir scale. While the examples provided above are relevant, specific models that incorporate the key geochemical and mechanical processes that occur during carbon mineralization are necessary. To arrive at this, key challenges need to be addressed, which have been discussed above and are summarized below.

4.7. Challenges With the Development of Representative Carbon Mineralization Models

Several challenges exist with the development of realistic carbon mineralization models that incorporate all aspects of carbon mineralization. Current models either specialize in THM or THC processes and a fully coupled THMC model does not exist at the reservoir scale. Given that the development of a successful carbon mineralization operation is likely to depend on the optimization of the coupled effects between geochemistry and geomechanics to create positive feedback to access sufficient host rock, moving toward a fully coupled model is a priority. The disparate timescales of THM and THC make a fully coupled model problematic. Model decomposition techniques that correctly model short- and long-term scale processes are a possibility. Pseudo-steady state assumptions can also be attempted.

Carbon mineralization is inherently a multi-scale problem and therefore large-scale macroscopic field observations, controlled small-scale laboratory experiments, and reduced complexity models are needed to inform and constrain multi-scale simulations that include UQ. Another challenge is unconstrained, uncertain, and unknown reaction and fracture parameters, which could yield inaccurate results that are not reproducible at the field scale. Robust and representative experimental studies are needed to accurately derive these parameters.

5. Conclusions and Outlook

To mitigate the current global climate crisis, immediate action must be taken to reduce atmospheric CO₂ levels. Carbon mineralization in mafic and ultramafic geologic reservoirs has been proven through recent field studies at CarbFix1 and CarbFix2 in Iceland and Wallula in Washington, USA, to be a promising means for quickly and securely storing CO₂ in the subsurface. However, many unknowns remain that must be addressed before storage operations can be scaled up and expanded to other favorable subsurface lithologies. In this review, we have outlined the critical first-order processes that must be considered while exploring this complex system, outstanding questions to be answered through experimental and modeling efforts, and ongoing pilot-scale field tests.

First, regarding the field scale studies of carbon mineralization, while rapid and highly efficient mineralization was observed in CarbFix, CarbFix2, and Wallula, generalization of these results to other potential field sites necessitates answering key questions including (a) whether upscaling using CO₂-saturated water can be feasible given the water requirements or if supercritical CO₂ injection is needed to scale-up efforts; (b) whether performance can be maintained over extended periods; and (c) how these findings can be applied to less permeable lithologies. The last question is currently being explored through field tests in relatively impermeable Oman

ophiolite, however, it opens the door to many further questions surrounding how mineralization within fractured systems will impact the connected fracture network. These include whether reaction-driven fracturing and sub-critical fracturing could enhance storage volumes and formation permeability, or whether carbonate precipitation leads to passivation of reactive surfaces or fracture clogging, quickly depleting the storage potential.

Second, we refine the extensive published literature on experimental studies of carbon mineralization to gain insight into how this reaction will proceed within fractured systems. While many studies exist to quantify the rates of carbonate mineral precipitation, particularly from the reaction of CO₂ with olivine, major uncertainties remain as to how this reaction will occur within fractures in the field, where reaction rates will be a function of the available surface area and the extent of reaction front penetration into an impermeable rock is uncertain. Flow through laboratory experiments can better reflect the reaction system in the field, where the relative reaction versus transport rates will greatly influence mineralization regimes. However, these experiments must also capture the impacts of the reaction on fracture propagation and activation. Lastly, differences between experimental studies and field observations must be considered. This includes the effects of surface passivation and differences in reaction conditions, typically employed to accelerate reaction rates to be observable at faster timescales. The effects of field-scale fracture networks and connectivity on these reaction processes must also be considered.

Finally, we explore currently available mathematical models and computational tools for simulating carbon mineralization on the pore-to-reservoir scale and make recommendations for improving these simulations to capture critical mechanisms observed through experiments and in the field. The biggest perceived challenge is coupling developed thermo-hydro-mechanical and thermo-hydro-chemical models to THMC models, which can simulate the simultaneous dissolution and precipitation processes that drive carbon mineralization while also capturing how this process can drive fracturing through stress corrosion and reaction-driven fracturing. An equally important challenge is that many parameters needed for models must still be constrained through further experiments and field studies or the models will not be predictive. Defensible predictions within uncertainty bounds of field-scale carbon mineralization in fractured systems, achieved through closing the knowledge gaps outlined in this review, will enable us to take full advantage of this strategy to reduce atmospheric CO₂ emissions and address the current climate crisis.

Conflict of Interest

The authors declare no conflicts of interest relevant to this study.

Data Availability Statement

Data were not used, nor created for this research.

Acknowledgments

The research was primarily supported as part of the Center on Geo-processes in Mineral Carbon Storage, an Energy Frontier Research Center funded by the U. S. Department of Energy (DOE), Office of Science, Basic Energy Sciences (BES), under Award Number DE-SC0023429. This award provided financial support for G. Buscarnera, J.W. Carey, M.A. Chen, E. Detournay, H. Huang, J.D. Hyman, P.K. Kang, Q. Kang, J.F. Labuz, W. Li, J. Matter, C.W. Neil, G. Srinivasan, M.R. Sweeney, V.R. Voller, W. Yang, Y. Yang, and H.S. Viswanathan. H. Nisbet, J.D. Hyman, W. Li, M.R. Sweeney, and H.S. Viswanathan gratefully acknowledge support from the Department of Energy, Office of Science, Office of Basic Energy Sciences, Geoscience Research program under Award Number LANL3W1. H. Nisbet thanks the support of the Laboratory Directed Research and Development program of Los Alamos National Laboratory under Project Number 20220809PRD4. J. Matter gratefully acknowledges the support from the ClimateWorks Foundation under Award Number G-21030802317354.

References

- Adeoye, J. T., Menefee, A. H., Xiong, W., Wells, R. K., Skemer, P., Giammar, D. E., & Ellis, B. R. (2017). Effect of transport limitations and fluid properties on reaction products in fractures of unaltered and serpentinized basalt exposed to high PCO fluids. *International Journal of Greenhouse Gas Control*, 63, 310–320. <https://doi.org/10.1016/j.ijggc.2017.06.003>
- Ahoulou, A. W. A., Tinet, A.-J., Oltéan, C., & Golfier, F. (2020). Experimental insights into the interplay between buoyancy, convection, and dissolution reaction. *Journal of Geophysical Research: Solid Earth*, 125(11), e2020JB020854. <https://doi.org/10.1029/2020JB020854>
- Al-Busaidi, A., Hazzard, J. F., & Young, R. P. (2005). Distinct element modeling of hydraulically fractured Lac du Bonnet granite. *Journal of Geophysical Research*, 110(B6), B06302. <https://doi.org/10.1029/2004jb003297>
- Alfredsson, H. A., Oelkers, E. H., Hardarsson, B. S., Franzson, H., Gunnlaugsson, E., & Gislason, S. R. (2013). The geology and water chemistry of the Hellisheidi, SW-Iceland carbon storage site. *International Journal of Greenhouse Gas Control*, 12, 399–418. <https://doi.org/10.1016/j.ijggc.2012.11.019>
- Aminu, M. D., Nabavi, S. A., Rochelle, C. A., & Manovic, V. (2017). A review of developments in carbon dioxide storage. *Applied Energy*, 208, 1389–1419. <https://doi.org/10.1016/j.apenergy.2017.09.015>
- Amor, M. B., Zgolli, D., Tlili, M. M., & Manzola, A. S. (2004). Influence of water hardness, substrate nature and temperature on heterogeneous calcium carbonate nucleation. *Desalination*, 166, 79–84. <https://doi.org/10.1016/j.desal.2004.06.061>
- Andre, B., Molins, S., Johnson, J., & Steefel, C. (2013). *Alquimia* (Technical Report). Lawrence Berkeley National Lab (LBNL).
- Andreani, M., Luquot, L., Gouze, P., Godard, M., Hoisé, E., & Gibert, B. (2009). Experimental study of carbon sequestration reactions controlled by the percolation of CO₂-rich brine through peridotites. *Environmental Science & Technology*, 43(4), 1226–1231. <https://doi.org/10.1021/es8018429>
- Andrews, E., & Navarre-Sitchler, A. (2021). Temporal and spatial heterogeneity of mineral dissolution rates in fractured media. *Geochimica et Cosmochimica Acta*, 312, 124–138. <https://doi.org/10.1016/j.gca.2021.08.008>
- Andrews, E. M., Hyman, J. D., Sweeney, M. R., Karra, S., Moulton, J. D., & Navarre-Sitchler, A. (2023). Fracture intensity impacts on reaction front propagation and mineral weathering in three-dimensional fractured media. *Water Resources Research*, 59(2), e2022WR032121. <https://doi.org/10.1029/2022WR032121>

- Aradóttir, E. S. P., Sonnenthal, E. L., Björnsson, G., & Jónsson, H. (2012). Multidimensional reactive transport modeling of CO₂ mineral sequestration in basalts at the Hellisheidi geothermal field, Iceland. *International Journal of Greenhouse Gas Control*, 9, 24–40. <https://doi.org/10.1016/j.ijggc.2012.02.006>
- Arvidson, R. S., Ertan, I. E., Amonette, J. E., & Luttge, A. (2003). Variation in calcite dissolution rates: A fundamental problem? *Geochimica et Cosmochimica Acta*, 67(9), 1623–1634. [https://doi.org/10.1016/S0016-7037\(02\)01177-8](https://doi.org/10.1016/S0016-7037(02)01177-8)
- Atchley, A. L., Maxwell, R. M., & Navarre-Sitchler, A. K. (2013). Using streamlines to simulate stochastic reactive transport in heterogeneous aquifers: Kinetic metal release and transport in CO₂ impacted drinking water aquifers. *Advances in Water Resources*, 52, 93–106. <https://doi.org/10.1016/j.advwatres.2012.09.005>
- Atkinson, B. K. (1984). Subcritical crack growth in geological materials. *Journal of Geophysical Research*, 89(B6), 4077–4114. <https://doi.org/10.1029/jb089ib06p04077>
- Aubele, J. C., Crumpler, L. S., & Elston, W. E. (1988). Vesicle zonation and vertical structure. *Journal of Volcanology and Geothermal Research*, 35(4), 349–374. [https://doi.org/10.1016/0377-0273\(88\)90028-5](https://doi.org/10.1016/0377-0273(88)90028-5)
- Baek, S.-H., Hong, J.-W., Kim, K. Y., Yeom, S., & Kwon, T.-H. (2019). X-ray computed microtomography imaging of abiogenic carbonate precipitation in porous media from a supersaturated solution: Insights into effect of CO₂ mineral trapping on permeability. *Water Resources Research*, 55(5), 3835–3855. <https://doi.org/10.1029/2018WR023578>
- Barati, R., & Liang, J. (2014). A review of fracturing fluid systems used for hydraulic fracturing of oil and gas wells. *Journal of Applied Polymer Science*, 131(16), 40735. <https://doi.org/10.1002/app.40735>
- Barenblatt, G. I. (1996). *Scaling, self-similarity, and intermediate asymptotics: Dimensional analysis and intermediate asymptotics*. Cambridge University Press.
- Bear, J. (1988). *Dynamics of fluids in porous media*. Dover Publications.
- Béarat, H., McKelvy, M. J., Chizmeshya, A. V. G., Gormley, D., Nunez, R., Carpenter, R. W., et al. (2006). Carbon sequestration via aqueous olivine mineral carbonation: Role of passivating layer formation. *Environmental Science & Technology*, 40(15), 4802–4808. <https://doi.org/10.1021/es052334o>
- Becker, M. W., & Shapiro, A. M. (2000). Tracer transport in fractured crystalline rock: Evidence of nondiffusive breakthrough tailing. *Water Resources Research*, 36(7), 1677–1686. <https://doi.org/10.1029/2000WR900080>
- Beinlich, A., Plümper, O., Boter, E., Müller, I. A., Kourim, F., Ziegler, M., et al. (2020). Ultramafic rock carbonation: Constraints from listvenite core BT1B, Oman Drilling Project. *Journal of Geophysical Research: Solid Earth*, 125(6), e2019JB019060. <https://doi.org/10.1029/2019jb019060>
- Beisman, J. J., Maxwell, R. M., Navarre-Sitchler, A. K., Steefel, C. I., & Molins, S. (2015). ParCrunchFlow: An efficient, parallel reactive transport simulation tool for physically and chemically heterogeneous saturated subsurface environments. *Computational Geosciences*, 19(2), 403–422. <https://doi.org/10.1007/s10596-015-9475-x>
- Berkowitz, B. (2002). Characterizing flow and transport in fractured geological media: A review. *Advances in Water Resources*, 25(8–12), 861–884. [https://doi.org/10.1016/S0309-1708\(02\)00042-8](https://doi.org/10.1016/S0309-1708(02)00042-8)
- Berkowitz, B., & Scher, H. (1997). Anomalous transport in random fracture networks. *Physical Review Letters*, 79(20), 4038–4041. <https://doi.org/10.1103/PhysRevLett.79.4038>
- Berre, I., Doster, F., & Keilegavlen, E. (2019). Flow in fractured porous media: A review of conceptual models and discretization approaches. *Transport in Porous Media*, 130(1), 215–236. <https://doi.org/10.1007/s11242-018-1171-6>
- Birkholzer, J. T., Morris, J., Bargar, J. R., Brondolo, F., Cihan, A., Crandall, D., et al. (2021). A new modeling framework for multi-scale simulation of hydraulic fracturing and production from unconventional reservoirs. *Energies*, 14(3), 641. <https://doi.org/10.3390/en14030641>
- Boese, C. M., Kwiatek, G., Fischer, T., Plenkers, K., Starke, J., Blümle, F., et al. (2022). Seismic monitoring of the STIMTEC hydraulic stimulation experiment in anisotropic metamorphic gneiss. *Solid Earth*, 13(2), 323–346. <https://doi.org/10.5194/se-13-323-2022>
- Bonnet, E., Bour, O., Odling, N. E., Davy, P., Main, I., Cowie, P., & Berkowitz, B. (2001). Scaling of fracture systems in geological media. *Reviews of Geophysics*, 39(3), 347–383. <https://doi.org/10.1029/1999RG000074>
- Boutt, D. F., Cook, B. K., & Williams, J. R. (2011). A coupled fluid–solid model for problems in geomechanics: Application to sand production. *International Journal for Numerical and Analytical Methods in Geomechanics*, 35(9), 997–1018. <https://doi.org/10.1002/nag.938>
- Brantut, N., Heap, M. J., Meredith, P. G., & Baud, P. (2013). Time-dependent cracking and brittle creep in crustal rocks: A review. *Journal of Structural Geology*, 52, 17–43. <https://doi.org/10.1016/j.jsg.2013.03.007>
- Bunger, A. P., Detournay, E., & Garagash, D. I. (2005). Toughness-dominated hydraulic fracture with leak-off. *International Journal of Fracture*, 134(2), 175–190. <https://doi.org/10.1007/s10704-005-0154-0>
- Burns, E. R., Williams, C. F., Ingebritsen, S. E., Voss, C. I., Spane, F. A., & DeAngelo, J. (2015). Understanding heat and groundwater flow through continental flood basalt provinces: Insights gained from alternative models of permeability/depth relationships for the Columbia Plateau, USA. *Geofluids*, 15(1–2), 120–138. <https://doi.org/10.1111/gfl.12095>
- Cao, H., Yoon, S., Xu, Z., Pyrak-Nolte, L., Bresciani, E., & Kang, P. (2023). Emergence of unstable focused flow induced by variable-density flows in vertical fracture. *Water Resources Research*, 59(12), e2023WR034729. <https://doi.org/10.1029/2023wr034729>
- Caprarello, G., & Reidel, S. P. (2004). Physical evolution of Grande Ronde Basalt magmas, Columbia River Basalt Group, north-western USA. *Mineralogy and Petrology*, 80(1–2), 1–25. <https://doi.org/10.1007/s00710-003-0017-1>
- Cardona, A., & Santamarina, J. C. (2023). Immiscible imbibition in fractured media: A dual-porosity microfluidics study. *International Journal of Rock Mechanics and Mining Sciences*, 170, 105555. <https://doi.org/10.1016/j.ijrmms.2023.105555>
- Carman, P. (1939). Permeability of saturated sands, soils and clays. *The Journal of Agricultural Science*, 29(2), 262–273. <https://doi.org/10.1017/s0021859600051789>
- Carman, P. C. (1956). *Flow of gases through porous media*. Academic Press New York.
- Chen, L., He, A., Zhao, J., Kang, Q., Li, Z.-Y., Carmeliet, J., et al. (2022). Pore-scale modeling of complex transport phenomena in porous media. *Progress in Energy and Combustion Science*, 88, 100968. <https://doi.org/10.1016/j.pecs.2021.100968>
- Chen, L., Kang, Q., Carey, B., & Tao, W.-Q. (2014). Pore-scale study of diffusion–reaction processes involving dissolution and precipitation using the lattice Boltzmann method. *International Journal of Heat and Mass Transfer*, 75, 483–496. <https://doi.org/10.1016/j.ijheatmasstransfer.2014.03.074>
- Chen, L., Kang, Q., Viswanathan, H. S., & Tao, W.-Q. (2014). Pore-scale study of dissolution-induced changes in hydrologic properties of rocks with binary minerals. *Water Resources Research*, 50(12), 9343–9365. <https://doi.org/10.1002/2014wr015646>
- Chen, Z., Jin, X., & Wang, M. (2018). A new thermo-mechanical coupled DEM model with non-spherical grains for thermally induced damage of rocks. *Journal of the Mechanics and Physics of Solids*, 116, 54–69. <https://doi.org/10.1016/j.jmps.2018.03.023>
- Chen, Z., & Wang, M. (2017). Pore-scale modeling of hydromechanical coupled mechanics in hydrofracturing process. *Journal of Geophysical Research: Solid Earth*, 122(5), 3410–3429. <https://doi.org/10.1002/2017jb013989>

- Chen, Z., Yang, Z., & Wang, M. (2018). Hydro-mechanical coupled mechanisms of hydraulic fracture propagation in rocks with cemented natural fractures. *Journal of Petroleum Science and Engineering*, 163, 421–434. <https://doi.org/10.1016/j.petrol.2017.12.092>
- Chen, Z.-Y., O'Connor, W. K., & Gerdemann, S. J. (2006). Chemistry of aqueous mineral carbonation for carbon sequestration and explanation of experimental results. *Environmental Progress*, 25(2), 161–166. <https://doi.org/10.1002/ep.10127>
- Clark, D. E., Gunnarsson, I., Aradóttir, E. S., P. Arnarson, M., Þorgeirsson, P. A., Sigurðardóttir, S. S., et al. (2018). The chemistry and potential reactivity of the CO₂-H₂S charged injected waters at the basaltic CarbFix2 site, Iceland. *Energy Procedia*, 146, 121–128. <https://doi.org/10.1016/j.egypro.2018.07.016>
- Clark, D. E., Oelkers, E. H., Gunnarsson, I., Sigfússon, B., Snæbjörnsdóttir, S. Ó., Aradóttir, E. S., & Gíslason, S. R. (2020). CarbFix2: CO₂ and H₂S mineralization during 3.5 years of continuous injection into basaltic rocks at more than 250°C. *Geochimica et Cosmochimica Acta*, 279, 45–66. <https://doi.org/10.1016/j.gca.2020.03.039>
- Colombani, J. (2008). Measurement of the pure dissolution rate constant of a mineral in water. *Geochimica et Cosmochimica Acta*, 72(23), 5634–5640. <https://doi.org/10.1016/j.gca.2008.09.007>
- Correns, C. W. (1949). Growth and dissolution of crystals under linear pressure. *Discussions of the Faraday Society*, 5, 267. <https://doi.org/10.1039/d19490500267>
- Crevacore, E., Tosco, T., Sethi, R., Boccardo, G., & Marchisio, D. L. (2016). Recirculation zones induce non-Fickian transport in three-dimensional periodic porous media. *Physical Review E*, 94(5), 053118. <https://doi.org/10.1103/PhysRevE.94.053118>
- Cubillas, P., Köhler, S., Prieto, M., Causserand, C., & Oelkers, E. H. (2005). How do mineral coatings affect dissolution rates? An experimental study of coupled CaCO₃ dissolution—CdCO₃ precipitation. *Geochimica et Cosmochimica Acta*, 69(23), 5459–5476. <https://doi.org/10.1016/j.gca.2005.07.016>
- Cui, X., & Wong, L. N. Y. (2021). A 3D thermo-hydro-mechanical coupling model for enhanced geothermal systems. *International Journal of Rock Mechanics and Mining Sciences*, 143, 104744. <https://doi.org/10.1016/j.ijrmms.2021.104744>
- Dai, Z., Xu, L., Xiao, T., McPherson, B., Zhang, X., Zheng, L., et al. (2020). Reactive chemical transport simulations of geologic carbon sequestration: Methods and applications. *Earth-Science Reviews*, 208, 103265. <https://doi.org/10.1016/j.earscirev.2020.103265>
- Datta, S. S., Battiatto, I., Fernø, M. A., Juanes, R., Parsa, S., Prigiobbe, V., et al. (2023). Lab on a chip for a low-carbon future. *Lab on a Chip*, 23(5), 1358–1375. <https://doi.org/10.1039/D2LC00020B>
- De Choudens-Sánchez, V., & Gonzalez, L. A. (2009). Calcite and aragonite precipitation under controlled instantaneous supersaturation: Elucidating the role of CaCO₃ saturation state and Mg/Ca ratio on calcium carbonate polymorphism. *Journal of Sedimentary Research*, 79(6), 363–376. <https://doi.org/10.2110/jsr.2009.043>
- Deng, H., Dai, Z., Wolfsberg, A., Lu, Z., Ye, M., & Reimus, P. (2010). Upscaling of reactive mass transport in fractured rocks with multimodal reactive mineral facies. *Water Resources Research*, 46(6), 2009WR008363. <https://doi.org/10.1029/2009WR008363>
- Deng, H., Fitts, J. P., Tappero, R. V., Kim, J. J., & Peters, C. A. (2020). Acid erosion of carbonate fractures and accessibility of arsenic-bearing minerals: In operando synchrotron-based microfluidic experiment. *Environmental Science & Technology*, 54(19), 12502–12510. <https://doi.org/10.1021/acs.est.0c03736>
- Deng, H., Molins, S., Trebotich, D., Steefel, C., & DePaolo, D. (2018). Pore-scale numerical investigation of the impacts of surface roughness: Upscaling of reaction rates in rough fractures. *Geochimica et Cosmochimica Acta*, 239, 374–389. <https://doi.org/10.1016/j.gca.2018.08.005>
- Deng, H., & Spycher, N. (2019). Modeling reactive transport processes in fractures. *Reviews in Mineralogy and Geochemistry*, 85(1), 49–74. <https://doi.org/10.2138/rmg.2019.85.3>
- Deng, H., Steefel, C., Molins, S., & DePaolo, D. (2018). Fracture evolution in multimaterial systems: The role of mineral composition, flow rate, and fracture aperture heterogeneity. *ACS Earth and Space Chemistry*, 2(2), 112–124. <https://doi.org/10.1021/acsearthspacechem.7b00130>
- De Obeso, J. C., Awolayo, A. N., Nightingale, M. J., Tan, C., & Tutolo, B. M. (2023). Experimental study on plagioclase dissolution rates at conditions relevant to mineral carbonation of seafloor basalts. *Chemical Geology*, 620, 121348. <https://doi.org/10.1016/j.chemgeo.2023.121348>
- DePaolo, D. J., & Cole, D. R. (2013). Geochemistry of geologic carbon sequestration: An overview. *Reviews in Mineralogy and Geochemistry*, 77(1), 1–14. <https://doi.org/10.2138/rmg.2013.77.1>
- Detournay, E. (2016). Mechanics of hydraulic fractures. *Annual Review of Fluid Mechanics*, 48(1), 311–339. <https://doi.org/10.1146/annurev-fluid-010814-014736>
- Detwiler, R. L., & Morris, J. P. (2018). Fracture initiation, propagation, and permeability evolution. *Geological carbon storage: Subsurface seals and caprock integrity* (pp. 119–135).
- Dewandel, B., Lachassagne, P., Boudier, F., Al-Hattali, S., Ladouche, B., Pinault, J.-L., & Al-Suleimani, Z. (2005). A conceptual hydrogeological model of ophiolite hard-rock aquifers in Oman based on a multiscale and a multidisciplinary approach. *Hydrogeology Journal*, 13(5–6), 708–726. <https://doi.org/10.1007/s10040-005-0449-2>
- Dormieux, L. (2006). *Microporomechanics*. Wiley.
- Dormieux, L., & Kondo, D. (2016). *Micromechanics of fracture and damage* (1st ed.). John Wiley & Sons.
- Dreybrodt, W., Eisenlohr, L., Madry, B., & Ringer, S. (1997). Precipitation kinetics of calcite in the system CaCO₃-H₂O-CO₂: The conversion to CO₂ by the slow process H⁺ + HCO₃⁻ → CO₂ + H₂O as a rate limiting step. *Geochimica et Cosmochimica Acta*, 61(18), 3897–3904. [https://doi.org/10.1016/s0016-7037\(97\)00201-9](https://doi.org/10.1016/s0016-7037(97)00201-9)
- Ederly, Y., Geiger, S., & Berkowitz, B. (2016). Structural controls on anomalous transport in fractured porous rock. *Water Resources Research*, 52(7), 5634–5643. <https://doi.org/10.1002/2016wr018942>
- Eisenlohr, L., Meteva, K., Gabrovšek, F., & Dreybrodt, W. (1999). The inhibiting action of intrinsic impurities in natural calcium carbonate minerals to their dissolution kinetics in aqueous H₂O-CO₂ solutions. *Geochimica et Cosmochimica Acta*, 63(7–8), 989–1001. [https://doi.org/10.1016/S0016-7037\(98\)00301-9](https://doi.org/10.1016/S0016-7037(98)00301-9)
- Ellis, B. R., Fitts, J. P., Bromhal, G. S., McIntyre, D. L., Tappero, R., & Peters, C. A. (2013). Dissolution-driven permeability reduction of a fractured carbonate caprock. *Environmental Engineering Science*, 30(4), 187–193. <https://doi.org/10.1089/ees.2012.0337>
- English, J. M. (2012). Thermomechanical origin of regional fracture systems. *AAPG Bulletin*, 96(9), 1597–1625. <https://doi.org/10.1306/01021211018>
- Ennis-King, J., & Paterson, L. (2007). Coupling of geochemical reactions and convective mixing in the long-term geological storage of carbon dioxide. *International Journal of Greenhouse Gas Control*, 1(1), 86–93. [https://doi.org/10.1016/S1750-5836\(07\)00034-5](https://doi.org/10.1016/S1750-5836(07)00034-5)
- Eppes, M. A., & Keanini, R. (2017). Mechanical weathering and rock erosion by climate-dependent subcritical cracking. *Reviews of Geophysics*, 55(2), 470–508. <https://doi.org/10.1002/2017rg000557>
- Evans, O., Spiegelman, M., & Kelemen, P. B. (2020). Phase-field modeling of reaction-driven cracking: Determining conditions for extensive olivine serpentinization. *Journal of Geophysical Research: Solid Earth*, 125(1), e2019JB018614. <https://doi.org/10.1029/2019JB018614>

- Falk, E. S., & Kelemen, P. B. (2015). Geochemistry and petrology of listvenite in the Samail ophiolite, Sultanate of Oman: Complete carbonation of peridotite during ophiolite emplacement. *Geochimica et Cosmochimica Acta*, 160, 70–90. <https://doi.org/10.1016/j.gca.2015.03.014>
- Farkas, M. P., Yoon, J. S., Zang, A., Zimmermann, G., Stephansson, O., Lemon, M., & Dankó, G. (2019). Effect of foliation and fluid viscosity on hydraulic fracturing tests in mica schists investigated using distinct element modeling and field data. *Rock Mechanics and Rock Engineering*, 52(2), 555–574. <https://doi.org/10.1007/s00603-018-1598-7>
- Fazeli, H., Nooraiepour, M., & Hellevang, H. (2020). Microfluidic study of fracture dissolution in carbonate-rich caprocks subjected to CO₂-charged brine. *Industrial & Engineering Chemistry Research*, 59(1), 450–457. <https://doi.org/10.1021/acs.iecr.9b06048>
- Feng, J., Zhang, X., Luo, P., Li, X., & Du, H. (2019). Mineral filling pattern in complex fracture system of carbonate reservoirs: Implications from geochemical modeling of water-rock interaction. *Geofluids*, 2019, 1–19. <https://doi.org/10.1155/2019/3420142>
- Fisher, K., & Warpinski, N. (2012). Hydraulic-fracture-height growth: Real data. *SPE Production & Operations*, 27(1), 8–19. <https://doi.org/10.2118/145949-pa>
- Fletcher, R., Buss, H., & Brantley, S. (2006). A spheroidal weathering model coupling porewater chemistry to soil thicknesses during steady-state denudation. *Earth and Planetary Science Letters*, 244(1–2), 444–457. <https://doi.org/10.1016/j.epsl.2006.01.055>
- Forjanes, P., Astilleros, J. M., & Fernández-Díaz, L. (2020). The formation of barite and celestite through the replacement of gypsum. *Minerals*, 10(2), 189. <https://doi.org/10.3390/min10020189>
- Fredd, C. N., & Fogler, H. S. (1998). Influence of transport and reaction on wormhole formation in porous media. *AIChE Journal*, 44(9), 1933–1949. <https://doi.org/10.1002/aic.690440902>
- French, M. E., Zhu, W., & Banker, J. (2016). Fault slip controlled by stress path and fluid pressurization rate. *Geophysical Research Letters*, 43(9), 4330–4339. <https://doi.org/10.1002/2016GL068893>
- Fu, P., Schoenball, M., Ajo-Franklin, J. B., Chai, C., Maceira, M., Morris, J. P., et al. (2021). Close observation of hydraulic fracturing at EGS Collab Experiment 1: Fracture trajectory, microseismic interpretations, and the role of natural fractures. *Journal of Geophysical Research: Solid Earth*, 126(7), e2020JB020840. <https://doi.org/10.1029/2020JB020840>
- Gadikota, G., Matter, J., Kelemen, P., Brady, P. V., & Park, A.-H. A. (2020). Elucidating the differences in the carbon mineralization behaviors of calcium and magnesium bearing aluminosilicates and magnesium silicates for CO₂ storage. *Fuel*, 277, 117900. <https://doi.org/10.1016/j.fuel.2020.117900>
- Gadikota, G., Matter, J., Kelemen, P., & Park, A. A. (2014). Chemical and morphological changes during olivine carbonation for CO₂ storage in the presence of NaCl and NaHCO₃. *Physical Chemistry Chemical Physics*, 16(10), 4679. <https://doi.org/10.1039/c3cp54903h>
- Gale, J. F. W., Elliott, S. J., & Laubach, S. E. (2018). Hydraulic fractures in core from stimulated reservoirs: Core fracture description of HFTs slant core, Midland Basin, West Texas. In *SPE/AAPG/SEG Unconventional Resources Technology Conference 2018, URTC 2018*. Society of Exploration Geophysicists, American Association of Petroleum Geologists, Society of Petroleum Engineers.
- Gale, J. F. W., Laubach, S. E., Olson, J. E., Eichhubl, P., & Fall, A. (2014). Natural fractures in shale; a review and new observations. *AAPG Bulletin*, 98(11), 2165–2216. <https://doi.org/10.1306/08121413151>
- Gan, Q., Candela, T., Wassing, B., Wasch, L., Liu, J., & Elsworth, D. (2021). The use of supercritical CO₂ in deep geothermal reservoirs as a working fluid: Insights from coupled THMC modeling. *International Journal of Rock Mechanics and Mining Sciences*, 147, 104872. <https://doi.org/10.1016/j.ijrmms.2021.104872>
- Garcia, B., Beaumont, V., Perfetti, E., Rouchon, V., Blanchet, D., Oger, P., et al. (2010). Experiments and geochemical modelling of CO₂ sequestration by olivine: Potential, quantification. *Applied Geochemistry*, 25(9), 1383–1396. <https://doi.org/10.1016/j.apgeochem.2010.06.009>
- Garipov, T. T., & Hui, M. H. (2019). Discrete fracture modeling approach for simulating coupled thermo-hydro-mechanical effects in fractured reservoirs. *International Journal of Rock Mechanics and Mining Sciences*, 122, 104075. <https://doi.org/10.1016/j.ijrmms.2019.104075>
- Geiger, S., Cortis, A., & Birkholzer, J. (2010). Upscaling solute transport in naturally fractured porous media with the continuous time random walk method. *Water Resources Research*, 46(12), W12530. <https://doi.org/10.1029/2010wr009133>
- Ghassemi, A. (2012). A review of some rock mechanics issues in geothermal reservoir development. *Geotechnical and Geological Engineering*, 30(3), 647–664. <https://doi.org/10.1007/s10706-012-9508-3>
- Ghassemi, A., & Suresh Kumar, G. (2007). Changes in fracture aperture and fluid pressure due to thermal stress and silica dissolution/precipitation induced by heat extraction from subsurface rocks. *Geothermics*, 36(2), 115–140. <https://doi.org/10.1016/j.geothermics.2006.10.001>
- Giammar, D. E., Bruant, R. G., & Peters, C. A. (2005). Forsterite dissolution and magnesite precipitation at conditions relevant for deep saline aquifer storage and sequestration of carbon dioxide. *Chemical Geology*, 217(3–4), 257–276. <https://doi.org/10.1016/j.chemgeo.2004.12.013>
- Gislason, S. R., & Oelkers, E. H. (2014). Carbon storage in basalt. *Science*, 344(6182), 373–374. <https://doi.org/10.1126/science.1250828>
- Gislason, S. R., Wolff-Boenisch, D., Stefansson, A., Oelkers, E. H., Gunnlaugsson, E., Sigurdardottir, H., et al. (2010). Mineral sequestration of carbon dioxide in basalt: A pre-injection overview of the CarbFix project. *International Journal of Greenhouse Gas Control*, 4(3), 537–545. <https://doi.org/10.1016/j.ijggc.2009.11.013>
- Golfier, F., Zarcone, C., Bazin, B., Lenormand, R., Lasseux, D., & Quintard, M. (2002). On the ability of a Darcy-scale model to capture wormhole formation during the dissolution of a porous medium. *Journal of Fluid Mechanics*, 457, 213–254. <https://doi.org/10.1017/s0022112002007735>
- Golubev, S. V., Pokrovsky, O. S., & Schott, J. (2005). Experimental determination of the effect of dissolved CO₂ on the dissolution kinetics of Mg and Ca silicates at 25°C. *Chemical Geology*, 217(3–4), 227–238. <https://doi.org/10.1016/j.chemgeo.2004.12.011>
- Gudbrandsson, S., Wolff-Boenisch, D., Gislason, S. R., & Oelkers, E. H. (2014). Experimental determination of plagioclase dissolution rates as a function of its composition and pH at 22°C. *Geochimica et Cosmochimica Acta*, 139, 154–172. <https://doi.org/10.1016/j.gca.2014.04.028>
- Gunnarsson, I., Aradóttir, E. S., Oelkers, E. H., Clark, D. E., Arnarson, M. Þ., Sigfússon, B., et al. (2018). The rapid and cost-effective capture and subsurface mineral storage of carbon and sulfur at the CarbFix2 site. *International Journal of Greenhouse Gas Control*, 79, 117–126. <https://doi.org/10.1016/j.ijggc.2018.08.014>
- Gysi, A. P., & Stefansson, A. (2012). Mineralogical aspects of CO₂ sequestration during hydrothermal basalt alteration—An experimental study at 75 to 250°C and elevated pCO₂. *Chemical Geology*, 306–307, 146–159. <https://doi.org/10.1016/j.chemgeo.2012.03.006>
- Hadgu, T., Karra, S., Kalinina, E., Makedonska, N., Hyman, J. D., Klise, K., et al. (2017). A comparative study of discrete fracture network and equivalent continuum models for simulating flow and transport in the far field of a hypothetical nuclear waste repository in crystalline host rock. *Journal of Hydrology*, 553, 59–70. <https://doi.org/10.1016/j.jhydrol.2017.07.046>
- Haggerty, R., Fleming, S. W., Meigs, L. C., & McKenna, S. A. (2001). Tracer tests in a fractured dolomite 2. Analysis of mass transfer in single-well injection-withdrawal tests. *Water Resources Research*, 37(5), 1129–1142. <https://doi.org/10.1029/2000wr900334>
- Haimson, B., & Fairhurst, C. (1967). Initiation and extension of hydraulic fractures in rocks. *Society of Petroleum Engineers Journal*, 7(3), 310–318. <https://doi.org/10.2118/1710-pa>
- Hartley, L., & Joyce, S. (2013). Approaches and algorithms for groundwater flow modeling in support of site investigations and safety assessment of the Forsmark site, Sweden. *Journal of Hydrology*, 500, 200–216. <https://doi.org/10.1016/j.jhydrol.2013.07.031>

- Hashin, Z., & Shtrikman, S. (1963). A variational approach to the theory of the elastic behaviour of multiphase materials. *Journal of the Mechanics and Physics of Solids*, 11(2), 127–140. [https://doi.org/10.1016/0022-5096\(63\)90060-7](https://doi.org/10.1016/0022-5096(63)90060-7)
- Hellevang, H., Pham, V. T. H., & Aagaard, P. (2013). Kinetic modelling of CO₂–water–rock interactions. *International Journal of Greenhouse Gas Control*, 15, 3–15. <https://doi.org/10.1016/j.ijggc.2013.01.027>
- Hou, B., Zhang, R., Tan, P., Song, Y., Fu, W., Chang, Z., et al. (2018). Characteristics of fracture propagation in compact limestone formation by hydraulic fracturing in central Sichuan, China. *Journal of Natural Gas Science and Engineering*, 57, 122–134. <https://doi.org/10.1016/j.jngse.2018.06.035>
- Huang, J. M., Tong, J., Shelley, M., & Ristroph, L. (2020). Ultra-sharp pinnacles sculpted by natural convective dissolution. *Proceedings of the National Academy of Sciences*, 117(38), 23339–23344. <https://doi.org/10.1073/pnas.2001524117>
- Huseby, O., Thovert, J.-F., & Adler, P. M. (2001). Dispersion in three-dimensional fracture networks. *Physics of Fluids*, 13(3), 594–615. <https://doi.org/10.1063/1.1345718>
- Hyman, J. D., Karra, S., Makedonska, N., Gable, C. W., Painter, S. L., & Viswanathan, H. S. (2015). dfnWorks: A discrete fracture network framework for modeling subsurface flow and transport. *Computers & Geosciences*, 84, 10–19. <https://doi.org/10.1016/j.cageo.2015.08.001>
- Hyman, J. D., Navarre-Sitchler, A., Andrews, E., Sweeney, M. R., Karra, S., Carey, J. W., & Viswanathan, H. S. (2022). A geo-structurally based correction factor for apparent dissolution rates in fractured media. *Geophysical Research Letters*, 49(15), e2022GL099513. <https://doi.org/10.1029/2022GL099513>
- Hyman, J. D., Rajaram, H., Srinivasan, S., Makedonska, N., Karra, S., Viswanathan, H., & Srinivasan, G. (2019). Matrix diffusion in fractured media: New insights into power law scaling of breakthrough curves. *Geophysical Research Letters*, 46(23), 13785–13795. <https://doi.org/10.1029/2019GL085454>
- Hyman, J. D., Sweeney, M. R., Gable, C. W., Svyatsky, D., Lipnikov, K., & Moulton, J. D. (2022). Flow and transport in three-dimensional discrete fracture matrix models using mimetic finite difference on a conforming multi-dimensional mesh. *Journal of Computational Physics*, 466, 111396. <https://doi.org/10.1016/j.jcp.2022.111396>
- Inskip, W. P., & Bloom, P. R. (1985). An evaluation of rate equations for calcite precipitation kinetics at pCO₂ less than 0.01 atm and pH greater than 8. *Geochimica et Cosmochimica Acta*, 49(10), 2165–2180. [https://doi.org/10.1016/0016-7037\(85\)90074-2](https://doi.org/10.1016/0016-7037(85)90074-2)
- Iraola, A., Trinchero, P., Karra, S., & Molinero, J. (2019). Assessing dual continuum method for multicomponent reactive transport. *Computers & Geosciences*, 130, 11–19. <https://doi.org/10.1016/j.cageo.2019.05.007>
- Ishida, T., Chen, Q., Mizuta, Y., & Roegiers, J.-C. (2004). Influence of fluid viscosity on the hydraulic fracturing mechanism. *Journal of Energy Resources Technology*, 126(3), 190–200. <https://doi.org/10.1115/1.1791651>
- Jackson, C. P., Hoch, A. R., & Todman, S. (2000). Self-consistency of a heterogeneous continuum porous medium representation of a fractured medium. *Water Resources Research*, 36(1), 189–202. <https://doi.org/10.1029/1999WR900249>
- Jacques, D., Simunek, J., Mallants, D., & Van Genuchten, M. T. (2018). The HPx software for multicomponent reactive transport during variably-saturated flow: Recent developments and applications. *Journal of Hydrology and Hydromechanics*, 66(2), 211–226. <https://doi.org/10.1515/johh-2017-0049>
- Jamtveit, B., Malthe-Sørenssen, A., & Kostenko, O. (2008). Reaction enhanced permeability during retrogressive metamorphism. *Earth and Planetary Science Letters*, 267(3–4), 620–627. <https://doi.org/10.1016/j.epsl.2007.12.016>
- Jamtveit, B., Putnis, C. V., & Malthe-Sørenssen, A. (2009). Reaction induced fracturing during replacement processes. *Contributions to Mineralogy and Petrology*, 157(1), 127–133. <https://doi.org/10.1007/s00410-008-0324-y>
- Jayne, R. S., Wu, H., & Pollyea, R. M. (2019). A probabilistic assessment of geomechanical reservoir integrity during CO₂ sequestration in flood basalt formations. *Greenhouse Gases: Science and Technology*, 9(5), 979–998. <https://doi.org/10.1002/ghg.1914>
- Jiménez-Martínez, J., Hyman, J. D., Chen, Y., Carey, J. W., Porter, M. L., Kang, Q., et al. (2020). Homogenization of dissolution and enhanced precipitation induced by bubbles in multiphase flow systems. *Geophysical Research Letters*, 47(7), e2020GL087163. <https://doi.org/10.1029/2020GL087163>
- Jones, T. A., & Detwiler, R. L. (2019). Mineral precipitation in fractures: Using the Level-Set method to quantify the role of mineral heterogeneity on transport properties. *Water Resources Research*, 55(5), 4186–4206. <https://doi.org/10.1029/2018wr024287>
- Jöns, N., Kahl, W.-A., & Bach, W. (2017). Reaction-induced porosity and onset of low-temperature carbonation in abyssal peridotites: Insights from 3D high-resolution microtomography. *Lithos*, 268–271, 274–284. <https://doi.org/10.1016/j.lithos.2016.11.014>
- Jung, H., & Navarre-Sitchler, A. (2018a). Physical heterogeneity control on effective mineral dissolution rates. *Geochimica et Cosmochimica Acta*, 227, 246–263. <https://doi.org/10.1016/j.gca.2018.02.028>
- Jung, H., & Navarre-Sitchler, A. (2018b). Scale effect on the time dependence of mineral dissolution rates in physically heterogeneous porous media. *Geochimica et Cosmochimica Acta*, 234, 70–83. <https://doi.org/10.1016/j.gca.2018.05.009>
- Kachanov, M., & Sevostianov, I. (2018). *Micromechanics of materials, with applications* (1st ed., Vol. 249). Springer Nature. <https://doi.org/10.1007/978-3-319-76204-3>
- Kang, P., Hyman, J. D., Han, W. S., & Dentz, M. (2020). Anomalous transport in three-dimensional discrete fracture networks: Interplay between aperture heterogeneity and particle injection modes. *Water Resources Research*, 56(11), e2020WR027378. <https://doi.org/10.1029/2020WR027378>
- Kang, Q., Chen, L., Valocchi, A. J., & Viswanathan, H. S. (2014). Pore-scale study of dissolution-induced changes in permeability and porosity of porous media. *Journal of Hydrology*, 517, 1049–1055. <https://doi.org/10.1016/j.jhydrol.2014.06.045>
- Kang, Q., Liu, M., Carey, J. W., & Viswanathan, H. S. (2023). 3D pore-scale modeling of mineral dissolution and precipitation in fractured rocks. In *ARMA US Rock Mechanics/Geomechanics Symposium* (ARMA-2023-0737). ARMA. <https://doi.org/10.56952/ARMA-2023-0737>
- Kang, Q., Lichtner, P. C., & David R. Janecky, D. R. J. (2010). Lattice Boltzmann method for reacting flows in porous media. *Advances in Applied Mathematics and Mechanics*, 2(5), 545–563. <https://doi.org/10.4208/aamm.10-m10S02>
- Kang, Q., Zhang, D., Chen, S., & He, X. (2002). Lattice Boltzmann simulation of chemical dissolution in porous media. *Physical Review E*, 65(3), 036318. <https://doi.org/10.1103/PhysRevE.65.036318>
- Kc, B., & Ghazanfari, E. (2021). Geothermal reservoir stimulation through hydro-shearing: An experimental study under conditions close to enhanced geothermal systems. *Geothermics*, 96, 102200. <https://doi.org/10.1016/j.geothermics.2021.102200>
- Kelemen, P., Benson, S. M., Pilorgé, H., Psarras, P., & Wilcox, J. (2019). An overview of the status and challenges of CO₂ storage in minerals and geological formations. *Frontiers in Climate*, 1, 9. <https://doi.org/10.3389/fclim.2019.00009>
- Kelemen, P. B., Aines, R., Bennett, E., Benson, S. M., Carter, E., Coggon, J. A., et al. (2018). In situ carbon mineralization in ultramafic rocks: Natural processes and possible engineered methods. *Energy Procedia*, 146, 92–102. <https://doi.org/10.1016/j.egypro.2018.07.013>
- Kelemen, P. B., & Hirth, G. (2012). Reaction-driven cracking during retrograde metamorphism: Olivine hydration and carbonation. *Earth and Planetary Science Letters*, 345–348, 81–89. <https://doi.org/10.1016/j.epsl.2012.06.018>

- Kelemen, P. B., Leong, J. A., Carlos de Obeso, J., Matter, J. M., Ellison, E. T., Templeton, A., et al. (2021). Initial results from the Oman drilling project multi-borehole observatory: Petrogenesis and ongoing alteration of mantle peridotite in the weathering horizon. *Journal of Geophysical Research: Solid Earth*, *126*(12), e2021JB022729. <https://doi.org/10.1029/2021jb022729>
- Kelemen, P. B., & Matter, J. (2008). In situ carbonation of peridotite for CO₂ storage. *Proceedings of the National Academy of Sciences*, *105*(45), 17295–17300. <https://doi.org/10.1073/pnas.0805794105>
- Kelemen, P. B., Matter, J., Streit, E. E., Rudge, J. F., Curry, W. B., & Blusztajn, J. (2011). Rates and mechanisms of mineral carbonation in peridotite: Natural processes and recipes for enhanced, in situ CO₂ capture and storage. *Annual Review of Earth and Planetary Sciences*, *39*(1), 545–576. <https://doi.org/10.1146/annurev-earth-092010-152509>
- Kelemen, P. B., Matter, J. M., Teagle, D. A. H., & Coggon, J. A. (2020). Proceedings of the Oman Drilling Project: Scientific Drilling in the Samail Ophiolite, Sultanate of Oman. In Oman Drilling Project Science Team (Ed.), (Vol. Phase 1 and 2). *International Ocean Discovery Program*. <https://doi.org/10.14379/OmanDP.proc.2020>
- Kelemen, P. B., McQueen, N., Wilcox, J., Renforth, P., Dipple, G., & Vankeuren, A. P. (2020). Engineered carbon mineralization in ultramafic rocks for CO₂ removal from air: Review and new insights. *Chemical Geology*, *550*, 119628. <https://doi.org/10.1016/j.chemgeo.2020.119628>
- Kim, K. T., Jagannath, M. S. P., Su, G. M., Freychet, G., Zeng, T., Mohanty, K. K., et al. (2021). Surfactant inhibition mechanisms of carbonate mineral dissolution in shale. *Colloids and Surfaces A: Physicochemical and Engineering Aspects*, *625*, 126857. <https://doi.org/10.1016/j.colsurfa.2021.126857>
- Klein, F., & Garrido, C. J. (2011). Thermodynamic constraints on mineral carbonation of serpentinized peridotite. *Lithos*, *126*(3–4), 147–160. <https://doi.org/10.1016/j.lithos.2011.07.020>
- Klein, F., & McCollom, T. M. (2013). From serpentinization to carbonation: New insights from a CO₂ injection experiment. *Earth and Planetary Science Letters*, *379*, 137–145. <https://doi.org/10.1016/j.epsl.2013.08.017>
- Knauss, G., Nguyen, S. N., & Weed, H. C. (1993). Diopside dissolution kinetics as a function of pH, CO₂, temperature, and time. *Geochimica et Cosmochimica Acta*, *57*(2), 285–294. [https://doi.org/10.1016/0016-7037\(93\)90431-u](https://doi.org/10.1016/0016-7037(93)90431-u)
- Knight, E. E., Rougier, E., Lei, Z., Euser, B., Chau, V., Boyce, S. H., et al. (2020). HOSS: An implementation of the combined finite-discrete element method. *Computational Particle Mechanics*, *7*(5), 765–787. <https://doi.org/10.1007/s40571-020-00349-y>
- Kolditz, O., Bauer, S., Bilke, L., Böttcher, N., Delfs, J.-O., Fischer, T., et al. (2012). OpenGeoSys: An open-source initiative for numerical simulation of thermo-hydro-mechanical/chemical (THM/C) processes in porous media. *Environmental Earth Sciences*, *67*(2), 589–599. <https://doi.org/10.1007/s12665-012-1546-x>
- Kong, X.-Z., Ahkami, M., Naets, I., & Saar, M. O. (2023). The role of high-permeability inclusion on solute transport in a 3D-printed fractured porous medium: An LIF-PIV integrated study. *Transport in Porous Media*, *146*(1), 283–305. <https://doi.org/10.1007/s11242-022-01827-y>
- Kostenko, O., Jamtveit, B., Austrheim, H., Pollok, K., & Putnis, C. (2002). The mechanism of fluid infiltration in peridotites at Almklovdalen, western Norway. *Geofluids*, *2*(3), 203–215. <https://doi.org/10.1046/j.1468-8123.2002.00038.x>
- Kozeny, J. (1927). Ueber kapillare leitung des wassers im boden. *Sitzungsberichte Der Akademie Der Wissenschaften in Wien*, *136*, 271.
- Kuleci, H., Ulven, O. I., Rybacki, E., Wunder, B., & Abart, R. (2017). Reaction-induced fracturing in a hot pressed calcite-periclase aggregate. *Journal of Structural Geology*, *94*, 116–135. <https://doi.org/10.1016/j.jsg.2016.11.009>
- Lafay, R., Montes-Hernandez, G., Renard, F., & Vonlanthen, P. (2018). Intracrystalline reaction-induced cracking in olivine evidenced by hydration and carbonation experiments. *Minerals*, *8*(9), 412. <https://doi.org/10.3390/min8090412>
- Lasaga, A. C. (1981). Transition state theory. *Reviews in Mineralogy*, *8*, 135–168.
- Lasaga, A. C. (2014). *Kinetic theory in the Earth sciences*. Princeton University Press.
- Laubach, S. E., Lander, R., Criscenti, L. J., Anovitz, L. M., Urai, J., Pollyea, R. M., et al. (2019). The role of chemistry in fracture pattern development and opportunities to advance interpretations of geological materials. *Reviews of Geophysics*, *57*(3), 1065–1111. <https://doi.org/10.1029/2019rg000671>
- Lebedeva, M. I., & Brantley, S. L. (2017). Weathering and erosion of fractured bedrock systems. *Earth Surface Processes and Landforms*, *42*(13), 2090–2108. <https://doi.org/10.1002/esp.4177>
- Lee, S. H., & Kang, P. K. (2020). Three-dimensional vortex-induced reaction hot spots at flow intersections. *Physical Review Letters*, *124*(14), 144501. <https://doi.org/10.1103/PhysRevLett.124.144501>
- Lei, Q., Latham, J. P., & Tsang, C. F. (2017). The use of discrete fracture networks for modelling coupled geomechanical and hydrological behaviour of fractured rocks. *Computers and Geotechnics*, *85*, 151–176. <https://doi.org/10.1016/j.compgeo.2016.12.024>
- Lei, Z., Rougier, E., Munjiza, A., Viswanathan, H., & Knight, E. E. (2019). Simulation of discrete cracks driven by nearly incompressible fluid via 2D combined finite-discrete element method. *International Journal for Numerical and Analytical Methods in Geomechanics*, *43*(9), 1724–1743. <https://doi.org/10.1002/nag.2929>
- Lei, Z., Zhang, Y., Cui, Q., & Shi, Y. (2023). The injection-production performance of an enhanced geothermal system considering fracture network complexity and thermo-hydro-mechanical coupling in numerical simulations. *Scientific Reports*, *13*(1), 14558. <https://doi.org/10.1038/s41598-023-41745-7>
- Li, L., Steefel, C. I., & Yang, L. (2008). Scale dependence of mineral dissolution rates within single pores and fractures. *Geochimica et Cosmochimica Acta*, *72*(2), 360–377. <https://doi.org/10.1016/j.gca.2007.10.027>
- Li, Q., Fernandez-Martinez, A., Lee, B., Waychunas, G. A., & Jun, Y.-S. (2014). Interfacial energies for heterogeneous nucleation of calcium carbonate on mica and quartz. *Environmental Science & Technology*, *48*(10), 5745–5753. <https://doi.org/10.1021/es405141j>
- Li, S., Feng, X.-T., Zhang, D., & Tang, H. (2019). Coupled thermo-hydro-mechanical analysis of stimulation and production for fractured geothermal reservoirs. *Applied Energy*, *247*, 40–59. <https://doi.org/10.1016/j.apenergy.2019.04.036>
- Li, S., Xu, J., & Luo, G. (2007). Control of crystal morphology through supersaturation ratio and mixing conditions. *Journal of Crystal Growth*, *304*(1), 219–224. <https://doi.org/10.1016/j.jcrysgro.2007.01.032>
- Li, W., Frash, L. P., Carey, J. W., Welch, N. J., Meng, M., Nguyen, H., et al. (2021). Injection parameters that promote branching of hydraulic cracks. *Geophysical Research Letters*, *48*(12), e2021GL093321. <https://doi.org/10.1029/2021GL093321>
- Li, W., Frash, L. P., Carey, J. W., Welch, N. J., Meng, M., & Viswanathan, H. S. (2022). Transparent true-triaxial apparatus for investigation of hydraulic fracture branching. In *56th U.S. Rock Mechanics/Geomechanics Symposium*.
- Liao, J., Hu, K., Mehmood, F., Xu, B., Teng, Y., Wang, H., et al. (2023). Embedded discrete fracture network method for numerical estimation of long-term performance of CO₂-EGS under THM coupled framework. *Energy*, *285*, 128734. <https://doi.org/10.1016/j.energy.2023.128734>
- Lichtner, P. C. (2000). *Critique of dual continuum formulations of multicomponent reactive transport in fractured porous media*. Los Alamos National Laboratory (LANL).
- Lichtner, P. C., Hammond, G. E., Lu, C., Karra, S., Bisht, G., Andre, B., et al. (2015). *PFLOTRAN user manual: A massively parallel reactive flow and transport model for describing surface and subsurface processes* (Report No.: LA-UR-15-20403). Los Alamos National Laboratory.

- Ling, B., Sodwatana, M., Kohli, A., Ross, C. M., Jew, A., Kovscek, A. R., & Battiato, I. (2022). Probing multiscale dissolution dynamics in natural rocks through microfluidics and compositional analysis. *Proceedings of the National Academy of Sciences*, *119*(32), e2122520119. <https://doi.org/10.1073/pnas.2122520119>
- Lipnikov, K., Manzini, G., & Shashkov, M. (2014). Mimetic finite difference method. *Journal of Computational Physics*, *257*, 1163–1227. <https://doi.org/10.1016/j.jcp.2013.07.031>
- Lisabeth, H. P., Zhu, W., Kelemen, P. B., & Ilgen, A. (2017). Experimental evidence for chemo-mechanical coupling during carbon mineralization in ultramafic rocks. *Earth and Planetary Science Letters*, *474*, 355–367. <https://doi.org/10.1016/j.epsl.2017.06.045>
- Liu, D., & Lecampion, B. (2022). Laboratory investigation of hydraulic fracture growth in Zimbabwe gabbro. *Journal of Geophysical Research: Solid Earth*, *127*(11), e2022JB025678. <https://doi.org/10.1029/2022JB025678>
- Liu, M., Kwon, B., & Kang, P. K. (2022). Machine learning to predict effective reaction rates in 3D porous media from pore structural features. *Scientific Reports*, *12*(1), 5486. <https://doi.org/10.1038/s41598-022-09495-0>
- Liu, M., & Mostaghimi, P. (2017). Pore-scale simulation of dissolution-induced variations in rock mechanical properties. *International Journal of Heat and Mass Transfer*, *111*, 842–851. <https://doi.org/10.1016/j.ijheatmasstransfer.2017.04.049>
- Liu, M., Starchenko, V., Anovitz, L. M., & Stack, A. G. (2020). Grain detachment and transport clogging during mineral dissolution in carbonate rocks with permeable grain boundaries. *Geochimica et Cosmochimica Acta*, *280*, 202–220. <https://doi.org/10.1016/j.gca.2020.04.022>
- Lods, G., Roubinet, D., Matter, J. M., Leprovost, R., & Gouze, P. (2020). Groundwater flow characterization of an ophiolitic hard-rock aquifer from cross-borehole multi-level hydraulic experiments. *Journal of Hydrology*, *589*, 125152. <https://doi.org/10.1016/j.jhydrol.2020.125152>
- Løge, I. A., Anabaraonye, B. U., Bovet, N., & Fosbøl, P. L. (2023). Crystal nucleation and growth: Supersaturation and crystal resilience determine stickability. *Crystal Growth & Design*, *23*(4), 2619–2627. <https://doi.org/10.1021/acs.cgd.2c01459>
- Luhmann, A. J., Tutolo, B. M., Bagley, B. C., Mildner, D. F. R., Seyfried, W. E., Jr., & Saar, M. O. (2017). Permeability, porosity, and mineral surface area changes in basalt cores induced by reactive transport of CO₂-rich brine. *Water Resources Research*, *53*(3), 1908–1927. <https://doi.org/10.1002/2016wr019216>
- Luhmann, A. J., Tutolo, B. M., Tan, C., Moskowitz, B. M., Saar, M. O., & Seyfried, W. E. (2017). Whole rock basalt alteration from CO₂-rich brine during flow-through experiments at 150°C and 150 bar. *Chemical Geology*, *453*, 92–110. <https://doi.org/10.1016/j.chemgeo.2017.02.002>
- Luquot, L., & Gouze, P. (2009). Experimental determination of porosity and permeability changes induced by injection of CO₂ into carbonate rocks. *Chemical Geology*, *265*(1), 148–159. <https://doi.org/10.1016/j.chemgeo.2009.03.028>
- Ma, J., Ahkami, M., Saar, M. O., & Kong, X.-Z. (2021). Quantification of mineral accessible surface area and flow-dependent fluid-mineral reactivity at the pore scale. *Chemical Geology*, *563*, 120042. <https://doi.org/10.1016/j.chemgeo.2020.120042>
- MacQuarrie, K. T., & Mayer, K. U. (2005). Reactive transport modeling in fractured rock: A state-of-the-science review. *Earth-Science Reviews*, *72*(3–4), 189–227. <https://doi.org/10.1016/j.earscirev.2005.07.003>
- Malvoisin, B., Brantut, N., & Kaczmarek, M.-A. (2017). Control of serpentinisation rate by reaction-induced cracking. *Earth and Planetary Science Letters*, *476*, 143–152. <https://doi.org/10.1016/j.epsl.2017.07.042>
- Matter, J. M., & Kelemen, P. B. (2009). Permanent storage of carbon dioxide in geological reservoirs by mineral carbonation. *Nature Geoscience*, *2*(12), 837–841. <https://doi.org/10.1038/ngeo683>
- Matter, J. M., Stute, M., Snæbjörnsdóttir, S. Ó., Oelkers, E. H., Gislason, S. R., Aradottir, E. S., et al. (2016). Rapid carbon mineralization for permanent disposal of anthropogenic carbon dioxide emissions. *Science*, *352*(6291), 1312–1314. <https://doi.org/10.1126/science.aad8132>
- McCollom, T. M., & Bach, W. (2009). Thermodynamic constraints on hydrogen generation during serpentinization of ultramafic rocks. *Geochimica et Cosmochimica Acta*, *73*(3), 856–875. <https://doi.org/10.1016/j.gca.2008.10.032>
- McGrail, B. P., Schaefer, H. T., Glezakou, V.-A., Dang, L. X., & Owen, A. T. (2009). Water reactivity in the liquid and supercritical CO₂ phase: Has half the story been neglected? *Energy Procedia*, *1*(1), 3415–3419. <https://doi.org/10.1016/j.egypro.2009.02.131>
- McGrail, B. P., Schaefer, H. T., Ho, A. M., Chien, Y.-J., Dooley, J. J., & Davidson, C. L. (2006). Potential for carbon dioxide sequestration in flood basalts. *Journal of Geophysical Research*, *111*(B12), B12201. <https://doi.org/10.1029/2005jb004169>
- McGrail, B. P., Schaefer, H. T., Spane, F. A., Cliff, J. B., Qafoku, O., Horner, J. A., et al. (2017). Field validation of supercritical CO₂ reactivity with basalts. *Environmental Science & Technology Letters*, *4*(1), 6–10. <https://doi.org/10.1021/acs.estlett.6b00387>
- McGrail, B. P., Schaefer, H. T., Spane, F. A., Horner, J. A., Owen, A. T., Cliff, J. B., et al. (2017). Wallula basalt pilot demonstration project: Post-injection results and conclusions. *Energy Procedia*, *114*, 5783–5790. <https://doi.org/10.1016/j.egypro.2017.03.1716>
- McGrail, B. P., Spane, F. A., Amonette, J. E., Thompson, C. R., & Brown, C. F. (2014). Injection and monitoring at the Wallula Basalt Pilot Project. *Energy Procedia*, *63*, 2939–2948. <https://doi.org/10.1016/j.egypro.2014.11.316>
- McGrail, B. P., Spane, F. A., Sullivan, E. C., Bacon, D. H., & Hund, G. (2011). The Wallula basalt sequestration pilot project. *Energy Procedia*, *4*, 5653–5660. <https://doi.org/10.1016/j.egypro.2011.02.557>
- McGrail, B. P., Sullivan, E., Spane, F. A., Bacon, D. H., Hund, G., Thorne, P., et al. (2009). *Preliminary hydrogeologic characterization results from the Wallula Basalt Pilot Study* (No. PNWD-4129). Battelle Pacific Northwest Division.
- Meeussen, J. C. (2003). ORCHESTRA: An object-oriented framework for implementing chemical equilibrium models. *Environmental Science & Technology*, *37*(6), 1175–1182. <https://doi.org/10.1021/es025597s>
- Meigs, L. C., & Beauheim, R. L. (2001). Tracer tests in a fractured dolomite: 1. Experimental design and observed tracer recoveries. *Water Resources Research*, *37*(5), 1113–1128. <https://doi.org/10.1029/2000wr900335>
- Menefee, A. H., Giammar, D. E., & Ellis, B. R. (2018). Permanent CO₂ trapping through localized and chemical gradient-driven basalt carbonation. *Environmental Science & Technology*, *52*(15), 8954–8964. <https://doi.org/10.1021/acs.est.8b01814>
- Menefee, A. H., Li, P., Giammar, D. E., & Ellis, B. R. (2017). Roles of transport limitations and mineral heterogeneity in carbonation of fractured basalts. *Environmental Science & Technology*, *51*(16), 9352–9362. <https://doi.org/10.1021/acs.est.7b00326>
- Menefee, A. H., Welch, N. J., Frash, L. P., Hicks, W., Carey, J. W., & Ellis, B. R. (2020). Rapid mineral precipitation during shear fracturing of carbonate-rich shales. *Journal of Geophysical Research: Solid Earth*, *125*(6), e2019JB018864. <https://doi.org/10.1029/2019jb018864>
- Meng, M., Frash, L. P., Li, W., Welch, N. J., Carey, J. W., Morris, J., et al. (2022). Hydro-mechanical measurements of sheared crystalline rock fractures with applications for EGS Collab Experiments 1 and 2. *Journal of Geophysical Research: Solid Earth*, *127*(2), e2021JB023000. <https://doi.org/10.1029/2021jb023000>
- Menzel, M. D., Urai, J. L., Ukar, E., Hirth, G., Schwedt, A., Kovács, A., et al. (2022). Ductile deformation during carbonation of serpentinized peridotite. *Nature Communications*, *13*(1), 3478. <https://doi.org/10.1038/s41467-022-31049-1>
- Mervine, E. M., Humphris, S. E., Sims, K. W. W., Kelemen, P. B., & Jenkins, W. J. (2014). Carbonation rates of peridotite in the Samail Ophiolite, Sultanate of Oman, constrained through ¹⁴C dating and stable isotopes. *Geochimica et Cosmochimica Acta*, *126*, 371–397. <https://doi.org/10.1016/j.gca.2013.11.007>

- Miller, Q. R. S., Schaefer, H. T., Kaszuba, J. P., Gadikota, G., McGrail, B. P., & Rosso, K. M. (2019). Quantitative review of olivine carbonation kinetics: Reactivity trends, mechanistic insights, and research frontiers. *Environmental Science & Technology Letters*, 6(8), 431–442. <https://doi.org/10.1021/acs.estlett.9b00301>
- Min, Y., Kubicki, J. D., & Jun, Y.-S. (2015). Plagioclase dissolution during CO₂–SO₂ cosequestration: Effects of sulfate. *Environmental Science & Technology*, 49(3), 1946–1954. <https://doi.org/10.1021/es504586u>
- Molins, S., Trebotich, D., Arora, B., Steefel, C. I., & Deng, H. (2019). Multi-scale model of reactive transport in fractured media: Diffusion limitations on rates. *Transport in Porous Media*, 128(2), 701–721. <https://doi.org/10.1007/s11242-019-01266-2>
- Moosavi, R., Kumar, A., De Wit, A., & Schröter, M. (2019). Influence of mineralization and injection flow rate on flow patterns in three-dimensional porous media. *Physical Chemistry Chemical Physics*, 21(27), 14605–14611. <https://doi.org/10.1039/C9CP01382B>
- Moulton, J. D., Berndt, M., Garimella, R., Prichett-Sheats, L., Hammond, G., Day, M., & Meza, J. (2012). *High-level design of Amanzi, the multi-process high performance computing simulator* (No. ASCEM-HPC-2011-03-1 (LANL: LA-UR 12-22193)). United States Department of Energy, Office of Environmental Management.
- Munjiza, A. A. (2004). *The combined finite-discrete element method*. John Wiley & Sons. Retrieved from <http://ebookcentral.proquest.com/lib/alamoz/detail.action?docID=219752>
- Nadimi, S., Forbes, B., Moore, J., Podgorney, R., & McLennan, J. D. (2020). Utah FORGE: Hydrogeothermal modeling of a granitic based discrete fracture network. *Geothermics*, 87, 101853. <https://doi.org/10.1016/j.geothermics.2020.101853>
- National Research Council. (1996). Rock fractures and fluid flow: Contemporary understanding and applications. In F. Flow (Ed.), *Committee on fracture characterization*. National Academy Press.
- Neil, C. W., Yang, Y., Nisbet, H., Iyare, U. C., Boampong, L. O., Li, W., et al. (2024). An integrated experimental–modeling approach to identify key processes for carbon mineralization in fractured mafic and ultramafic rocks. *PNAS Nexus*, 3(9). <https://doi.org/10.1093/pnasnexus/pgae388>
- Neuman, S. P. (2005). Trends, prospects and challenges in quantifying flow and transport through fractured rocks. *Hydrogeology Journal*, 13(1), 124–147. <https://doi.org/10.1007/s10040-004-0397-2>
- Neuville, A., Renaud, L., Luu, T. T., Minde, M. W., Jettestuen, E., Vinningland, J. L., et al. (2017). Xurography for microfluidics on a reactive solid. *Lab on a Chip*, 17(2), 293–303. <https://doi.org/10.1039/c6lc01253a>
- Ng, L. W. T., & Willcox, K. E. (2014). Multifidelity approaches for optimization under uncertainty. *International Journal for Numerical Methods in Engineering*, 100(10), 746–772. <https://doi.org/10.1002/nme.4761>
- Nicolas, A., & Jackson, M. (1982). High temperature dikes in peridotites: Origin by hydraulic fracturing. *Journal of Petrology*, 23(4), 568–582. <https://doi.org/10.1093/petrology/23.4.568>
- Noiriel, C., Gouze, P., & Madé, B. (2013). 3D analysis of geometry and flow changes in a limestone fracture during dissolution. *Journal of Hydrology*, 486, 211–223. <https://doi.org/10.1016/j.jhydrol.2013.01.035>
- Noiriel, C., Oursin, M., & Daval, D. (2020). Examination of crystal dissolution in 3D: A way to reconcile dissolution rates in the laboratory? *Geochimica et Cosmochimica Acta*, 273, 1–25. <https://doi.org/10.1016/j.gca.2020.01.003>
- Noiriel, C., Seigneur, N., Le Guern, P., & Lagneau, V. (2021). Geometry and mineral heterogeneity controls on precipitation in fractures: An X-ray micro-tomography and reactive transport modeling study. *Advances in Water Resources*, 152, 103916. <https://doi.org/10.1016/j.advwatres.2021.103916>
- Noiriel, C., & Soulaire, C. (2021). Pore-scale imaging and modelling of reactive flow in evolving porous media: Tracking the dynamics of the fluid–rock interface. *Transport in Porous Media*, 140(1), 181–213. <https://doi.org/10.1007/s11242-021-01613-2>
- NRCC. (1996). Physical characteristics of fractures and fracture patterns. In *Rock fractures and fluid flow: Contemporary understanding and applications* (pp. 29–102). National Academies Press.
- Oelkers, E., & Gislason, S. (2023). Carbon capture and storage: From global cycles to global solutions. *Geochemical Perspectives*, 12(2), 179–349. <https://doi.org/10.7185/geochempersp.12.2>
- Oelkers, E. H., Declercq, J., Saldi, G. D., Gislason, S. R., & Schott, J. (2018). Olivine dissolution rates: A critical review. *Chemical Geology*, 500, 1–19. <https://doi.org/10.1016/j.chemgeo.2018.10.008>
- Oelkers, E. H., Gislason, S. R., & Matter, J. (2008). Mineral carbonation of CO₂. *Elements*, 4(5), 333–337. <https://doi.org/10.2113/gselements.4.5.333>
- Oldenburg, C., Dobson, P., Wu, Y., Cook, P., Kneafsey, T., Nakagawa, S., et al. (2020). *Hydraulic fracturing experiments at 1500 m depth in a deep mine: Highlights from the kISMET project*. Lawrence Berkeley National Laboratory (LBNL).
- Olsson, J., Bovet, N., Makovicky, E., Bechgaard, K., Balogh, Z., & Stipp, S. L. S. (2012). Olivine reactivity with CO₂ and H₂O on a microscale: Implications for carbon sequestration. *Geochimica et Cosmochimica Acta*, 77, 86–97. <https://doi.org/10.1016/j.gca.2011.11.001>
- O'Malley, D., Karra, S., Hyman, H., Viswanathan, J. D., & Srinivasan, G. (2018). Efficient Monte Carlo with graph-based subsurface flow and transport models. *Water Resources Research*, 54(5), 3758–3766. <https://doi.org/10.1029/2017wr022073>
- Osselin, F., Kondratiuk, P., Budek, A., Cybulski, O., Garstecki, P., & Szymczak, P. (2016). Microfluidic observation of the onset of reactive-infiltration instability in an analog fracture. *Geophysical Research Letters*, 43(13), 6907–6915. <https://doi.org/10.1002/2016GL069261>
- Otu, S., Rinehart, A. J., Luhmann, A. J., Simmons, J., & Mozley, P. (2023). Effects of CO₂ on creep deformation in sandstones at carbon sequestration reservoir conditions: An experimental study. *International Journal of Greenhouse Gas Control*, 129, 103970. <https://doi.org/10.1016/j.ijggc.2023.103970>
- Pachalieuva, A. A., Sweeney, M. R., Viswanathan, H., Stein, E., Leone, R., & Hyman, J. D. (2023). Impact of artificial topological changes on flow and transport through fractured media due to mesh resolution. *Computational Geosciences*, 27(6), 1145–1163. <https://doi.org/10.1007/s10596-023-10253-y>
- Painter, S., Cvetkovic, V., & Selroos, J.-O. (2002). Power-law velocity distributions in fracture networks: Numerical evidence and implications for tracer transport. *Geophysical Research Letters*, 29(14), 20-1–20-4. <https://doi.org/10.1029/2002gl014960>
- Pandey, S., & Rajaram, H. (2016). Modeling the influence of preferential flow on the spatial variability and time-dependence of mineral weathering rates. *Water Resources Research*, 52(12), 9344–9366. <https://doi.org/10.1002/2016wr019026>
- Pandey, S. N., Chaudhuri, A., & Kelkar, S. (2017). A coupled thermo-hydro-mechanical modeling of fracture aperture alteration and reservoir deformation during heat extraction from a geothermal reservoir. *Geothermics*, 65, 17–31. <https://doi.org/10.1016/j.geothermics.2016.08.006>
- Park, S., Anggraini, T. M., Chung, J., Kang, P. K., & Lee, S. (2021). Microfluidic pore model study of precipitates induced by the pore-scale mixing of an iron sulfate solution with simulated groundwater. *Chemosphere*, 271, 129857. <https://doi.org/10.1016/j.chemosphere.2021.129857>
- Parkhurst, D. L., & Appelo, C. (2013). Description of input and examples for PHREEQC version 3—A computer program for speciation, batch-reaction, one-dimensional transport, and inverse geochemical calculations. *US Geological Survey Techniques and Methods*, 6(A43), 497.

- Paukert, A. N., Matter, J. M., Kelemen, P. B., Shock, E. L., & Havig, J. R. (2012). Reaction path modeling of enhanced in situ CO₂ mineralization for carbon sequestration in the peridotite of the Samail Ophiolite, Sultanate of Oman. *Chemical Geology*, 330–331, 86–100. <https://doi.org/10.1016/j.chemgeo.2012.08.013>
- Peherstorfer, B., Willcox, K., & Gunzburger, M. (2016). Optimal model management for multifidelity Monte Carlo estimation. *SIAM Journal on Scientific Computing*, 38(5), A3163–A3194. <https://doi.org/10.1137/15M1046472>
- Phukan, M., Jyoti, A., Black, J. R., & Haese, R. R. (2021). Changes in pore geometry and connectivity in the basalt pore network adjacent to fractures in response to CO₂-saturated fluid. *Water Resources Research*, 57(12), e2021WR030275. <https://doi.org/10.1029/2021WR030275>
- Plümper, O., & Matter, J. (2023). Olivine—The alteration rock star. *Elements*, 19(3), 165–172. <https://doi.org/10.2138/gselements.19.3.165>
- Pogge von Strandmann, P. A. E., Burton, K. W., Snæbjörnsdóttir, S. Ó., Sigfússon, B., Aradóttir, E. S., Gunnarsson, I., et al. (2019). Rapid CO₂ mineralisation into calcite at the CarbFix storage site quantified using calcium isotopes. *Nature Communications*, 10(1), 1983. <https://doi.org/10.1038/s41467-019-10003-8>
- Pokrovsky, O. S., & Schott, J. (2000). Kinetics and mechanism of forsterite dissolution at 25°C and pH from 1 to 12. *Geochimica et Cosmochimica Acta*, 64(19), 3313–3325. [https://doi.org/10.1016/S0016-7037\(00\)00434-8](https://doi.org/10.1016/S0016-7037(00)00434-8)
- Polites, E. G., Schaeff, H. T., Horner, J. A., Owen, A. T., Holliman, J. E., McGrail, B. P., & Miller, Q. R. S. (2022). Exotic carbonate mineralization recovered from a deep basalt carbon storage demonstration. *Environmental Science & Technology*, 56(20), 14713–14722. <https://doi.org/10.1021/acs.est.2c03269>
- Poonosamy, J., Soulaïne, C., Burmeister, A., Deissmann, G., Bosbach, D., & Roman, S. (2020). Microfluidic flow-through reactor and 3D Raman imaging for in situ assessment of mineral reactivity in porous and fractured porous media. *Lab on a Chip*, 20(14), 2562–2571. <https://doi.org/10.1039/d0lc00360c>
- Porter, M. L., Jiménez-Martínez, J., Martínez, R., McCulloch, Q., Carey, J. W., & Viswanathan, H. S. (2015). Geo-material microfluidics at reservoir conditions for subsurface energy resource applications. *Lab on a Chip*, 15(20), 4044–4053. <https://doi.org/10.1039/C5LC00704F>
- Power, I. M., Dipple, G. M., & Francis, P. S. (2017). Assessing the carbon sequestration potential of magnesium oxychloride cement building materials. *Cement and Concrete Composites*, 78, 97–107. <https://doi.org/10.1016/j.cemconcomp.2017.01.003>
- Power, I. M., Harrison, A. L., Dipple, G. M., Wilson, S. A., Kelemen, P. B., Hitch, M., & Southam, G. (2013). Carbon mineralization: From natural analogues to engineered systems. *Reviews in Mineralogy and Geochemistry*, 77(1), 305–360. <https://doi.org/10.2138/rmg.2013.77.9>
- Prommer, H., Barry, D., & Zheng, C. (2003). MODFLOW/MT3DMS-based reactive multicomponent transport modeling. *Groundwater*, 41(2), 247–257. <https://doi.org/10.1111/j.1745-6584.2003.tb02588.x>
- Qin, F., & Beckingham, L. E. (2021). The impact of mineral reactive surface area variation on simulated mineral reactions and reaction rates. *Applied Geochemistry*, 124, 104852. <https://doi.org/10.1016/j.apgeochem.2020.104852>
- Rahimi-Aghdam, S., Chau, V.-T., Lee, H., Nguyen, H., Li, W., Karra, S., et al. (2019). Branching of hydraulic cracks enabling permeability of gas or oil shale with closed natural fractures. *Proceedings of the National Academy of Sciences - PNAS*, 116(5), 1532–1537. <https://doi.org/10.1073/pnas.1818529116>
- Rashid, M. I., Benhelal, E., Anderberg, L., Farhang, F., Oliver, T., Rayson, M. S., & Stockenhuber, M. (2022). Aqueous carbonation of peridotites for carbon utilisation: A critical review. *Environmental Science and Pollution Research*, 29(50), 75161–75183. <https://doi.org/10.1007/s11356-022-23116-3>
- Rasoulzadeh, M., Yekta, A., Deng, H., & B. Ghahfarokhi, R. (2020). Semi-analytical models of mineral dissolution in rough fractures with permeable walls. *Physics of Fluids*, 32(5), 052003. <https://doi.org/10.1063/5.0005878>
- Ratouis, T. M. P., Snæbjörnsdóttir, S. Ó., Voigt, M. J., Sigfússon, B., Gunnarsson, G., Aradóttir, E. S., & Hjørleifsdóttir, V. (2022). Carbfix 2: A transport model of long-term CO₂ and H₂S injection into basaltic rocks at Hellisheidi, SW-Iceland. *International Journal of Greenhouse Gas Control*, 114, 103586. <https://doi.org/10.1016/j.ijggc.2022.103586>
- Raza, A., Glatz, G., Gholami, R., Mahmoud, M., & Alafnan, S. (2022). Carbon mineralization and geological storage of CO₂ in basalt: Mechanisms and technical challenges. *Earth-Science Reviews*, 229, 104036. <https://doi.org/10.1016/j.earscirev.2022.104036>
- Raza, A., Mahmoud, M., Murtaza, M., Arif, M., Hassan, A., Glatz, G., et al. (2023). Experimental investigation of mafic rocks for carbon mineralization prospect. *Energy & Fuels*, 37(8), 5976–5985. <https://doi.org/10.1021/acs.energyfuels.3c00370>
- Reches, Z., & Dewers, T. (2005). Gouge formation by dynamic pulverization during earthquake rupture. *Earth and Planetary Science Letters*, 235(1–2), 361–374. <https://doi.org/10.1016/j.epsl.2005.04.009>
- Reidel, S. P., Spang, F. A., & Johnson, V. G. (2002). *Natural gas storage in basalt aquifers of the Columbia Basin, Pacific Northwest USA: A guide to site characterization* (No. PNNL-13962, 15020781). Pacific Northwest National Laboratory (PNNL). <https://doi.org/10.2172/15020781>
- Renard, F. (2021). Reaction-induced fracturing: When chemistry breaks rocks. *Journal of Geophysical Research: Solid Earth*, 126(2), e2020JB021451. <https://doi.org/10.1029/2020jb021451>
- Renshaw, C. E., & Pollard, D. D. (1995). An experimentally verified criterion for propagation across unbounded frictional interfaces in brittle, linear elastic materials. *International Journal of Rock Mechanics and Mining Sciences & Geomechanics Abstracts*, 32(3), 237–249. [https://doi.org/10.1016/0148-9062\(94\)00037-4](https://doi.org/10.1016/0148-9062(94)00037-4)
- Rezvani Khalilabad, M., Axelsson, G., & Gislason, S. R. (2008). Aquifer characterization with tracer test technique; permanent CO₂ sequestration into basalt, SW Iceland. *Mineralogical Magazine*, 72(1), 121–125. <https://doi.org/10.1180/minmag.2008.072.1.121>
- Rinaldi, A. P., & Rutqvist, J. (2019). Joint opening or hydroshearing? Analyzing a fracture zone stimulation at Fenton Hill. *Geothermics*, 77, 83–98. <https://doi.org/10.1016/j.geothermics.2018.08.006>
- Rinehart, A. J., Dewers, T. A., Broome, S. T., & Eichhubl, P. (2016). Effects of CO₂ on mechanical variability and constitutive behavior of the Lower Tuscaloosa Formation, Cranfield Injection Site, USA. *International Journal of Greenhouse Gas Control*, 53, 305–318. <https://doi.org/10.1016/j.ijggc.2016.08.013>
- Romanov, V., Soong, Y., Carney, C., Rush, G. E., Nielsen, B., & O'Connor, W. (2015). Mineralization of carbon dioxide: A literature review. *ChemBioEng Reviews*, 2(4), 231–256. <https://doi.org/10.1002/cben.201500002>
- Ruiz-Agudo, E., Putnis, C. V., & Putnis, A. (2014). Coupled dissolution and precipitation at mineral–fluid interfaces. *Chemical Geology*, 383, 132–146. <https://doi.org/10.1016/j.chemgeo.2014.06.007>
- Schaeff, H. T., & McGrail, B. P. (2009). Dissolution of Columbia River Basalt under mildly acidic conditions as a function of temperature: Experimental results relevant to the geological sequestration of carbon dioxide. *Applied Geochemistry*, 24(5), 980–987. <https://doi.org/10.1016/j.apgeochem.2009.02.025>
- Schaeff, H. T., McGrail, B. P., & Owen, A. T. (2009). Basalt- CO₂-H₂O interactions and variability in carbonate mineralization rates. *Energy Procedia*, 1(1), 4899–4906. <https://doi.org/10.1016/j.egypro.2009.02.320>
- Scherer, G. W. (2004). Stress from crystallization of salt. *Cement and Concrete Research*, 34(9), 1613–1624. <https://doi.org/10.1016/j.cemconres.2003.12.034>

- Schincariol, R. A., & Schwartz, F. W. (1990). An experimental investigation of variable density flow and mixing in homogeneous and heterogeneous media. *Water Resources Research*, 26(10), 2317–2329. <https://doi.org/10.1029/WR026i10p02317>
- Scott, S. R., Sims, K. W. W., Frost, B. R., Kelemen, P. B., Evans, K. A., & Swapp, S. M. (2017). On the hydration of olivine in ultramafic rocks: Implications from Fe isotopes in serpentinites. *Geochimica et Cosmochimica Acta*, 215, 105–121. <https://doi.org/10.1016/j.gca.2017.07.011>
- Severino, G., Tartakovsky, D. M., Srinivasan, G., & Viswanathan, H. (2012). Lagrangian models of reactive transport in heterogeneous porous media with uncertain properties. *Proceedings of the Royal Society A: Mathematical, Physical and Engineering Sciences*, 468(2140), 1154–1174. <https://doi.org/10.1098/rspa.2011.0375>
- Sharafisafa, M., Aliabadian, Z., Sato, A., & Shen, L. (2023). Coupled thermo-hydro-mechanical simulation of hydraulic fracturing in deep reservoirs using finite-discrete element method. *Rock Mechanics and Rock Engineering*, 56(7), 5039–5075. <https://doi.org/10.1007/s00603-023-03325-z>
- Shibuya, T., Yoshizaki, M., Masaki, Y., Suzuki, K., Takai, K., & Russell, M. J. (2013). Reactions between basalt and CO₂-rich seawater at 250 and 350°C, 500 bars: Implications for the CO₂ sequestration into the modern oceanic crust and the composition of hydrothermal vent fluid in the CO₂-rich early ocean. *Chemical Geology*, 359, 1–9. <https://doi.org/10.1016/j.chemgeo.2013.08.044>
- Shimizu, H., Murata, S., & Ishida, T. (2011). The distinct element analysis for hydraulic fracturing in hard rock considering fluid viscosity and particle size distribution. *International Journal of Rock Mechanics and Mining Sciences*, 48(5), 712–727. <https://doi.org/10.1016/j.ijrmm.2011.04.013>
- Shiraki, R., & Brantley, S. L. (1995). Kinetics of near-equilibrium calcite precipitation at 100°C: An evaluation of elementary reaction-based and affinity-based rate laws. *Geochimica et Cosmochimica Acta*, 59(8), 1457–1471. [https://doi.org/10.1016/0016-7037\(95\)00055-5](https://doi.org/10.1016/0016-7037(95)00055-5)
- Shovkun, I., & Espinoza, D. N. (2019). Fracture propagation in heterogeneous porous media: Pore-scale implications of mineral dissolution. *Rock Mechanics and Rock Engineering*, 52(9), 3197–3211. <https://doi.org/10.1007/s00603-019-01766-z>
- Sigfusson, B., Gislason, S. R., Matter, J. M., Stute, M., Gunnlaugsson, E., Gunnarsson, I., et al. (2015). Solving the carbon-dioxide buoyancy challenge: The design and field testing of a dissolved CO₂ injection system. *International Journal of Greenhouse Gas Control*, 37, 213–219. <https://doi.org/10.1016/j.ijggc.2015.02.022>
- Singh, R., Sivaguru, M., Fried, G. A., Fouke, B. W., Sanford, R. A., Carrera, M., & Werth, C. J. (2017). Real rock-microfluidic flow cell: A test bed for real-time in situ analysis of flow, transport, and reaction in a subsurface reactive transport environment. *Journal of Contaminant Hydrology*, 204, 28–39. <https://doi.org/10.1016/j.jconhyd.2017.08.001>
- Sneðbjörnsdóttir, S. Ó., Oelkers, E. H., Mesfin, K., Aradóttir, E. S., Dideriksen, K., Gunnarsson, I., et al. (2017). The chemistry and saturation states of subsurface fluids during the in situ mineralisation of CO₂ and H₂S at the CarbFix site in SW-Iceland. *International Journal of Greenhouse Gas Control*, 58, 87–102. <https://doi.org/10.1016/j.ijggc.2017.01.007>
- Sneðbjörnsdóttir, S. Ó., Sigfusson, B., Marieni, C., Goldberg, D., Gislason, S. R., & Oelkers, E. H. (2020). Carbon dioxide storage through mineral carbonation. *Nature Reviews Earth & Environment*, 1(2), 90–102. <https://doi.org/10.1038/s43017-019-0011-8>
- Srinivasan, G., Hyman, J. D., Osthus, D. A., Moore, B. A., O'Malley, D., Karra, S., et al. (2018). Quantifying topological uncertainty in fractured systems using graph theory and machine learning. *Scientific Reports*, 8(1), 11665. <https://doi.org/10.1038/s41598-018-30117-1>
- Srinivasan, G., Tartakovsky, D. M., Robinson, B. A., & Aceves, A. B. (2007). Quantification of uncertainty in geochemical reactions. *Water Resources Research*, 43(12), 2007WR006003. <https://doi.org/10.1029/2007WR006003>
- Starchenko, V., Marra, C. J., & Ladd, A. J. C. (2016). Three-dimensional simulations of fracture dissolution. *Journal of Geophysical Research: Solid Earth*, 121(9), 6421–6444. <https://doi.org/10.1002/2016jb013321>
- Steefel, C. I. (2009). CrunchFlow. *Software for modeling multicomponent reactive flow and transport. User's manual* (pp. 12–91).
- Steefel, C. I., Appelo, C., Arora, B., Jacques, D., Kalbacher, T., Kolditz, O., et al. (2015). Reactive transport codes for subsurface environmental simulation. *Computational Geosciences*, 19(3), 445–478. <https://doi.org/10.1007/s10596-014-9443-x>
- Steefel, C. I., & Hu, M. (2022). Reactive transport modeling of mineral precipitation and carbon trapping in discrete fracture networks. *Water Resources Research*, 58(9), e2022WR032321. <https://doi.org/10.1029/2022wr032321>
- Steefel, C. I., & Lasaga, A. C. (1994). A coupled model for transport of multiple chemical species and kinetic precipitation/dissolution reactions with application to reactive flow in single phase hydrothermal systems. *American Journal of Science*, 294(5), 529–592. <https://doi.org/10.2475/ajs.294.5.529>
- Steefel, C. I., & Lichtner, P. C. (1994). Diffusion and reaction in rock matrix bordering a hyperalkaline fluid-filled fracture. *Geochimica et Cosmochimica Acta*, 58(17), 3595–3612. [https://doi.org/10.1016/0016-7037\(94\)90152-x](https://doi.org/10.1016/0016-7037(94)90152-x)
- Steefel, C. I., & Lichtner, P. C. (1998). Multicomponent reactive transport in discrete fractures: I. Controls on reaction front geometry. *Journal of Hydrology*, 209(1–4), 186–199. [https://doi.org/10.1016/S0022-1694\(98\)00146-2](https://doi.org/10.1016/S0022-1694(98)00146-2)
- Steefel, C. I., & MacQuarrie, K. T. (2018). Approaches to modeling of reactive transport in porous media. *Reactive transport in porous media* (pp. 83–130).
- Stefansson, I., Berre, I., & Keilegavlen, E. (2021). A fully coupled numerical model of thermo-hydro-mechanical processes and fracture contact mechanics in porous media. *Computer Methods in Applied Mechanics and Engineering*, 386, 114122. <https://doi.org/10.1016/j.cma.2021.114122>
- Stephanson, O., Jing, L., & Tsang, C. F. (1997). *Coupled thermo-hydro-mechanical processes of fractured media - Mathematical and experimental studies* (1st ed., Vol. 79). Elsevier.
- Su, D., Mayer, K. U., & MacQuarrie, K. T. (2021). MIN3P-HPC: A high-performance unstructured grid code for subsurface flow and reactive transport simulation. *Mathematical Geosciences*, 53(4), 517–550. <https://doi.org/10.1007/s11004-020-09898-7>
- Sweeney, M. R., Gable, C. W., Karra, S., Stauffer, P. H., Pawar, R. J., & Hyman, J. D. (2020). Upscaled discrete fracture matrix model (UDFM): An octree-refined continuum representation of fractured porous media. *Computational Geosciences*, 24, 1–18. <https://doi.org/10.1007/s10596-019-09921-9>
- Tan, P., Jin, Y., Han, K., Hou, B., Chen, M., Guo, X., & Gao, J. (2017). Analysis of hydraulic fracture initiation and vertical propagation behavior in laminated shale formation. *Fuel*, 206, 482–493. <https://doi.org/10.1016/j.fuel.2017.05.033>
- Teng, H. H., Dove, P. M., & De Yoreo, J. J. (2000). Kinetics of calcite growth: Surface processes and relationships to macroscopic rate laws. *Geochimica et Cosmochimica Acta*, 64(13), 2255–2266. [https://doi.org/10.1016/S0016-7037\(00\)00341-0](https://doi.org/10.1016/S0016-7037(00)00341-0)
- Tenthorey, E., & Cox, S. F. (2006). Cohesive strengthening of fault zones during the interseismic period: An experimental study. *Journal of Geophysical Research*, 111(B9), 2005JB004122. <https://doi.org/10.1029/2005JB004122>
- The National Academies of Sciences, Engineering, and Medicine. (2021). *Characterization, modeling, monitoring, and remediation of fractured rock*. National Academies Press.
- Thom, J. G. M., Dipple, G. M., Power, I. M., & Harrison, A. L. (2013). Chrysotile dissolution rates: Implications for carbon sequestration. *Applied Geochemistry*, 35, 244–254. <https://doi.org/10.1016/j.apgeochem.2013.04.016>

- Townend, J., & Zoback, M. D. (2000). How faulting keeps the crust strong. *Geology*, 28(5), 399–402. [https://doi.org/10.1130/0091-7613\(2000\)028<0399:hfkts>2.3.co;2](https://doi.org/10.1130/0091-7613(2000)028<0399:hfkts>2.3.co;2)
- Tsang, C. F. (1991). Coupled hydromechanical-thermomechanical processes in rock fractures. *Reviews of Geophysics*, 29(4), 537–551. <https://doi.org/10.1029/91rg01832>
- Tsang, Y., Tsang, C., Hale, F., & Dverstorp, B. (1996). Tracer transport in a stochastic continuum model of fractured media. *Water Resources Research*, 32(10), 3077–3092. <https://doi.org/10.1029/96wr01397>
- Uno, M., Koyanagawa, K., Kasahara, H., Okamoto, A., & Tsuchiya, N. (2022). Volatile-consuming reactions fracture rocks and self-accelerate fluid flow in the lithosphere. *Proceedings of the National Academy of Sciences*, 119(3), e2110776118. <https://doi.org/10.1073/pnas.2110776118>
- Vafaie, A., Cama, J., Soler, J. M., Kivi, I. R., & Vilarrasa, V. (2023). Chemo-hydro-mechanical effects of CO₂ injection on reservoir and seal rocks: A review on laboratory experiments. *Renewable and Sustainable Energy Reviews*, 178, 113270. <https://doi.org/10.1016/j.rser.2023.113270>
- van Der Lee, J., De Windt, L., Lagneau, V., & Goblet, P. (2003). Module-oriented modeling of reactive transport with HYTEC. *Computers & Geosciences*, 29(3), 265–275. [https://doi.org/10.1016/s0098-3004\(03\)00004-9](https://doi.org/10.1016/s0098-3004(03)00004-9)
- Van Noort, R., Spiers, C. J., Drury, M. R., & Kandianis, M. T. (2013). Peridotite dissolution and carbonation rates at fracture surfaces under conditions relevant for in situ mineralization of CO₂. *Geochimica et Cosmochimica Acta*, 106, 1–24. <https://doi.org/10.1016/j.gca.2012.12.001>
- Van Noort, R., Wolterbeek, T. K. T., Drury, M. R., Kandianis, M. T., & Spiers, C. J. (2017). The force of crystallization and fracture propagation during in-situ carbonation of peridotite. *Minerals*, 7(10), 190. <https://doi.org/10.3390/min7100190>
- Verberg, R., & Ladd, A. J. C. (2002). Simulation of chemical erosion in rough fractures. *Physical Review E*, 65(5), 056311. <https://doi.org/10.1103/PhysRevE.65.056311>
- Verhaeghe, F., Arnout, S., Blanpain, B., & Wollants, P. (2005). Lattice Boltzmann model for diffusion-controlled dissolution of solid structures in multicomponent liquids. *Physical Review E*, 72(3), 036308. <https://doi.org/10.1103/PhysRevE.72.036308>
- Verhaeghe, F., Arnout, S., Blanpain, B., & Wollants, P. (2006). Lattice-Boltzmann modeling of dissolution phenomena. *Physical Review E*, 73(3), 036316. <https://doi.org/10.1103/PhysRevE.73.036316>
- Viswanathan, H. S., Ajo-Franklin, J., Birkholzer, J. T., Carey, J. W., Guglielmi, Y., Hyman, J. D., et al. (2022). From fluid flow to coupled processes in fractured rock: Recent advances and new frontiers. *Reviews of Geophysics*, 60(1), e2021RG000744. <https://doi.org/10.1029/2021RG000744>
- Viswanathan, H. S., Robinson, B. A., Valocchi, A. J., & Triay, I. R. (1998). A reactive transport model of neptunium migration from the potential repository at Yucca Mountain. *Journal of Hydrology*, 209(1–4), 251–280. [https://doi.org/10.1016/S0022-1694\(98\)00122-X](https://doi.org/10.1016/S0022-1694(98)00122-X)
- Voigt, M., Marieni, C., Baldernann, A., Galeczka, I. M., Wolff-Boenisch, D., Oelkers, E. H., & Gislason, S. R. (2021). An experimental study of basalt–seawater–CO₂ interaction at 130°C. *Geochimica et Cosmochimica Acta*, 308, 21–41. <https://doi.org/10.1016/j.gca.2021.05.056>
- Vrolijk, P., & van der Pluijm, B. A. (1999). Clay Gouge. *Journal of Structural Geology*, 21(8–9), 1039–1048. [https://doi.org/10.1016/s0191-8141\(99\)00103-0](https://doi.org/10.1016/s0191-8141(99)00103-0)
- Wang, F., Dreisinger, D., Jarvis, M., & Hitchens, T. (2019). Kinetics and mechanism of mineral carbonation of olivine for CO₂ sequestration. *Minerals Engineering*, 131, 185–197. <https://doi.org/10.1016/j.mineng.2018.11.024>
- Wang, J. S. Y. (1991). Flow and transport in fractured rocks. *Reviews of Geophysics*, 29(S1), 254–262. <https://doi.org/10.1002/rog.1991.29.s1.254>
- Wen, H., & Li, L. (2018). An upscaled rate law for mineral dissolution in heterogeneous media: The role of time and length scales. *Geochimica et Cosmochimica Acta*, 235, 1–20. <https://doi.org/10.1016/j.gca.2018.04.024>
- Weng, X., Kresse, O., Cohen, C., Wu, R., & Gu, H. (2011). Modeling of hydraulic-fracture-network propagation in a naturally fractured formation. *SPE Production & Operations*, 26(4), 368–380. <https://doi.org/10.2118/140253-pa>
- White, A. F., & Brantley, S. L. (2003). The effect of time on the weathering of silicate minerals: Why do weathering rates differ in the laboratory and field? *Chemical Geology*, 202(3–4), 479–506. <https://doi.org/10.1016/j.chemgeo.2003.03.001>
- White, M. D., & Oostrom, M. (2003). *STOMP subsurface transport over multiple phases version 3.0 User's guide*. Pacific Northwest National Laboratory.
- White, S. K., Spane, F. A., Schaeff, H. T., Miller, Q. R. S., White, M. D., Horner, J. A., & McGrail, B. P. (2020). Quantification of CO₂ mineralization at the Wallula Basalt Pilot Project. *Environmental Science & Technology*, 54(22), 14609–14616. <https://doi.org/10.1021/acs.est.0c05142>
- Wood, B. D. (2007). Inertial effects in dispersion in porous media. *Water Resources Research*, 43(12), 2006WR005790. <https://doi.org/10.1029/2006WR005790>
- Wood, B. D., He, X., & Apte, S. V. (2020). Modeling turbulent flows in porous media. *Annual Review of Fluid Mechanics*, 52(1), 171–203. <https://doi.org/10.1146/annurev-fluid-010719-060317>
- Wu, W., Reece, J. S., Gensterblum, Y., & Zoback, M. D. (2017). Permeability evolution of slowly slipping faults in shale reservoirs. *Geophysical Research Letters*, 44(22), 11368–11375. <https://doi.org/10.1002/2017GL075506>
- Wu, Z., Luhmann, A. J., Rinehart, A. J., Mozley, P. S., Dewers, T. A., Heath, J. E., & Majumdar, B. S. (2020). Chemo-mechanical alterations induced from CO₂ injection in carbonate-cemented sandstone: An experimental study at 71°C and 29 MPa. *Journal of Geophysical Research: Solid Earth*, 125(3), e2019JB019096. <https://doi.org/10.1029/2019jb019096>
- Xiao-Dong, N., Chunming, Z., & Yuan, W. (2015). Hydro-mechanical analysis of hydraulic fracturing based on an improved DEM-CFD coupling model at micro-level. *Journal of Computational and Theoretical Nanoscience*, 12(9), 2691–2700. <https://doi.org/10.1166/jctn.2015.4164>
- Xing, T., Zhu, W., Fusses, F., & Lisabeth, H. (2018). Generating porosity during olivine carbonation via dissolution channels and expansion cracks. *Solid Earth*, 9(4), 879–896. <https://doi.org/10.5194/se-9-879-2018>
- Xiong, W., & Giammar, D. (2014). Forsterite carbonation in zones with transport limited by diffusion. *Environmental Science & Technology Letters*, 1(8), 333–338. <https://doi.org/10.1021/ez500182s>
- Xiong, W., Wells, R. K., & Giammar, D. E. (2017). Carbon sequestration in olivine and basalt powder packed beds. *Environmental Science & Technology*, 51(4), 2105–2112. <https://doi.org/10.1021/acs.est.6b05011>
- Xiong, W., Wells, R. K., Horner, J. A., Schaeff, H. T., Skemer, P. A., & Giammar, D. E. (2018). CO₂ mineral sequestration in naturally porous basalt. *Environmental Science & Technology Letters*, 5(3), 142–147. <https://doi.org/10.1021/acs.estlett.8b00047>
- Xiong, W., Wells, R. K., Menefee, A. H., Skemer, P., Ellis, B. R., & Giammar, D. E. (2017). CO₂ mineral trapping in fractured basalt. *International Journal of Greenhouse Gas Control*, 66, 204–217. <https://doi.org/10.1016/j.ijggc.2017.10.003>
- Xu, T., Spycher, N., Sonnenthal, E., Zhang, G., Zheng, L., & Pruess, K. (2011). TOUGHREACT Version 2.0: A simulator for subsurface reactive transport under non-isothermal multiphase flow conditions. *Computers & Geosciences*, 37(6), 763–774. <https://doi.org/10.1016/j.cageo.2010.10.007>

- Xu, Z., Cao, H., Yoon, S., Kang, P. K., Jun, Y.-S., Kneafsey, T., et al. (2023). Gravity-driven controls on fluid and carbonate precipitation distributions in fractures. *Scientific Reports*, *13*(1), 9400. <https://doi.org/10.1038/s41598-023-36406-8>
- Yan, C., Xie, X., Ren, Y., Ke, W., & Wang, G. (2022). A FDEM-based 2D coupled thermal-hydro-mechanical model for multiphysical simulation of rock fracturing. *International Journal of Rock Mechanics and Mining Sciences*, *149*, 104964. <https://doi.org/10.1016/j.ijrmms.2021.104964>
- Yang, W., Chen, M. A., Lee, S. H., & Kang, P. K. (2024). Fluid inertia controls mineral precipitation and clogging in pore to network-scale flows. *Proceedings of the National Academy of Sciences*, *121*(28), e2401318121. <https://doi.org/10.1073/pnas.2401318121>
- Yao, J., Zhang, X., Sun, Z., Huang, Z., Liu, J., Li, Y., et al. (2018). Numerical simulation of the heat extraction in 3D-EGS with thermal-hydraulic-mechanical coupling method based on discrete fractures model. *Geothermics*, *74*, 19–34. <https://doi.org/10.1016/j.geothermics.2017.12.005>
- Ye, Z., & Ghassemi, A. (2018). Injection-induced shear slip and permeability enhancement in granite fractures. *Journal of Geophysical Research: Solid Earth*, *123*(10), 9009–9032. <https://doi.org/10.1029/2018jb016045>
- Yeh, G., & Tripathi, V. (1990). *HYDROGEOCHEM: A coupled model of HYDROlogic transport and GEOCHEMical equilibria in reactive multicomponent systems*. Oak Ridge National Laboratory.
- Yoon, H., Chojnicki, K. N., & Martinez, M. J. (2019). Pore-scale analysis of calcium carbonate precipitation and dissolution kinetics in a microfluidic device. *Environmental Science & Technology*, *53*(24), 14233–14242. <https://doi.org/10.1021/acs.est.9b01634>
- Yoon, S., & Kang, P. K. (2023). Mixing-induced bimolecular reactive transport in rough channel flows: Pore-scale simulation and stochastic upscaling. *Transport in Porous Media*, *146*(1), 329–350. <https://doi.org/10.1007/s11242-021-01662-7>
- Yuan, Y., Xu, T., Moore, J., Lei, H., & Feng, B. (2020). Coupled thermo-hydro-mechanical modeling of hydro-shearing stimulation in an enhanced geothermal system in the Raft River geothermal field, USA. *Rock Mechanics and Rock Engineering*, *53*(12), 5371–5388. <https://doi.org/10.1007/s00603-020-02227-8>
- Zakharova, N. V., Goldberg, D. S., Sullivan, E. C., Herron, M. M., & Grau, J. A. (2012). Petrophysical and geochemical properties of Columbia River flood basalt: Implications for carbon sequestration. *Geochemistry, Geophysics, Geosystems*, *13*(11), 2012GC004305. <https://doi.org/10.1029/2012GC004305>
- Zaoui, A. (2002). Continuum micromechanics: Survey. *Journal of Engineering Mechanics*, *128*(8), 808–816. [https://doi.org/10.1061/\(ASCE\)0733-9399\(2002\)128:8\(808\)](https://doi.org/10.1061/(ASCE)0733-9399(2002)128:8(808))
- Zhang, G., Zhou, D., Wang, P., Zhang, K., & Tang, M. (2020). Influence of supercritical CO₂-water on the micromechanical properties of sandstone. *International Journal of Greenhouse Gas Control*, *97*, 103040. <https://doi.org/10.1016/j.ijggc.2020.103040>
- Zhang, L., Wang, Y., Miao, X., Gan, M., & Li, X. (2019). Geochemistry in geologic CO₂ utilization and storage: A brief review. *Advances in Geo-Energy Research*, *3*(3), 304–313. <https://doi.org/10.26804/ager.2019.03.08>
- Zhang, Q., Deng, H., Dong, Y., Molins, S., Li, X., & Steefel, C. (2022). Investigation of coupled processes in fractures and the bordering matrix via a micro-continuum reactive transport model. *Water Resources Research*, *58*(2), e2021WR030578. <https://doi.org/10.1029/2021WR030578>
- Zhang, Y., & Dawe, R. A. (2000). Influence of Mg²⁺ on the kinetics of calcite precipitation and calcite crystal morphology. *Chemical Geology*, *163*(1–4), 129–138. [https://doi.org/10.1016/S0009-2541\(99\)00097-2](https://doi.org/10.1016/S0009-2541(99)00097-2)
- Zhang, Y., Shao, J., De Saxcé, G., Shi, C., & Liu, Z. (2019). Study of deformation and failure in an anisotropic rock with a three-dimensional discrete element model. *International Journal of Rock Mechanics and Mining Sciences*, *120*, 17–28. <https://doi.org/10.1016/j.ijrmms.2019.05.007>
- Zheng, X., Cordonnier, B., Zhu, W., Renard, F., & Jamtveit, B. (2018). Effects of confinement on reaction-induced fracturing during hydration of periclase. *Geochemistry, Geophysics, Geosystems*, *19*(8), 2661–2672. <https://doi.org/10.1029/2017gc007322>
- Zhu, J., & Cheng, Y. (2018). Effective permeability of fractal fracture rocks: Significance of turbulent flow and fractal scaling. *International Journal of Heat and Mass Transfer*, *116*, 549–556. <https://doi.org/10.1016/j.ijheatmasstransfer.2017.09.026>
- Zhu, W., Fuisseis, F., Lisabeth, H., Xing, T., Xiao, X., De Andrade, V., & Karato, S. (2016). Experimental evidence of reaction-induced fracturing during olivine carbonation: Fracturing during olivine carbonation. *Geophysical Research Letters*, *43*(18), 9535–9543. <https://doi.org/10.1002/2016GL070834>
- Zhuang, L., & Zang, A. (2021). Laboratory hydraulic fracturing experiments on crystalline rock for geothermal purposes. *Earth-Science Reviews*, *216*, 103580. <https://doi.org/10.1016/j.earscirev.2021.103580>
- Zoback, M. D., Rummel, F., Jungi, R., & Raleigh, C. B. (1977). Laboratory hydraulic fracturing experiments in intact and pre-fractured rock. *International Journal of Rock Mechanics and Mining Sciences*, *14*(2), 49–58. [https://doi.org/10.1016/0148-9062\(77\)90196-6](https://doi.org/10.1016/0148-9062(77)90196-6)
- Zyvoloski, G. (2007). FEHM: A control volume finite element code for simulating subsurface multi-phase multi-fluid heat and mass transfer. Los Alamos Unclassified Report LA-UR-07-3359.

Erratum

The originally published version of this article contained an error. In Figure 1, the labels for experimental and field scales were swapped. The error has been corrected, and this may be considered the authoritative version of record.